

Spring 2016

# Modular and Dynamic Approaches to the Formation of Single-chain Polymer Nanoparticles

Bryan Tyler Tuten

*University of New Hampshire, Durham*

Follow this and additional works at: <https://scholars.unh.edu/dissertation>

---

## Recommended Citation

Tuten, Bryan Tyler, "Modular and Dynamic Approaches to the Formation of Single-chain Polymer Nanoparticles" (2016). *Doctoral Dissertations*. 2242.

<https://scholars.unh.edu/dissertation/2242>

This Dissertation is brought to you for free and open access by the Student Scholarship at University of New Hampshire Scholars' Repository. It has been accepted for inclusion in Doctoral Dissertations by an authorized administrator of University of New Hampshire Scholars' Repository. For more information, please contact [nicole.hentz@unh.edu](mailto:nicole.hentz@unh.edu).

MODULAR AND DYNAMIC APPROACHES TO THE FORMATION OF SINGLE-  
CHAIN POLYMER NANOPARTICLES

BY

BRYAN TYLER TUTEN

DISSERTATION

Submitted to the University of New Hampshire in Partial Fulfillment of the Requirements  
for the Degree of

Doctor of Philosophy

In

Materials Science

May, 2016

ALL RIGHTS RESERVED

© 2016

Bryan Tyler Tuten

This dissertation has been examined and approved in partial fulfillment of the requirements of the degree Doctor of Philosophy in Materials Science by:

Dissertation Director, Erik Berda, Associate  
Professor in Chemistry and Materials Science

John Tsavalas, Associate Professor in  
Chemistry and Materials Science

Glen P. Miller, Professor in Chemistry and  
Materials Science

Carmela Amato-Wierda, Associate Professor  
in Materials Science

Arthur Greenberg, Professor in Chemistry

On January 22<sup>nd</sup>, 2016

Original approval signatures are on file with the University of New Hampshire Graduate School



# Table of Contents

<b>TABLE OF FIGURES:</b> .....	<b>VI</b>
<b>TABLE OF SCHEMES:</b> .....	<b>VIII</b>
<b>TABLE OF TABLES:</b> .....	<b>IX</b>
<b>DEDICATION</b> .....	<b>X</b>
<b>ACKNOWLEDGMENTS</b> .....	<b>XI</b>
<b>ABSTRACT</b> .....	<b>XVI</b>
<b>CHAPTER 1</b> .....	<b>1</b>
<b>INTRODUCTION TO SINGLE-CHAIN POLYMER NANOPARTICLES:</b> .....	<b>1</b>
1.1 SYNTHESIS OF SCNPs.....	2
1.1.1 Covalent cross-linking reactions: .....	7
1.1.2 Dynamic covalent chemistry.....	11
1.2 CHARACTERIZATION OF SCNPs .....	12
1.2.1 Size exclusion chromatography .....	13
1.2.2 Light scattering.....	14
1.2.3 Viscometry .....	15
1.2.4 Nuclear Magnetic Resonance Spectroscopy (NMR) .....	16
<b>CHAPTER 2</b> .....	<b>17</b>
<b>DYNAMIC DISULFIDE POLYMER NANOPARTICLES</b> .....	<b>17</b>
2.1 INTRODUCTION .....	17
2.2 RESULTS AND DISCUSSION .....	19
2.2.1 Polymer design .....	19
2.2.2 SEC characterization via standard calibration .....	20
2.2.3 Characterization via triple detection SEC .....	24
2.3 CONCLUSIONS .....	28
2.4 EXPERIMENTAL SECTION .....	29
2.4.1 General Methods .....	29
2.4.2 Synthesis of poly(norbornene- <i>exo</i> -anhydride): .....	30
2.4.3 Poly(cyclooctadiene- <i>co</i> -norbornene- <i>exo</i> -anhydride): .....	31
2.4.4 General Crosslinking Procedure (N1 and N2): .....	32
2.4.5 General Unfolding Procedure: .....	33
2.4.6 General Disulfide Oxidation (refolding) Procedure: .....	34
2.4.7 Supplemental Figures .....	34
2.4.8 Example Spectra .....	35
<b>CHAPTER 3</b> .....	<b>38</b>
<b>MODULAR DESIGN FOR HIERARCHICAL POLYMERIC MATERIALS</b> .....	<b>38</b>
3.1 INTRODUCTION .....	38
3.2 RESULTS/DISCUSSION:.....	40
3.2.1 Modularity via glycidyl methacrylate and pentafluorophenyl methacrylate .....	40
3.2.2 Modularity via propargyl methacrylate and pentafluorophenyl methacrylate .....	44
3.3 EXPERIMENTAL:.....	48
3.3.1 General Methods .....	48
3.3.2 Synthesis of pentafluorophenyl methacrylate: .....	49

3.3.3 Example polymerization for methyl methacrylate, glycidyl methacrylate, and pentafluorophenyl methacrylate. ....	50
3.3.4 TMS-Monomer synthesis .....	51
3.3.5 TMS Polymer synthesis.....	51
3.3.6 Polymer deprotection: .....	52
3.3.7 SCNP formation via thermally initiated thiol-yne click chemistry: .....	53
3.3.8 Synthesis of poly(propargyl methacrylate-co-methyl methacrylate-co-pentafluorophenyl methacrylate):.....	53
<b>CHAPTER 4 .....</b>	<b>55</b>
4.1 PENTAFLUOROPHENYL ACTIVATED ESTERS AND THEIR DOPING EFFECTS ON SECOND AND THIRD GENERATION GRUBBS' CATALYST .....	55
4.1.1 Introduction:.....	55
4.2 RESULTS AND DISCUSSION: .....	58
4.3 EXPERIMENTAL:.....	63
4.3.1 General Methods. ....	63
4.3.2 Synthesis of norbornene hexyl imide: .....	64
4.3.3 Synthesis of <i>exo</i> -norbornene hexanoic acid: .....	65
4.3.4 Synthesis of <i>exo</i> -norbornene hexanoic acid chloride: .....	66
4.3.5 Synthesis of <i>exo</i> -norbornene hexanoic pentafluorophenyl ester:.....	66
4.3.6 Synthesis of <i>exo</i> -norbornene dodecanoic acid: .....	67
4.3.7 Synthesis of <i>exo</i> -norbornene dodecanoic acid chloride: .....	67
4.3.8 Synthesis of <i>exo</i> -norbornene dodecanoic pentafluorophenyl ester:.....	68
4.3.9 An example procedure for ROMP (catalyst added last):.....	69
4.3.10 An example procedure for a "starve-fed" ROMP: .....	69
<b>CHAPTER 5 .....</b>	<b>71</b>
<b>NEW ROUTES IN POST-POLYMERIZATION MODIFICATION WITH PENTAFLUOROPHENYL ACTIVATED ESTERS .....</b>	<b>71</b>
5.1 INTRODUCTION .....	71
5.2 RESULTS AND DISCUSSION.....	73
5.3 EXPERIMENTAL.....	76
5.3.1 General Methods .....	76
5.3.2 Synthesis of pentafluorophenyl methacrylate .....	77
5.3.3 Polymer synthesis .....	78
5.3.4 Representative thiol- <i>para</i> fluoro post polymerization modification: .....	79
5.3.5 Representative post-polymerization modification of the active ester: .....	79
<b>APPENDIX .....</b>	<b>81</b>
<b>REFERENCES .....</b>	<b>122</b>

### TABLE OF FIGURES:

Figure 1.1 General overview of SCNP formation. ....	2
Figure 2.1 SEC before and after intramolecular cross-linking. ....	21
Figure 2.2 SEC traces of unfolded polymer uN1 compared to parent polymer P1. ....	22

Figure 2.3 SEC traces of showing the initial folding of P1 to N1, unfolding into uN1 following disulfide reduction, and refolding after thiol oxidation.....	23
Figure 2.4 Representative TEM image of single-chain nanoparticles N2. ....	27
Figure 2.5 MALS and RI detection traces for SEC of N2 and excess cross-linker. Although the concentration of multi-chain aggregates has a negligible impact on the RI trace, these larger particles scatter quite intensely as seen in the MALS trace.....	28
Figure 2.6 Full SEC trace for unfolded chains uN1, showing a small amount of intermolecular particle-particle coupling (see previous text for details). ....	34
Figure 2.7 SEC overlay of MALS detector trace for N2 and P2 for which data in Table 2.1 MALS and viscometric data for <b>P2</b> and <b>N2</b> (see above) was derived. ....	35
Figure 2.8 IR overlay for P2 and N2. Addition of cross-linker is confirmed by the shift in the anhydride carbonyl stretch to lower wavenumber, as well as the appearance of the Ph-H bend and the carboxylic acid –OH. ....	35
Figure 2.9 NMR overlay of N2 before and after treatment with DTT showing the appearance of the –SH peak confirming disulfide reduction.....	36
Figure 2.10 Full TEM image of SCNPs N2 from which Figure 2.4 was taken.....	37
Figure 3.1 Refractive Index SEC traces of before (blue) and after (red) of cross-linking with piperazine. SEC traces of A) P3.1, B) P3.2 and C) P3.3. Little, to no shift in retention time is observed using piperazine as a cross-linker.....	43
Figure 3.2 MALS trace of P3.3 showing large amounts of inter-chain crosslinking.....	44
Figure 3.3 Thermally initiated thiol-yne click-chemistry to form SCNPs.....	45
Figure 3.4 Compaction studies performed by Pomposo and coworkers. Column a) are SCNPs formed via thiol-ene click-chemistry analyzed by SEC and SAXS and column b)	



are SCNPs formed via thiol-yne click chemistry analyzed by SEC and SAXS. See reference <sup>105</sup> for further details. ....	47
Figure 4.1 A) A basic scheme for possible FAH interactions with Grubbs' catalyst. B) DFT optimized MD simulations for hexafluorobenzene (top) and benzene (bottom). See reference <sup>115</sup> for further details. ....	58
Figure 4.2 MALS trace (red) and RI trace (blue) of "starve-fed" polymerizations showing poor control over dispersity.....	61
Figure 4.3 MALS (top) and RI (bottom) traces of FAH containing polymer using Grubbs' 1 <sup>st</sup> generation catalyst showing low polydispersity. ....	62
Figure 5.1 <sup>19</sup> F NMR of the parent pentafluorophenyl methacrylate polymer (top), the thiol-para fluoro post-polymerization modification (middle), and the post-polymerization of the still activated ester via primary alkyl amine (bottom).....	75
Figure 5.2 <sup>1</sup> H NMR spectra of sequential post-polymerization modifications through the pentafluorophenyl-activated ester. ....	76

### TABLE OF SCHEMES:

Scheme 2.1 Synthetic scheme for dynamic covalent SCNPs. ....	20
Scheme 2.2 Synthesis of a copolymer with a discrete amount of reactive comonomer to control the extent of possible intramolecular cross-linking.....	25
Scheme 3.1 Example of post-polymerization modification of SCNPs.....	39
Scheme 3.2 SCNP formation with secondary amine, then SCNP functionalization with primary alkyl amine .....	40

Scheme 4.1 Attempted polymerizations of FAH-containing polymers with different Grubbs' catalysts .....	56
Scheme 5.1 Sequential post-polymerization modifications with pentafluorophenyl activated esters .....	71
Scheme 5.2 Scheme of the different thiols capable of performing thiol-para fluoro click-reactions on pentafluorophenyl-activated esters.....	73

**TABLE OF TABLES:**

Table 1.1 A list of the numerous types of chemistry utilized in the formation of SCNPs..	3
Table 2.1 MALS and viscometric data for <b>P2</b> and <b>N2</b> .....	25
Table 3.1 Varying comonomer parent polymers, <b>P</b> , and their subsequent cross-linking with piperazine, <b>N</b> . .....	41
Table 3.2 Initial results with thiol-yne polymers, <b>P</b> , and SCNP formation, <b>N</b> . .....	46
Table 4.1 Matrix of varying FAH containing ROMP monomers .....	60

## **DEDICATION**

To my loving mother and father, Jerilyn and Dave, my beautiful and hilarious baby sisters Bethany and Paige, the love of my life and the most amazing and loving woman I know, Jessie Kate Sexton, and finally to my late Grandmother, Charlotte Johnson.

## ACKNOWLEDGMENTS

Where to begin? Reflecting back on this adventure it seems an almost equally daunting task trying to acknowledge and thank the multitude of people responsible for my success here at the UNH, as it has been actually writing this dissertation. I think the most efficient course of action will be in a somewhat reverse chronological order.

To my advisor Prof. Erik Berda: I will forever, and eternally, be in your debt. From our first conversation in which you informed me on your experiments with *in vivo* alcohol dehydrogenase studies, all the way till now, you have for reasons I will probably never understand, stood by me and had my back every step of the way even when I didn't deserve it. My abilities and proficiencies as a polymer chemist are a direct reflection of you and your teachings and all of my many shortcomings and failings as a polymer chemist are my own. I could not have asked for a better advisor and mentor. Thank you.

To my committee: Prof. John Tsavalas, Prof. Glen Miller, Prof. Carmela Amato-Weirda, and Prof. Art Greeberg, thank you all so much for your patience, kind advice and guidance over the years. I'm truly thankful for you all.

To the Berda Group: There's a dissertation-worth of memories with you all. In the early stages of me writing this part, you each had your own write up, but in the interest of space, time, and professionalism, I will mention you all briefly here, but send you each what I had initially wrote later: Dr. Alka Prasher, Dr. Christopher Lyon, Peter Frank, Ashley Hanlon, Justin Cole, and honorary group member Kyle Rodriguez. Thank you all so much. On top of being brilliant scientists and colleagues, you are all great people. Thank you for all the friendship along the way.

To the Berda Group undergrads, past and present, there are quite literally too many of you to list, however, a very special thank you goes out to the two amazing

undergrads that I had work under me over the years: Karen Richards and Rachel Olsen, thank you both so much for your hard work and amazing attitudes. Karen, it was one of the highlights of my time in graduate school to watch you grow as a scientist from your freshman year all the way through your graduation and now being one of my closest friends. Rachel, I couldn't have asked for a funnier, more down-to-earth student that would take part in random lab dance-offs. Thank you both so much.

A special thank you to the people that actually taught me how to handle myself in a laboratory: Dr. Anita Augustyniak, Dr. Haoran Chen, and Dr. Danming Chao. Thank you guys for making sure I never blew myself up, as well as teaching me all of your tips and tricks.

Thank you to Katie Makem and Michelle Waltz in the Materials Science Program for helping me every time I dropped by Demeritt Hall with questions and concerns.

Thank you to Cindi Rowher, Peg Torch, Bob Constantine, and Kristen Blackwell in my adoptive home of the Chemistry Department for being my lifesavers more times than I can count.

To all of my professors that have taught me over the years that I haven't already mentioned, Dr. James Krzanowski, Dr. Charles Zercher, Dr. Gary Weisman, as well as Dr. Patricia Wilkinson for all of NMR help and training over the years, as well as all the German language books. Thank you all so much.

To my former advisor, Dr. Marshall Ming and the rest of the NPRC at the time I started at UNH: Dr. Don Sundberg and Dr. Yvon Durant, thank you all so much for being the ones to see potential in me and invite me to join your group at UNH. I'm forever in your debt.

To all my NH friends that don't fall into the spectrum that is UNH Chemistry/MSP: George Marshall, not a "NH" friend per se, but having one of my best

friends from college down in Boston has been amazing. I regret not hanging out more. Connor Roelke and the “Lee House”... that’s really all that I can say about you all while maintaining professionalism. Mike Thompson and all of our outdoor adventures. Brandon Montemuro and Wei Dai for all the ski trips. Kate Braland for being the first and only friend I’ve ever made on an airplane. Mollie Mitchem for being a long-lost high school acquaintance, turned great friend down in Boston. Adriana Duffin, former student, turned awesome friend over the years. I love Durham and UNH, but sometimes one needs to get away and you all have helped provide places to “runaway” too. Thank you all so much.

To my former chemistry professors at West Virginia Wesleyan College, Dr. Ed Wovchko, and Dr. Tim Troyer, thank you so much for your guidance during my undergraduate chemistry major, especially because I was absolutely more trouble than I was worth. Dr. Wovchko, you were an amazing advisor and your love for materials science is the reason I went to graduate school. Dr. Troyer, you saw something in me during organic chemistry that I didn’t even see in myself. I was struggling and you didn’t give up on me and even rewarded my efforts with an extra-curricular science experiment in thermite. Its because of you that the materials science group I joined was an organic chemistry intensive one.

To my KWBJJ family: I can’t even begin to put into words what you all mean to me. You have adopted me as one of your own, you have been there for me, without question, every single time. You have mentored me, you have taught me, you have loved me, you have taken care of me. I absolutely, 100% could not have done this without you all. A special mention to the two head coaches of KWBJJ, Kevin Watson and Jay Hanley: You two are the brothers I’ve never had. On top of the “jiu-jitsu family” that you both brought me into, you both have brought me into your actual families as well. I will never

in my life be able to repay you for the love that you and your families have shown me. I love you all.

Kelley, Mike, Alex, Mem and Pep, you absolutely have been my New Hampshire parents, and grandparents (and little brother). I can't even begin to list all the times that you have fed me, lodged me, loved me, taken me for birthday dinners, Thanksgiving's, Christmas', New Years', watched Jack, trips to the lake, and otherwise unconditionally adopted me into your family. I love you all.

Jack. I know you'll never read the words on this page, but I know you'll understand their sentiment. I wouldn't have been able to do this without you. You've come to work with me almost everyday for 4 years, sleeping under my desk, laying your head on my lap when I'm stressed out, making other people smile when they enter the office and sometimes even barfing on the floor. I love you buddy and I can't wait to start this new adventure in Germany with you.

Jessie Kate. The absolute love of my life. Never in my wildest dreams did I ever think that I would end up with someone as amazing as you. For the last six and a half years you have been by my side, unconditionally, no matter what. Through all of the stress, the long hours, the long distances, the late nights, you have been my rock through it all. I absolutely don't deserve you, but I'm thankful that you'll have me anyway. I love you with all my heart.

Beth and Paige. I haven't done a good enough job of letting you both know how much you have made me laugh, often to the point of tears and sore cheeks, over the years. Your constant text messages, phone calls, Bernie Sanders riding a unicorn with rainbow pistols, or thrift store tin print outs of Karlsruhe Germany have helped me get through the hard days more than you will ever know. I love you both so much.

Mamaw and Papaw Toots and my late Grandma and Papaw Johnson. I love you all so very much and without your unconditional love and support I would not be where I am today.

Last, but most certainly not least. Mom and Dad. How do I thank you for all that you've done for me? Any words I put to a page will not even come close to adequately describing how thankful and grateful I am to have you two as my parents. You've listened to me on my bad days, yelled at me on my lazy days, sent me money for food, student fees, and plane tickets. You've traveled thousands of miles, sometimes just to see me for a couple of days, and other times, you've put your life on hold in order to spend weeks with me. If I end up just being half the person that either of you are, I will be the luckiest person on Earth. I love you both so much and I wouldn't have been able to complete this journey if it wasn't for you two. Thank you both so much, I love you.

*“Eventually, all things merge into one, and a river runs through it.”*

*-Normal Maclean*



## ABSTRACT

### MODULAR AND DYNAMIC APPROACHES TO THE FORMATION OF SINGLE-CHAIN POLYMER NANOPARTICLES

BY

Bryan Tuten

University of New Hampshire, May, 2016

The methodology towards the creation of nanoscale polymeric objects by way of the folding of single polymer chains has been enjoying success in the field of polymer chemistry and materials science. By synthesizing polymer chains with built in functionality either through functional side groups, or direct incorporation into the polymer backbone, polymer chemists are able to fold single polymer chains onto themselves through a broad range of covalent and non-covalent interactions in dilute solution. These compact, nano-sized objects can now be used in a wide arrange of functions and applications.

The aim of this dissertation is to provide first, a comprehensive overview of the recent advances and success enjoyed by this field and second, to showcase some of the various routes towards the dynamic and modular creation of these single-chain polymer nanoparticles (SCNPs).

Chapter 2 of this work discusses the use of dynamic covalent cross-linking chemistry via reversible disulfide bridges in the folding and unfolding of SCNPs. Through the use of triple detection size-exclusion chromatography (SEC) it was shown

through changes in retention time, a phenomena indicative of hydrodynamic volume, a polymer was being folded into compact SCNPs and then unfolded and refolded via redox chemistry. Chapter 3 explores the design of polymers that had various different cross-linkable moieties incorporated into the monomer side units. By having cross-linkable moieties that can undergo different chemical cross-linking reactions (i.e thiol-yne click reactions, epoxide ring-opening reactions, activated esters), a modular approach towards the folding and subsequent functionalization of SCNPs is created. Looking to design a system with a greater degree of control over the modular functionality, chapter 4 investigates the use of norbornene imide monomers containing pentafluorophenyl activated esters with varying methylene spacer unites between the polymerizable olefin and the activated ester. It was here that an unexpected phenomena was observed; the doping effects of fluorinated aromatic hydrocarbons (FAHs) on second and third generation Grubbs' catalysts. This chapter aims to shed some light on this subject. Finally in chapter 5 an additional click-chemistry reaction is observed to take place with pentafluorophenyl methacrylate. Thiol-para fluoro click reactions are used to react with the pentafluorophenyl activated esters, while still leaving the ester moiety reactive towards primary alkyl amines.

## CHAPTER 1

### INTRODUCTION TO SINGLE-CHAIN POLYMER NANOPARTICLES:

Ubiquitous in nature are precisely defined linear polymers folded into functional nano-objects that are capable of performing complex tasks. With this in mind an obvious, yet unmet, research goal becomes apparent: exploiting our understanding of biological macromolecules to mimic this behavior in the laboratory using recent advances in controlled polymerization chemistry and the well-known theories of modern polymer physics. Applications for this emerging technology include catalysis<sup>1-5</sup>, sensors<sup>6</sup>, nanoreactors<sup>7</sup>, and nanomedicine.<sup>8-11</sup>

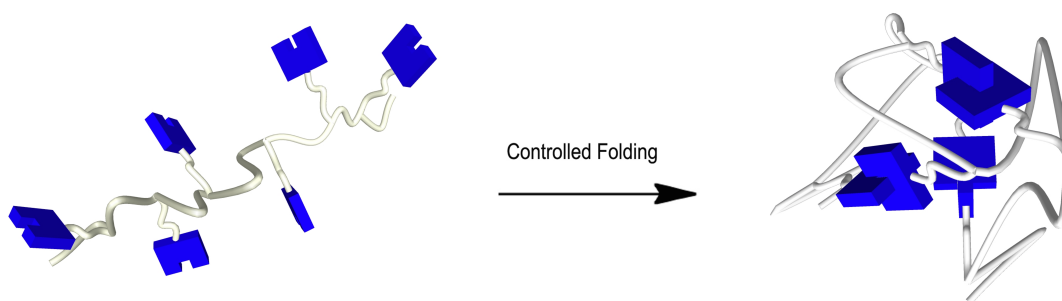
The elegance and utility of biomacromolecules lies in their perfectly defined tertiary structure or, in other words, a specific three-dimensional shape with precise placement of functionality either on the surface, or within the interior. It is by having a precise primary structure, that these biomacromolecules form their specific tertiary structures, which is not currently possible in traditional synthetic polymers. Recent advances in controlled polymerization chemistries have allowed the synthesis of multiblock polymers with narrow molecular weight distributions<sup>12</sup> or materials with controlled monomer sequences<sup>13,14</sup> by step-growth and chain-growth techniques. These methods are a leap forward, but still result in microstructure heterogeneities or broad molecular weight distributions. In analogy to nature's three-dimensional globular

structures, dendrimers have often been considered as a synthetic alternative due to their low molecular weight distributions and highly regular structures. Traditionally, however, their synthesis is tedious and often results in prohibitively low yields as well as the inability to precisely control the functionality and morphology of the interior. By using “click” chemistries, recent advances have been made upon traditional methods,<sup>15</sup> however, dendrimers still fall short of the precisely controlled architecture’s of nature.<sup>16</sup>

With biomacromolecules as the paragon of functional and structurally defined nano-objects, then the new paradigm in polymer synthesis must involve the manipulation and folding of single polymer chains.<sup>17</sup> Conceptually, this is a simple process (Figure 1.1 General overview of SCNP formation.<sup>18</sup>)

Single-chain polymer nanoparticles (SCNP), while in principle are easy to comprehend, they have exhibited far greater complexity than initially anticipated and are the subject of numerous research groups internationally<sup>19-22</sup> as well as our own.

### 1.1 Synthesis of SCNPs

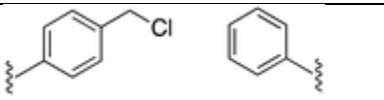
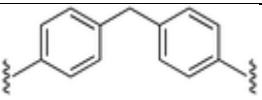
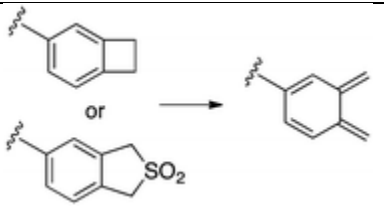
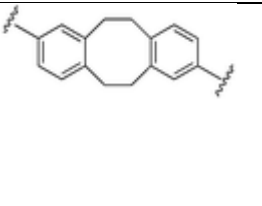


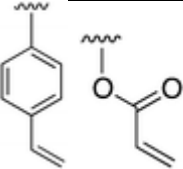
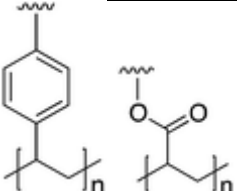
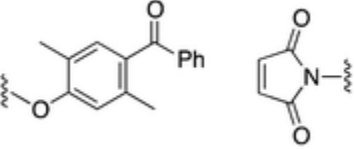
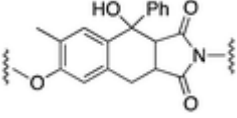
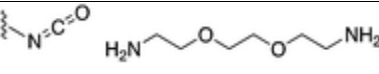
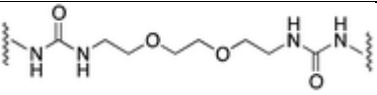
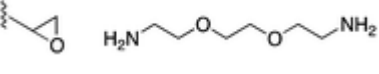
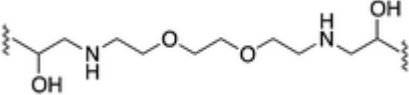
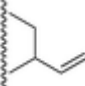
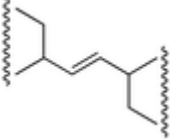
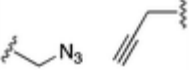
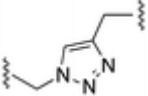
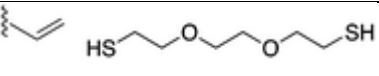
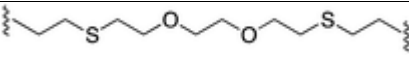
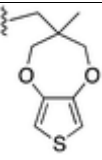
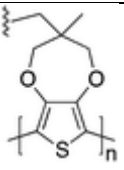
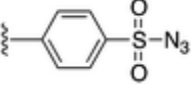
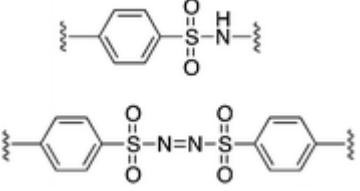
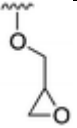
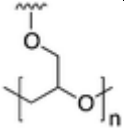
*Figure 1.1 General overview of SCNP formation.*



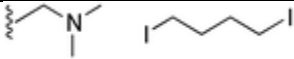
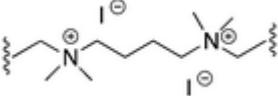
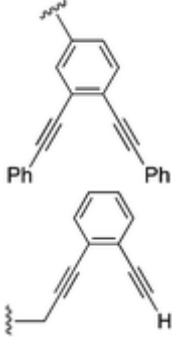
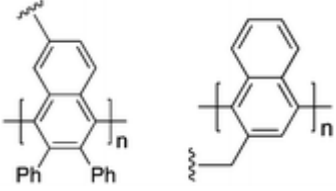
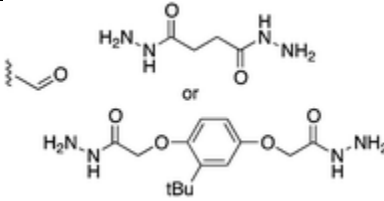
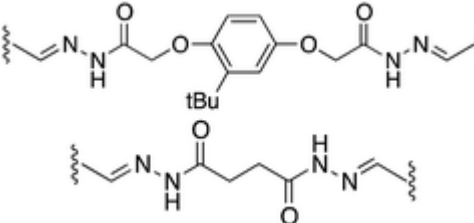
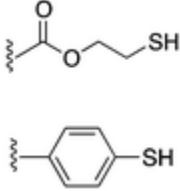
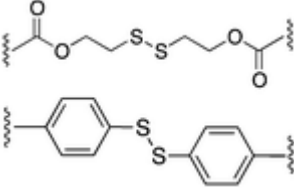
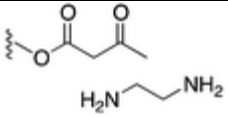
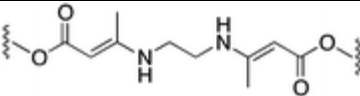
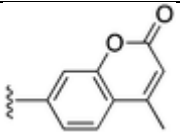
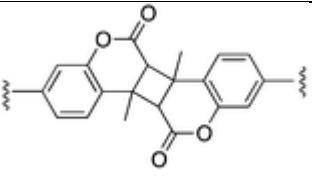
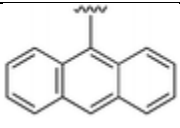
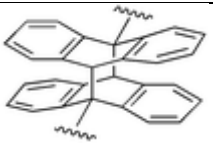
A wide array of various chemistries has been used to synthesize SCNPs. In most cases, functionalized polymers are created via post-polymerization modification techniques in dilute solution (most commonly  $<1 \text{ mg mL}^{-1}$ ) in order to promote intra-chain cross-linking as opposed to inter-chain cross-linking. Indicative of any post-polymerization modification technique, the chemistries utilized in SCNP formation must be efficient and produce no side-products.<sup>23</sup>

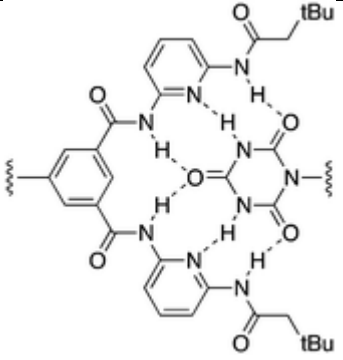
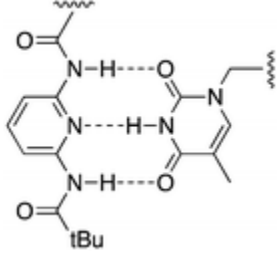
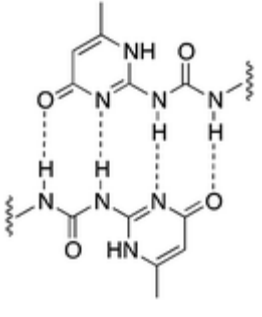
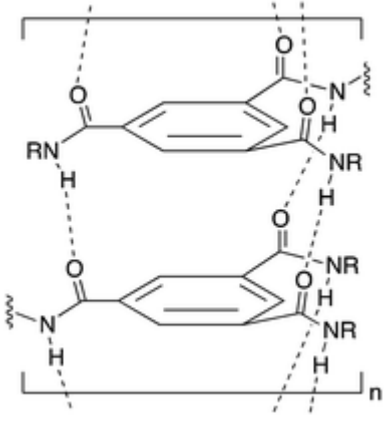
Nature takes advantage of many different orthogonal covalent cross-links (eg disulfides), dynamic covalent chemistry (eg acetal formation), and non-covalent interactions (eg hydrogen bonding, metal ligation), in folded biomacromolecules. Drawing on these ideas as inspiration, SCNPs can be created following these and similar motifs. In this section the discussion of intra-chain cross-linking chemistries will be divided into three sections: covalent, dynamic covalent, and non-covalent. Table 1.1 highlights these three themes.

*Table 1.1 A list of the numerous types of chemistry utilized in the formation of SCNPs.*

Before cross-linking	Structure of cross-link	Type of chemistry
		Friedel-Crafts alkylation <sup>24</sup>
		Thermal [4+4] cycloaddition <sup>25-28</sup>

Before cross-linking	Structure of cross-link	Type of chemistry
		Free radical polymerization <sup>29,30</sup>
		Photoinduced [4+2] cycloaddition <sup>31</sup>
		Isocyanate amine <sup>32</sup>
		Epoxide amine
		Olefin metathesis <sup>33</sup>
		Azide-alkyne "click" chemistry <sup>9,34-36</sup>
		Thiol-ene "click" chemistry <sup>37</sup>
		Oxidative polymerization of thiophene <sup>38</sup>
		Sulfonyl nitrene insertion/coupling <sup>39</sup>
		Cationic polymerization of epoxide <sup>1</sup>

Before cross-linking	Structure of cross-link	Type of chemistry
		Glaser-Hay coupling <sup>40</sup>
		Menschutkin reaction <sup>41</sup>
		Bergman cyclization <sup>42,43</sup>
		Hydrazone formation <sup>19,44</sup>
		Disulfide formation <sup>45,46</sup>
		Enamine formation <sup>47,48</sup>
		Photodimerization of coumarin <sup>7</sup>
		Photodimerization of anthracene <sup>49</sup>

Structure	Type of chemistry
	Hamilton wedge, cyanuric acid hydrogen bonding <sup>50,51</sup>
	Thymine, diaminopyridine hydrogen bonding <sup>51,52</sup>
	2-Ureido-4[1H]-pyrimidinone (UPy) hydrogen bonding <sup>53-57</sup>
	Benzene-1,3,5-tricarboxamide (BTA) hydrogen bonding <sup>2,3,6,17,58</sup>



Structure	Type of chemistry
	Dendritic self-complementary hydrogen bonding <sup>59</sup>

Before cross-linking	Structure of cross-link	Type of chemistry
		Rhodium coordination <sup>60</sup>
<p>Cu(OAc)<sub>2</sub></p>		Copper coordination <sup>5</sup>

### 1.1.1 Covalent cross-linking reactions:

Taking advantage of a benzylcyclobutene functional group, Hawker and coworkers synthesized architecturally defined SCNPs via intramolecular dimerization at high temperatures (thermal 4 + 4 cycloaddition). (Fig. 2<sup>27</sup>). As mentioned early, the formation of SCNPs is dependant on low concentrations in order to facilitate intramolecular cross-linking as opposed to intermolecular cross-linking. Hawker and coworkers reported

various syntheses of random copolymers of 4-vinylbenzylcyclobutene (BCB) and other various vinyl monomers via nitroxide mediated free radical polymerization (NMP). A continuous addition method was used in which concentrated polymer solutions were added to heated solvent, with overall concentration of 2.5 mg mL<sup>-1</sup> (0.05 M). This continuous addition method proved more efficient than typical ultra-dilute conditions as it required less solvent while still avoiding intermolecular cross-linking. Showcasing the versatility of this cross-linking chemistry, Harth and coworkers created a less synthetically challenging vinylbenzosulfone (VBS) monomer that displays similar cross-linking characteristics only at a much lower temperature than the BCB monomers.<sup>61</sup> While the electron withdrawing SO<sub>2</sub> moiety lowers the thermal barrier for the 4 + 4 cycloaddition to 150 °C, this is still too extreme for many sensitive functional groups. Also, while the continuous addition process lowers the amount of solvent required to form these SCNPs, the amount needed still precludes them from being synthesized on any kind of industrial scale. This lack in scalability is still an as of yet challenge solved by the SCNP community.

With their high efficiencies, high functional group tolerance, and mild reaction conditions, “click” reactions are an attractive route to the synthesis of SCNPs.<sup>22</sup> To date, copper-mediated azide-alkyne cycloadditions,<sup>9,34-36</sup> thiol-ene addition,<sup>37,62</sup> and amine-isocyanate addition<sup>32</sup> click reactions have all been used as routes to the creation of SCNPs. Due to their incompatibility with free radicals, alkene and alkyne “click” reactions often involve the protection/deprotection of protecting groups or accessed through post-polymerization modification methods. Another clever way around this issue is to have an external cross-linker containing the more reactive moieties.

Another interesting way around the high reactivity of alkynes to free-radicals was demonstrated by Pomoposo and coworkers by synthesizing a terminal alkyne monomer

which was created via redox-initiated RAFT polymerization.<sup>40</sup> Following the polymerization of the “naked” alkyne monomer the group used the copper-catalyzed Glaser-Hay coupling conditions to form SCNPs in appropriately dilute conditions.

While not technically considered a “click” reaction by the strict definition, O’Reily and coworkers utilized the tetrazine-norbornene reaction<sup>63</sup> in their formation of SCNPs. This reaction is both fast and quantitative, and can be carried out without the use of catalyst and at room temperature.

Another method for creating SCNPs with clean, high yielding, relatively fast, and no use of catalysts is with photochemical reactions. Popular photochemically triggered reactions for the creation of SCNPs include the photo-dimerization of coumarin,<sup>7</sup> the photo-dimerization of anthracene,<sup>64</sup> the photo-induced nitrile imine mediated tetrazole-ene cycloaddition,<sup>65</sup> and the photo-induced Diels-Alder reaction between 2,5-dimethylbenzophenone and maleimide.<sup>66</sup>

Another route to photoinduced SCNPs introduced by Zhu and coworkers was the intramolecular collapse via the photo-triggered Bergman Cyclization.<sup>42,43</sup> Possessing high photo-reactivity, the desired reactive motif had phenyl substituted triple bonds and double bonds locked in an amethylbenzoate ring. Using SET-LRP, a variety of random co-polymers were created containing enediyne monomers and butylacrylate. The resulting linear polymers were then dissolved in toluene under dilute conditions and subjected to Bergman Cyclization conditions to form the corresponding intramolecularly cross-linked polymer nanoparticles.

Another technique to intramolecular cross-linking polymers is with reactive sulfonyl nitrene moiety. This functional handle is created by the thermal extrusion of nitrogen from sulfonyl azide groups. Pu and coworkers demonstrated that SCNPs could be created with this method, albeit, at high temperatures (190 °C).<sup>39</sup> Due to the reactive

nature of sulfonyl nitrenes, the resulting cross-links that are formed are not very well defined. Similarly, Li and coworkers synthesized azido-functionalized polystyrene.<sup>67</sup> By exposing the azido group to UV radiation, a nitrene is formed, whereupon cross-links are formed via nitrene insertion. Furthermore using this chemistry, it is possible to functionalize any remaining azide groups with click-chemistry if the initial cross-linking is not carried all the way to completion.

Using olefin metathesis to synthesize polymeric nanoparticles from linear polycarbonates containing pendant vinyl groups was demonstrated by Coates and coworkers.<sup>33</sup> Copolymerizing vinylcyclohexene oxide, cyclohexene oxide, and CO<sub>2</sub> with a BDI-ligated zinc catalyst produced a polymer with the desired vinyl-functionalization. The extent of cross-linking mediated by Grubbs' catalyst is easily monitored spectroscopically.

Using styrene, Fmoc protected aminostyrene, and chloromethylstyrene, Thayumanavan and coworkers created linear polymers with various reactive functional handles.<sup>29</sup> Using post-polymerization modification techniques, the chloromethylstyrene was used in order to create polymers with pendant styrene groups, which subsequently, under dilute conditions, were polymerized using AIBN to form SCNPs. Following the intra-chain collapse of these polymers, the Fmoc group was removed which resulted in amine-functionalized nanoparticles.

While also utilizing pendant glycidyl groups, Pomposo and coworkers have reported the synthesis of SCNPs with catalytic activity.<sup>1</sup> These catalytic SCNPs were created by using the B(C<sub>6</sub>F<sub>5</sub>)<sub>3</sub> catalyzed ring-opening polymerization of glycidyl methacrylate in order to intramolecularly cross-link the linear polymers. If the polymer collapse went to completion then the remaining B(C<sub>6</sub>F<sub>5</sub>)<sub>3</sub> was trapped in the inside of the

SCNPs. Having the catalyst trapped on the inside of the SCNPs endowed the nanoparticles with a catalytic ability to polymerize tetrahydrofuran.

Using a novel propylenedioxy-thiophene functionalized polymer, Pyun and coworkers synthesized SCNPs via the oxidative polymerization of the thiophene units.<sup>38</sup> The ester linkage connecting the polystyrene backbone and the newly formed polythiophene was then cleaved in order to separate the polymers, leaving behind polymerized propylenedioxy-thiophene side chains.

The synthesis of SCNPs shape amphiphiles containing a hydrophobic polystyrene tail connected to a hydrophilic poly(2-dimethylamino)ethyl methacrylate)-based SCNPs has been reported by Zhao and coworkers.<sup>41</sup> These shape amphiphiles were created by taking the poly(DMAEMA) block and collapsing it with a quaternization reaction of the tertiary amine with 1,4-diiodobutane. These SCNPs shape amphiphiles represent multi-functional, well controlled, three-dimensional structures.

### **1.1.2 Dynamic covalent chemistry**

Dynamic covalent bonds represent an interesting route to adaptable and responsive SCNPs.<sup>68</sup> These dynamic covalent bonds are reversible in nature and, under the right conditions, can be kinetically fixed or cleaved in response to various changes in environmental conditions, such as pH, oxidation, or temperature.

Utilizing dynamic covalent acylhydrazone bonds, Fulton and coworkers synthesized SCNPs with reversible character.<sup>19</sup> Using a continuously added bis(hydrazide) cross-linker to an aldehyde functionalized polystyrene and catalytic amounts of trifluoroacetic acid (TFA), dynamic acylhydrazone bonds were formed. In

order for the SCNPs to remain intact upon isolation, the TFA had to be quenched with triethylamine in order to kinetically trap the hydrazone bonds. The cross-linking density was controlled directly by the amount of cross-linker added. The dynamic nature of these acylhydrazone bonds was proven via an exchange reaction of bis(hydrazide) cross-linker with copolymers adorned with monohydrazide. Building off of this work, Fulton and coworkers published another dynamic covalent SCNPs system using oligo(ethylene glycol) side chains to impart thermoresponsive behavior.<sup>44</sup> A solution of nanoparticles are kinetically trapped at low pH, however, upon exposure to acid and heat, the thermoresponsive nanoparticles precipitate following hydrogel formation. When the system is cooled, this process is reversed.

SCNPs that are capable of undergoing a reversible coil to globule transition have been reported by Pomposo and coworkers. These nanoparticles utilized enamine bond formation, a reversible process under acidic conditions.<sup>48</sup>

Of particular interest, in respect to this thesis, is the application of the dynamic nature of the disulfide bond. This will be elaborated on later in this document.

## **1.2 Characterization of SCNPs**

The corroboration of data provided by multiple techniques is often required to characterize SCNPs formation. The appearance or disappearance of functional groups involved in the cross-linking chemistry and changes in the size and morphology of polymer structure can be detected using the techniques described in this section. Importantly, it is often necessary to use techniques that are sensitive enough to detect

small concentrations of aggregates that may be formed by intermolecular cross-linking to prove the single molecule nature of these nanostructures.

### **1.2.1 Size exclusion chromatography**

Size exclusion chromatography (SEC) has been an invaluable tool in understanding and characterizing SCNPs. Early papers began with qualitative SEC measurements based on standards<sup>24,27</sup> and have since evolved into more quantitative measurements using multiple in-line detectors such as multiangle light scattering (MALS) and viscometry. Standalone SEC measurements are vital to understanding the behavior of SCNPs. While the molecular weight of globular SCNPs cannot be accurately measured using linear polymer standards, SEC provides other valuable data. An in depth study performed by Harth and coworkers provides an excellent example.<sup>27</sup> In this work random copolymers of styrene and vinylbenzocyclobutane (BCB) were used to create a family of SCNPs. The molecular weight of these linear polymers was measured using SEC with polystyrene standards. Upon collapse, SEC measurements showed that all of their polymers had an increase in retention time and a decrease in apparent molecular weight. Since the BCB cross-linking does not produce any side products, the decrease in apparent molecular weight can be directly attributed to a decrease in hydrodynamic volume, which is principally what is measured by traditional SEC. Additionally, the authors used the change in apparent molecular weight to calculate the decrease in hydrodynamic volume. This data was corroborated by dynamic light scattering (DLS) measurements. <sup>1</sup>H NMR was also used to confirm the complete disappearance of the BCB moiety, confirming spectroscopically that changes in solution volume can be attributed to this chemistry. Often, a decrease in polydispersity index ( $\mathcal{D}$ ) is observed via SEC when a chain transitions from a linear coil

to a SCNP. In a computational study,<sup>69</sup> Pomposo et al. examined SCNP formation assuming theta conditions for all samples so that a SCNP can be treated as a small linear polymer with a comparable hydrodynamic volume. They found this decrease in polydispersity index arises from the standard SEC calibration equation ( $M_{app} = cM\beta$ ), where the apparent molecular weight uses a scaling factor derived from a hydrodynamic radius equation. This research illustrates the merits in studying the complex physics of the intra-chain cross-linking of polymers via various mathematical and computational methods. Full three-dimensional modeling of these materials is still needed in order to include a wider range of collapsing chemistries and represents an open area of research opportunity. Even though quantitative data cannot be collected directly from standalone SEC, it still provides an important tool in characterizing SCNPs. Specifically, it is used to observe a qualitative decrease in hydrodynamic radius, and also provides insight regarding intramolecular vs. intermolecular coupling.

### **1.2.2 Light scattering**

The principles of light scattering were established by prominent scientists such as Einstein,<sup>70</sup> Raman,<sup>71</sup> Debye,<sup>72</sup> and Zimm<sup>73</sup> at the beginning of the 20th century. It has since been the basis of one of the most useful forms of absolute characterization of macromolecular suspensions and solutions. Light scattering is an absolute method; the molar mass of large macromolecules is calculated based on first principles and consequently does not produce data relative to standards.<sup>74</sup> In regard to SCNPs, dynamic light scattering (DLS) and multiangle light scattering (MALS) are both indispensable characterization techniques. Work from our laboratory has shown that using a MALS



detector in-line with an SEC can prove that the molecular weight is consistent from parent polymer to SCNP.<sup>49,75</sup> Several groups have also used DLS as a method for confirming this result.<sup>37,66,76</sup>

### **1.2.3 Viscometry**

Another valuable technique in the characterization of SCNPs is solution viscometry. A particle's intrinsic viscosity is related to its molecular weight by the Mark–Houwink equation (Equation 1). Using the intrinsic viscosity measurement gathered by the viscometer and the molar mass data from MALS, “K” and “a” coefficients can be calculated which relate to polymer conformation and the interaction between polymer and solvent. Viscometry is also useful in calculating hydrodynamic volume ( $V_h$ ) which can further be used to calculate hydrodynamic radius ( $R_h$ ) via the Einstein–Simha Relation (Equation 2 and Equation 3).

$$[\eta] = KM^a$$

*Equation 1 Mark-Houwink Equation*

$$V_h = M[\eta]/(2.5N_A)$$

*Equation 2 Einstein-Simha Relation for hydrodynamic volume ( $V_h$ )*

$$R_h = (3V_h/4\pi)^{1/3}$$

*Equation 3 Einstein-Simha Relation for hydrodynamic radius ( $R_h$ )*

$[\eta]$  is intrinsic viscosity,  $M$  is molar mass,  $V_h$  is hydrodynamic volume,  $N_A$  is the Avagadro constant, and  $R_h$  is hydrodynamic radius. Hawker et al. used viscometric measurements to characterize the formation of SCNPs synthesized using intra-chain isocyanate chemistry (Fig. 5).<sup>32</sup> The intrinsic viscosity of a polymer decreases as the degree of intramolecular cross-linking increases. In this case the authors used two polymer samples: 100 kDa, 150 kDa, and their SCNP counterparts, which were formed using an external diamine crosslinker. As expected, the higher molecular weight linear polymer had greater intrinsic viscosity than the lower. However, for the SCNPs, despite a 50% increase in molecular weight compared to the parent polymers, the intrinsic viscosities of both samples decreased, and were similar to one another. This is consistent with the prediction made by Einstein; that the intrinsic viscosity of a constant density sphere is independent of its molecular weight, i.e.  $5/2$  divided by the sphere density.

#### **1.2.4 Nuclear Magnetic Resonance Spectroscopy (NMR)**

The formation of SCNPs can be confirmed by monitoring the appearance or disappearance of various signals corresponding to characteristic moieties (or protons in the case of  $^1\text{H}$  NMR) in external and internal cross-linking chemistries. However, other laboratories have shown other useful NMR techniques in monitoring the globule to SCNP transition. By using spin-spin relaxation time ( $T_2$ ), Zhao and coworkers were able to observe the formation of SCNPs via the intramolecular photodimerization of coumarin moieties. Molecular motion in macromolecules directly alters the spin-spin relaxation time which is what allowed Zhao and coworkers to monitor SCNP formation.<sup>7</sup> They saw that with an increase in photodimerization there was an increase in the spin-spin

relaxation time. This is caused by the reduced mobility of the chain segments as they undergo intramolecular cross-linking.

Another interesting and useful NMR technique is the use of DOSY experiments to determine the diffusion coefficient of polymers, which is inversely proportional to hydrodynamic volume. Loinaz and coworkers demonstrated the utility of DOSY experiments by measuring the diffusion coefficient of poly(N-isopropylacrylamide) based thermoresponsive SCNPs in solution.<sup>34</sup> They saw that with an increase in intramolecular collapse there was an increase in the diffusion coefficient, thus leading to further evidence of the formation of collapsed SCNPs.

## **CHAPTER 2**

### **DYNAMIC DISULFIDE POLYMER NANOPARTICLES**

#### **2.1 Introduction**

In analogy to nature, the fabrication of functional nanodevices from well-defined discrete macromolecules remains an important yet elusive research objective. Single-chain polymer nanoparticles (SCNPs)<sup>2,7,9,19,25,27,29,32-35,43,51,53-55,58,59,61,69,77-85</sup> represent a significant step towards these ends. This technique is predicated on the concept that in

sufficiently dilute polymer solutions (concentrations below the overlap concentration,  $c^*$ ), inter-chain interactions are minimized because the dimensions of individual chains are smaller than the average distance between the chains. Thus, triggering a cross-linking reaction under these conditions will result in intra-chain, rather than inter-chain coupling, facilitating a change in conformation from an expanded coil to a collapsed globule or particle.

While only a small number of reports on this topic have appeared to date, this research area is growing rapidly. Based on reports currently in the literature, it is clear that this technique is general and can be applied to a variety of polymer scaffolds utilizing a host of cross-linking chemistries. Most involve some type of covalent linkage to induce the chain collapse process. This is effected either by chemistry built directly into the polymer (i.e. benzocyclobutane coupling<sup>25,27</sup> or azide–alkyne click chemistry,<sup>9,34,35</sup> or using an externally added cross-linking agent to collapse an appropriately decorated polymer (a dithiol coupled with an alkene functionalized polymer,<sup>86</sup> a diamine coupled with an isocyanate functionalized polymer.<sup>32</sup> These pioneering examples show that architecturally defined nano-objects can be prepared in a facile manner. Given the permanent nature of the covalent cross-links, however, the nano-particles reported in these instances lack any adaptability or sensitivity to their environment, which could be important in various applications.

Taking further inspiration from nature, a few reports demonstrate the use of supramolecular<sup>2,50,51,53-55,58,59,78</sup> or dynamic covalent linkages<sup>19</sup> to form metastable “folded” polymer particles that are reversibly held in an adaptable conformation. The Barner-Kowollik group recently developed a method to make alpha, omega functionalized folded polymer structures which can adopt cyclic<sup>50</sup> or figure-8 type conformations.<sup>51</sup> Some beautiful work from the Meijer lab<sup>2</sup> displays how this concept can

be used to make ordered assemblies in water that exhibit enzyme-like activity. A recent example from the Scherman group<sup>78</sup> shows that host guest chemistry is also quite effective in this regard. The first example of dynamic covalent chemistry applied to SCNP synthesis, published by Fulton and Murray,<sup>19</sup> demonstrates the potential of this method for making adaptable “intelligent” nanosystems. Two excellent reviews have recently been written on this emerging field.<sup>20,21</sup>

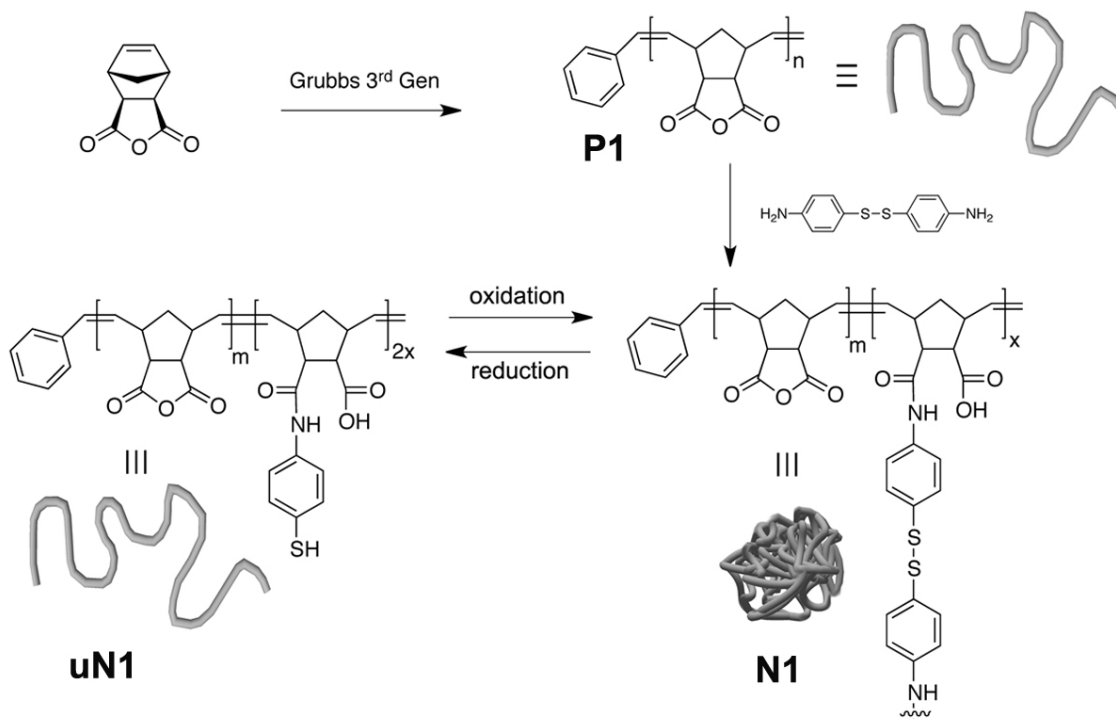
Our lab is interested in combining aspects of both covalently fixed and metastable SCNPs in an effort to carefully fold single chains into precisely defined conformations, similar to what is observed in nature. For this reason, we chose to investigate the use of disulfide bridges as reversible linkages to control the conformation of single chains in solution. Ubiquitous in nature and well studied in the dynamic covalent chemistry literature,<sup>87,88</sup> we report here that disulfide bridges provide a robust system for “folding” and “unfolding” single chains via reductive or oxidative stimuli.

## **2.2 Results and discussion**

### **2.2.1 Polymer design**

While many avenues exist for the incorporation of thiols or disulfides into synthetic polymer chains,<sup>45,89-91</sup> we envisioned the happiest route would be one where all starting materials are commercially available. This alleviates the need for complicated monomer synthesis or thiol protecting chemistry, and would therefore be amenable to scale up. This design is outlined in Scheme 1. Rather than directly incorporate thiols into the polymer, we adopted a strategy where the polymer chain is decorated with a reactive functional group, then folded by the introduction of a difunctional cross-linker that contains a premade disulfide bond (in this case *p*-aminophenyl disulfide). In our initial studies, we

chose to work with poly(norbornene-*exo*-anhydride) (polymer P1), synthesized via ROMP using third generation Grubbs catalyst as an initiator. In this case every monomer unit along the backbone is reactive, which allows us to vary the degree of collapse



*Scheme 2.1 Synthetic scheme for dynamic covalent SCNPs.*

that occurs during nanoparticle formation simply by varying the amount of difunctional cross-linker added. This method of using a single polymer sample to make several batches of nanoparticles lessens ambiguities that would be introduced due to heterogeneities between different samples of polymer.

### **2.2.2 SEC characterization via standard calibration**

As is typical in the SCNP literature,<sup>69</sup> we characterized the coil to particle transition by SEC. As the intramolecular cross-linking reaction progresses, the coil collapses, reducing in hydrodynamic volume and thus increasing the sample's retention time. Figure 2.1 shows

a series of SEC traces for a sample of polymer P1 and its corresponding nanoparticles N1 after various extents of intramolecular cross-linking. As expected, an increase in retention time is witnessed as increasing amounts of cross-linker are introduced. Interestingly, this behavior shows a limiting value at around 30% cross-linking. Apparently at this point the chain is collapsed to an extent where further penetration and reaction of the diamine is hindered, consistent with previous findings in this field.<sup>19</sup>

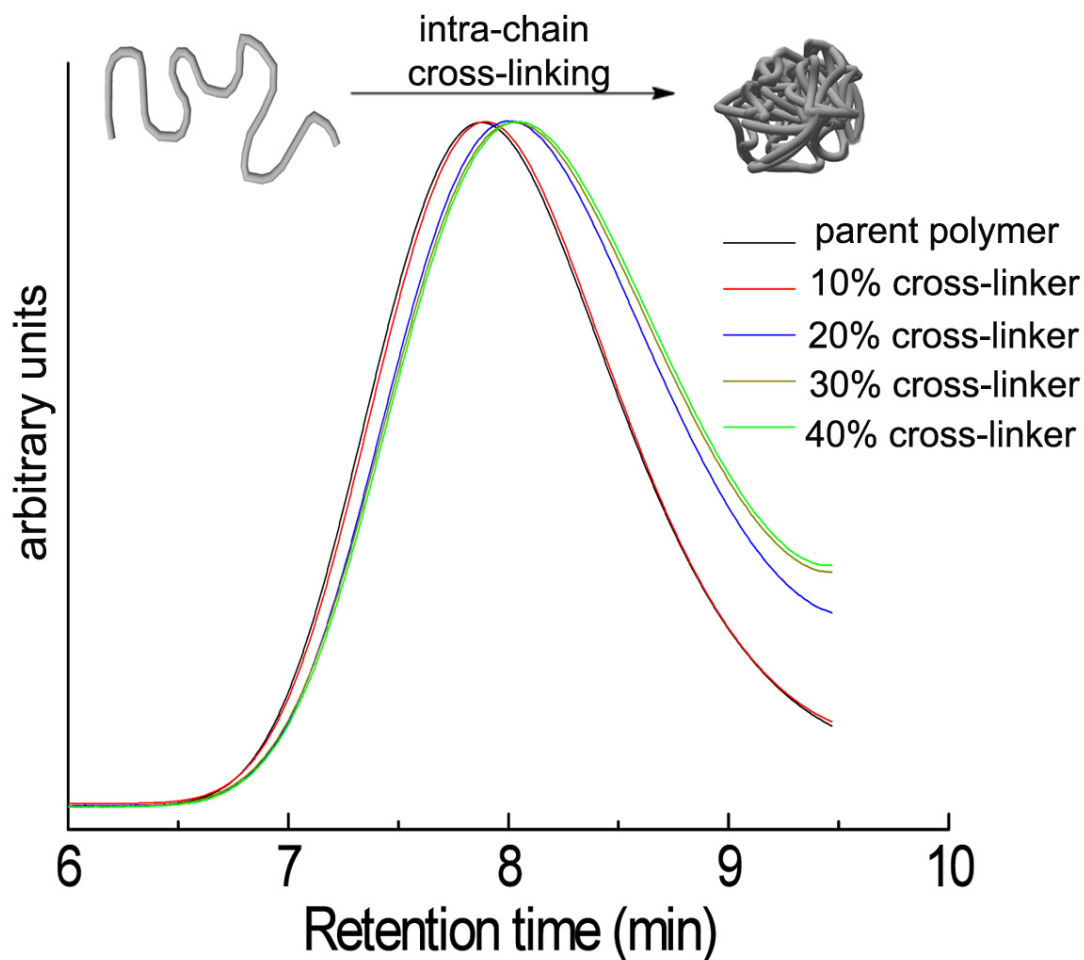


Figure 2.1 SEC before and after intramolecular cross-linking.

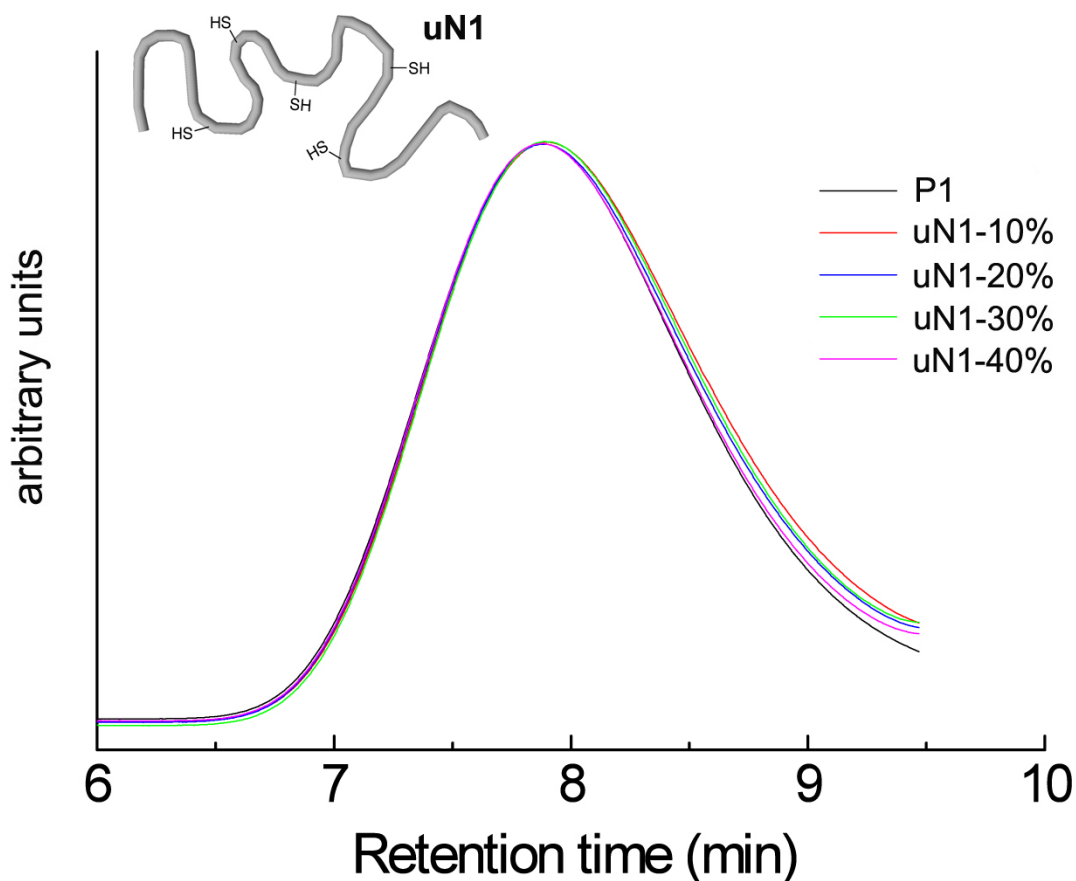


Figure 2.2 SEC traces of unfolded polymer uN1 compared to parent polymer P1.

Once we confirmed the folding of the chains into particles via SEC, dithiothreitol (DTT) was introduced to reduce the disulfide linkages to the corresponding thiols,<sup>45,87-89</sup> unfolding the N1 particles back to their original coil conformation (the notation uN1 is used here to indicate “unfolded N1”). This transition was confirmed via decreased SEC retention time, signifying an increase in hydrodynamic volume (Figure 2.2). Regardless of the amount of cross-linker originally added, on treatment with DTT the chains re-expand to their original hydrodynamic volume (based on retention time) when compared to the parent polymer P1. Interestingly, even at these low concentrations, a small amount of intermolecular coupling between chains due to thiol exchange is witnessed as evident in a



small peak at very low retention time, indicating the presence of much larger, high molecular weight species (Figure 2.6)

After reductive cleavage of the disulfide linkages, the resulting thiol functionalized polymer was re-folded via oxidation in the presence of catalytic amounts of  $\text{FeCl}_3$ . This results in a shift to longer SEC

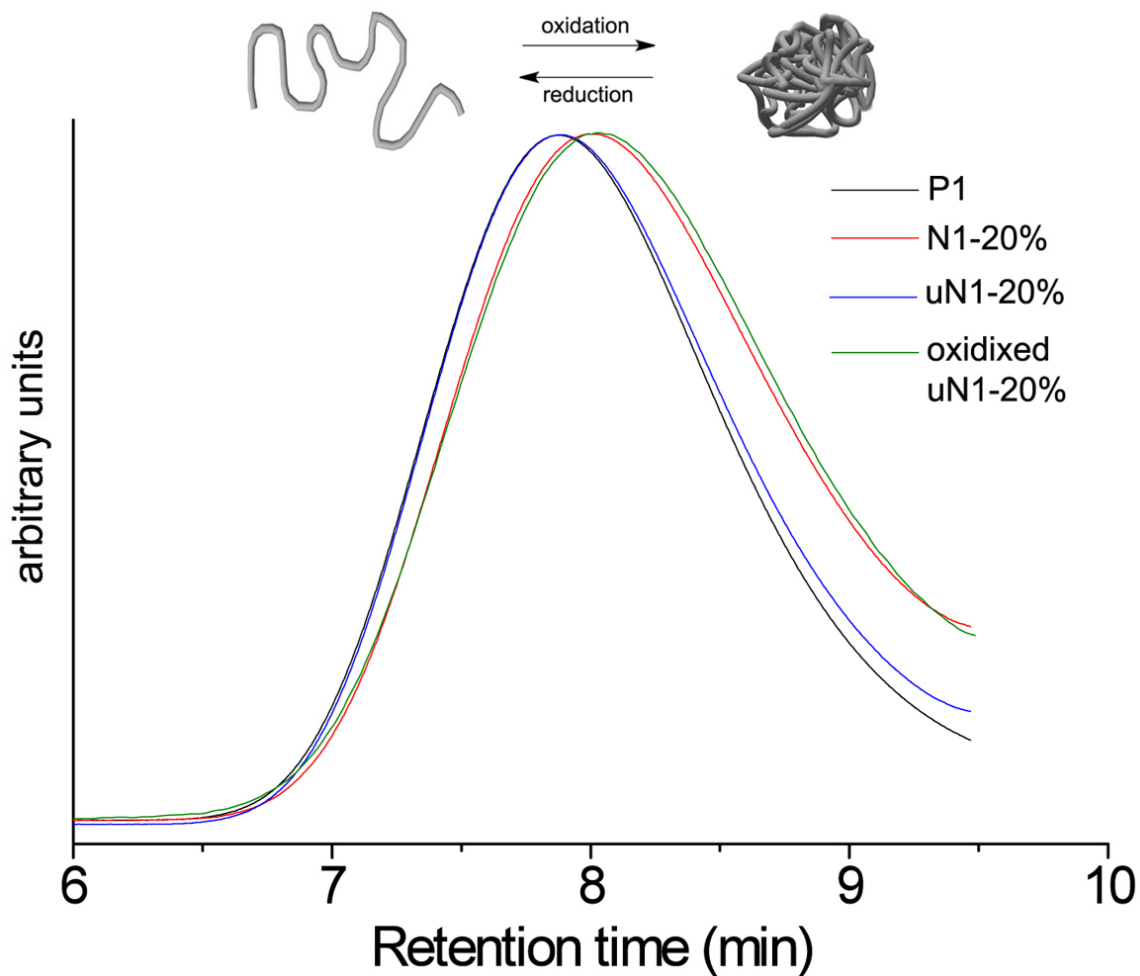


Figure 2.3 SEC traces of showing the initial folding of P1 to N1, unfolding into uN1 following disulfide reduction, and refolding after thiol oxidation.

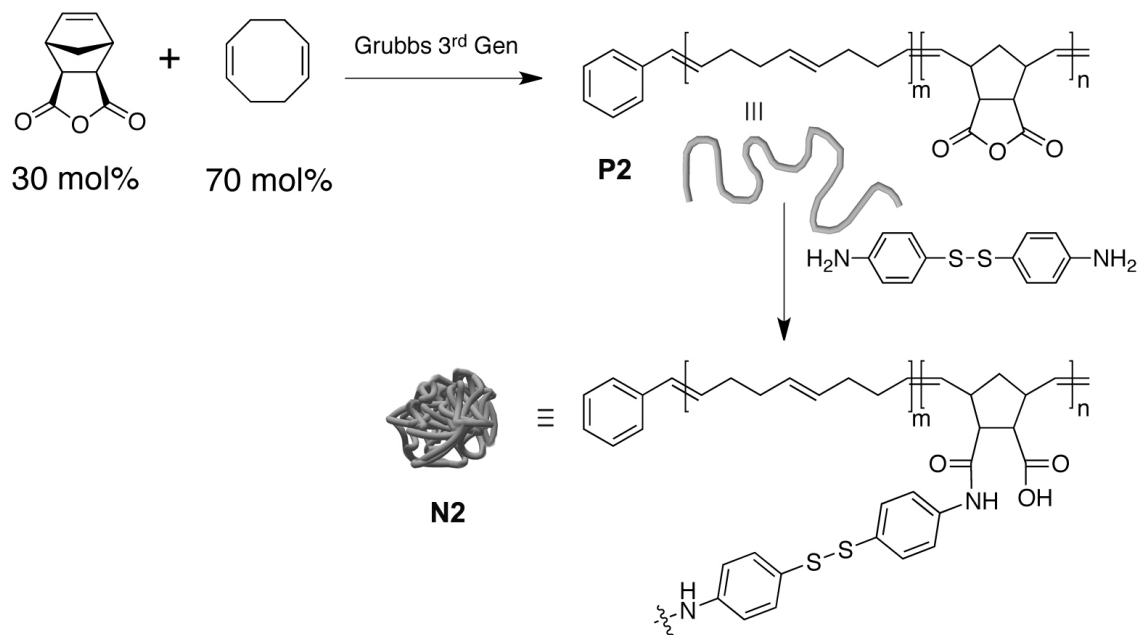
retention time, once again indicating a reduction in hydrodynamic volume with the reformation of the intramolecular disulfide bridges. Fig. 3 shows overlays of the chromatograms for the N1-20% nanoparticle, the corresponding expanded coil uN1 after

reductive disulfide cleavage, and the re-collapsed nanoparticle post thiol oxidation. The chromatogram for P1 is included for reference. These data highlight the efficacy of this chemistry for carefully controlling the solution conformation of individual synthetic chains.

### **2.2.3 Characterization via triple detection SEC**

Dynamic light scattering (DLS) is often used as a tool to characterize SCNPs as a way to confirm both the change in hydrodynamic volume and the well-defined three-dimensional architecture. DLS does have some limitations in this regard, however. Most significantly, the results will always be weighted towards the larger particles present. There is no way to separate between single-chain particles and aggregates of a few chains, which scatter more intensely than the unimolecular particles, skewing the measured particle size. We thought it would be extremely valuable to be able to characterize the size and conformation of each slice of the size exclusion chromatogram as it elutes from the columns. At the same time we thought it would be useful to use absolute molecular weight characterization, rather than relative molecular weight, to show that observed change in retention time is indeed due to a conformational change in chains of a known molecular weight. To accomplish both of these, we coupled our SEC to an external MALS detector and a differential viscometer.

For this set of experiments we adjusted the structure of the polymer used: here we incorporate a defined amount of anhydride units and render the rest of the chain unreactive towards the difunctional cross- linker. This was accomplished simply by replacing some of the



*Scheme 2.2 Synthesis of a copolymer with a discrete amount of reactive comonomer to control the extent of possible intramolecular cross-linking.*

*Table 2.1 MALS and viscometric data for P2 and N2*

	Peak retention time (min) <sup>a</sup>	M <sub>w</sub> <sup>a</sup> (KDa)	PDI <sup>a</sup>	[η] <sup>b</sup> mL g <sup>-1</sup>	R <sub>h</sub> <sup>b</sup> (nm)
<b>P2</b>	17.8	50.1	1.22	13.9	4.5
<b>N2</b>	18.8	59.3	1.32	8.7	3.9

<sup>a</sup> SEC data collected at 40 °C in THF from MALS. <sup>b</sup> SEC data collected at 40 °C in THF from viscometer.

norbornene-*exo*-anhydride with cyclooctadiene (COD) as a comonomer (Scheme 2.2). Doing so allows us to reasonably predict how much mass should be added during the folding reaction without the possibility of over functionalization that is present in the poly(norbornene anhydride) homopolymer.

Table 1 shows the results from the SEC-MALS-viscometry experiment. After folding, the characteristic shift to a longer retention time is observed as expected. Additionally, the absolute molecular weight from the MALS detector increases as is expected with the addition of the cross-linker. The viscometric data shows a decrease in intrinsic viscosity and hydrodynamic radius, consistent with the conformational change in going from a coil to a particle and in agreement with theory and other literature examples.<sup>32</sup> Additionally, TEM images of SCNP N2 drop cast on carbon coated copper grids show well-defined particles with dimensions in agreement with the viscometric data (Figure 2.4).

To highlight the effectiveness of this technique in determining the difference between single-chain and multi-chain behavior, we repeated the intra-molecular cross-linking reaction for an extended reaction time with a slight excess of cross-linker to encourage some amount of intermolecular coupling. Figure 2.5 shows an overlay of the MALS and refractive index detector traces for this experiment. While the RI detector shows only a single peak that can be attributed to single-chain particles, the MALS detector shows two peaks of nearly equal intensity. The peak at a shorter retention time is a result of strongly scattering multi-chain aggregates, which are not seen in the RI detection trace. For this sample, relying solely on traditionally calibrated SEC would not have revealed the presence of the larger aggregates while DLS without chromatographic separation would have likely over estimated the particle  $R_h$ .

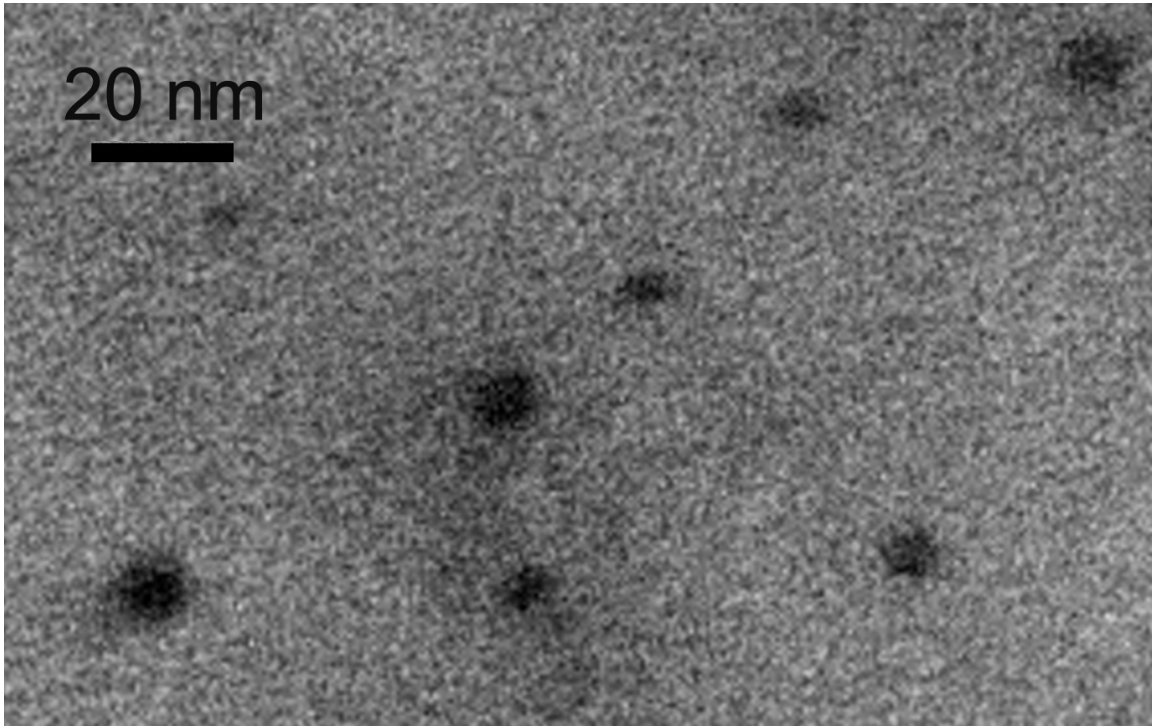


*Figure 2.4 Representative TEM image of single-chain nanoparticles N2.*

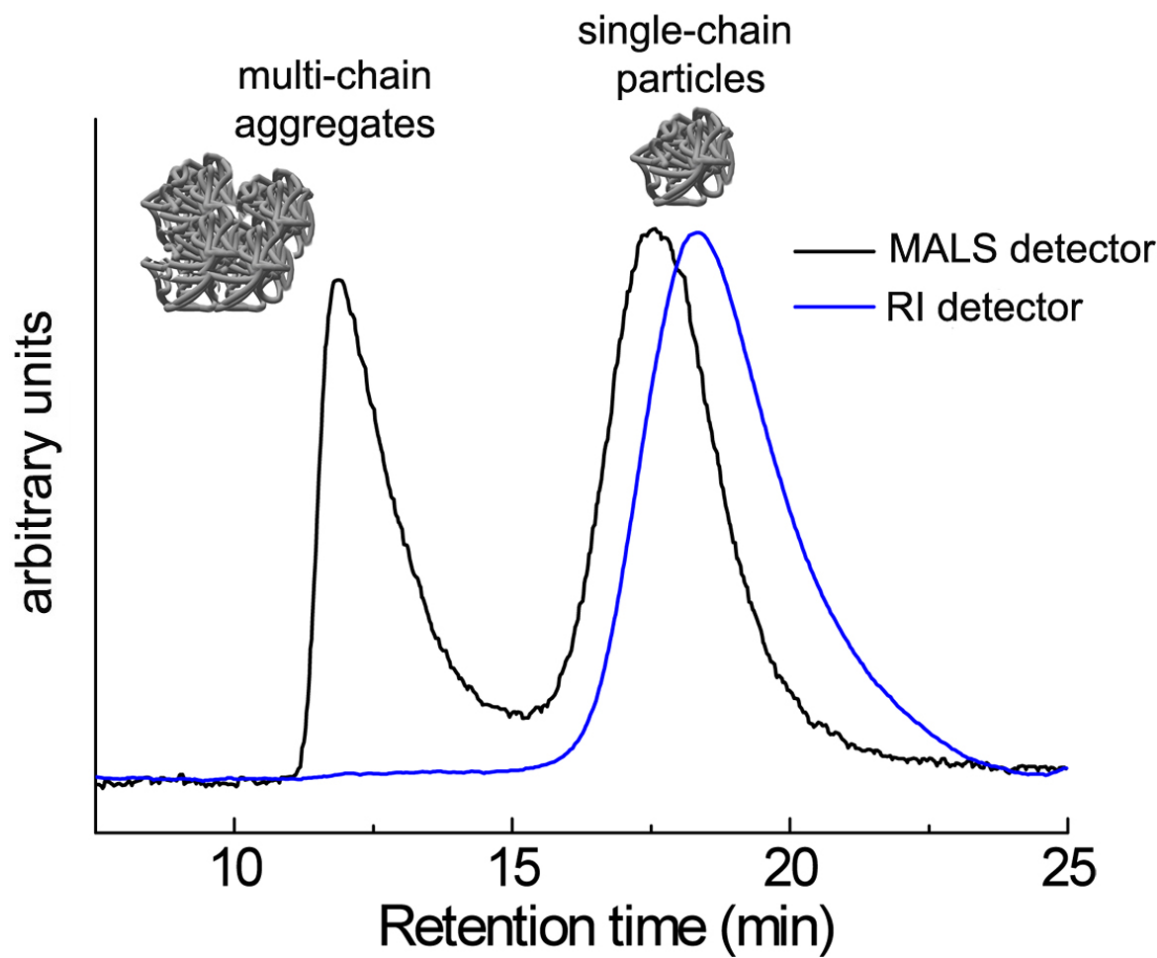


Figure 2.5 MALS and RI detection traces for SEC of N2 and excess cross-linker. Although the concentration of multi-chain aggregates has a negligible impact on the RI trace, these larger particles scatter quite intensely as seen in the MALS trace.

### 2.3 Conclusions

We demonstrate here the utility of disulfide bridges in the fabrication of dynamic covalent single-chain polymer nanoparticles. Increasing the number of disulfide bridges results in tighter folding of the polymer chain resulting in a longer retention time and therefore a smaller hydrodynamic radius. Reduction of the disulfide groups allows the particle to unfold into a coil; re-oxidation of the resultant thiols causes the coil to refold into a particle. We also demonstrate SEC coupled to a multi angle light scattering detector and differential viscometer as an excellent way to characterize single-chain

polymer nanoparticles. Our efforts in this area are ongoing, with particular interest in using multiple, orthogonal interactions to precisely program the conformations of single polymer chains.

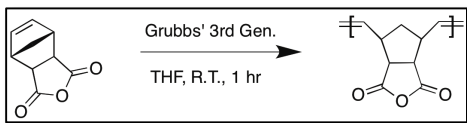
## **2.4 Experimental Section**

### **2.4.1 General Methods.**

Reagents were purchased from Aldrich and used as received except for cis-5-norbornene-exo-2,3-dicarboxylic anhydride, which although commercially available was synthesized from the endo isomer (purchased from Acros) according to the literature.<sup>92</sup> Size exclusion chromatography (SEC) was performed on a Tosoh EcoSEC dual detection (RI and UV) GPC system coupled to an external Wyatt Technologies miniDAWN Treos multi angle light scattering (MALS) detector and a Wyatt Technologies ViscoStarII differential viscometer. Samples were run in THF at 40 °C at a flow rate of 0.35 mL/min. The column set was two Tosoh TSKgel SuperMultipore HZ-M columns (4.6x150 mm), one Tosoh TSKgel SuperH3000 column (6x150mm) and one Tosoh TSKgel SuperH4000 column (6x150mm). (Note: SEC experiments on the poly(norbornene anhydride) homopolymer P1 and nanoparticles N1 were run using only the SuperMultipore columns without the external detectors). Increment refractive index values ( $dn/dc$ ) were calculated online assuming 100% mass recovery (RI as the concentration detector) using the Astra 6 software package (Wyatt Technologies) by selecting the entire trace from analyte peak onset to the onset of the solvent peak or flow marker. Absolute molecular weights and molecular weight distributions were calculated using the Astra 6 software package. Relative molecular weights were obtained vs. polystyrene standards (PStQuick MP-M, Tosoh) and calculated using the EcoSEC software package (Tosoh). Intrinsic viscosity

( $[\eta]$ ) and viscometric hydrodynamic radii ( $R_h$ ) were calculated from the differential viscometer detector trace and processed using the Astra 6 software. Transmission Electron Microscopy (TEM) images were recorded using a Zeiss LEO 922 $\Omega$  operating at 120kV with a Gatan Multi-scan bottom mount digital camera. Samples were prepared by drop casting 1.5  $\mu$ L of a nanoparticle solution ( $1.8 \times 10^{-4}$  mg/mL) on to Formvar carbon film coated 300 square mesh copper grids.  $^1\text{H}$  NMR (400 MHz) spectra were recorded on a Varian Associates Mercury 400 spectrometer. Solvents ( $\text{CDCl}_3$  or  $d_8$ -THF) contained 0.03% v/v TMS as an internal reference, chemical shifts ( $\delta$ ) are reported in ppm relative to TMS. Peak abbreviations are used as follows: s=singlet, d=doublet, t=triplet, m=multiplet, br=broad. Infrared spectra were recorded on a Thermo Scientific Nicolet iS10 FT-IR spectrometer with Smart iTR ATR accessory.

#### **2.4.2 Synthesis of poly(norbornene-exo-anhydride):**

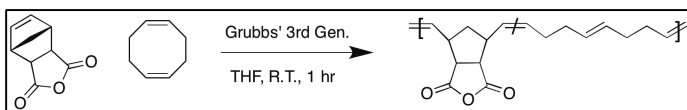


To a 100 mL three neck RBF was added Grubbs' third generation catalyst (0.009 g, 0.01 mmol) and 4 mL of dry THF. The solution was degassed via nitrogen purge (30 minutes). Norbornene-exo-anhydride monomer (0.492 g, 0.003 mmol) was dissolved in 6 mL of dry THF and added to an addition funnel and degassed via argon purge for ten minutes. The monomer solution was then added dropwise over 15 minutes into the flask with medium stirring at 25  $^{\circ}\text{C}$ . The reaction was run for one hour then quenched with excess ethyl vinyl ether. The polymer was then purified via precipitation into cold, dry hexanes and isolated as slightly grey powder  $^1\text{H}$  NMR (400 MHz,  $\text{CDCl}_3$ ):  $\delta$  ppm 9.15- 8.80 (br s), 8.05 (m), 5.75-5.63 (m), 5.54-5.52 (m), 5.39-5.25 (br m), 5.13 (s), 4.38-4.25 (br m),



4.21-3.83 (br m), 3.75-3.63 (br m), 2.5 (m), 2.25 (m), 2.21-1.62 (br m). IR  $\nu$  ( $\text{cm}^{-1}$ ) 2933 (br CH), 1858 & 1770 (anhydride C=O), 908 (=C-H bending) SEC (THF vs. polystyrene)  $M_w = 31.8$  kDa, PDI = 1.39.

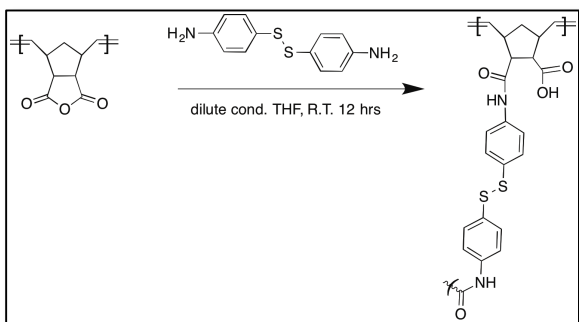
### **2.4.3 Poly(cyclooctadiene-co-norbornene-*exo*-anhydride):**



Cyclooctadiene (1.436 g, 13.3 mmol) was dissolved in 86 mL

of dry THF and added to a dry 250 mL three neck flask sealed with rubber septa. The solution was degassed via nitrogen purge for 30 minutes. Norbornene-*exo*-anhydride (0.935 g, 5.7 mmol) was dissolved in 5 mL of dry THF solution, which was degassed for 5 minutes via argon purge. Grubbs' first generation catalyst (0.034 g, 0.041 mmol) was dissolved in 0.5 mL of dry THF and was added to the stirring COD solution via gas tight syringe. Once the catalyst was added the norbornene-*exo*-anhydride monomer was added dropwise to the reaction over the course of 5 minutes. This helps circumvent the tendency for alternation previously reported for these two monomers.<sup>93</sup> The reaction was run for two hours then quenched with excess ethyl vinyl ether. The polymer solution was purified via precipitation into cold, dry hexanes yielding a gray adhesive gum.  $^1\text{H}$  NMR (400 MHz,  $\text{CDCl}_3$ ):  $\delta$  ppm 6.29 (s), 3.75 (t), 3.45 (s), 2.95 (s), 1.85-1.79 (br m), 1.65 (d) 1.45 (d), 1.25 (t). IR  $\nu$  ( $\text{cm}^{-1}$ ) 2933 (br CH), 1858 & 1770 (anhydride C=O), 908 (=C-H bending) SEC:  $M_w = 50.1$  kDa (MALS,  $dn/dc = 0.1667$ ); PDI = 1.22 (MALS)

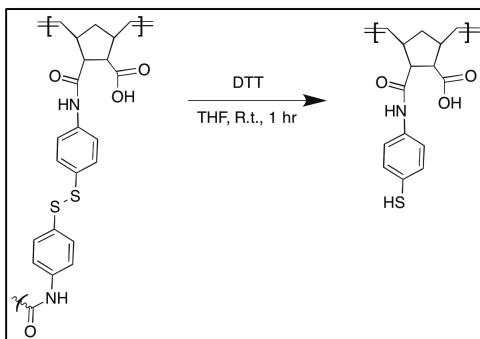
#### 2.4.4 General Crosslinking Procedure (N1 and N2):



Polymer was dissolved in dry THF under dilute conditions (1 mg/mL). The solution was then added to a dry three-neck flask capped with rubber septa. The solution was degassed via nitrogen purge

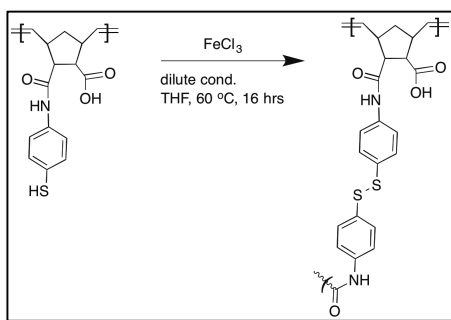
for 30 minutes. Depending on the polymer being cross-linked, varying molar percentages of 4-aminophenyl disulfide was added to the stirring polymer solution via a gas tight syringe (for N1 cross-linking percentages reported were calculated based on the percentage of backbone anhydride units consumed. For N2 0.5 equivalents of 4-aminophenyl disulfide per anhydride unit was used). The solutions were stirred at 25 °C for 12 hours, aliquots taken for direct SEC analysis, then purified by dialysis against THF (MWCO = 3500) for 18 hours and isolated via solvent evaporation. Nanoparticles remain stable in solution for weeks based on repeated SEC measurements. N1: IR  $\nu$  ( $\text{cm}^{-1}$ ): 3356 (carboxylic -OH), 2917 (br -CH), 1683 (amide C=O), 820 (ArH bending). N2:  $^1\text{H}$  NMR (400 MHz, d-THF):  $\delta$  ppm 7.30-7.00 (br m, ArH), 6.65-6.37 (br m, ArH), 5.47 (s), 5.29-5.13 (br d), 4.13 (t), 3.70-3.63 (m), 2.25 (t), 2.12-1.71 (br m), 1.17 (s). IR  $\nu$  ( $\text{cm}^{-1}$ ): 3356 (carboxylic -OH), 2917 (br -CH), 1683 (amide C=O), 820 (ArH bending). SEC:  $M_w$  = 50.1kDa (MALS  $dn/dc$  = 0.1526); PDI = 1.22 (MALS).

### **2.4.5 General Unfolding Procedure:**



The SCNPs (N1 or N2) were dissolved in dry THF under dilute conditions (1 mg/mL) and added to a dry three neck flask capped with rubber septa. The solution was degassed via nitrogen purge for 30 minutes. A large excess (3 mmol) of dithiothreitol (DTT) in THF was added to the SCNP solution and stirred at 25 °C for 1 hour. Aliquots were taken for direct SEC analysis, followed by dialysis against THF for 18 hours (MWCO = 3500) and isolation via solvent evaporation. N1: IR  $\nu$  ( $\text{cm}^{-1}$ ): 3353 (-OH), 3300 (-OH), 2230 (-SH), 2090 (-SH), 1644 (amide C=O), 819 (ArH bending). uN2  $^1\text{H}$  NMR (400 MHz, d- THF):  $\delta$  ppm 10.75 (s), 7.50-6.95 (br m), 6.59-6.37 (br m), 5.25 (s), 4.13 (t), 3.74-3.65 (br m), 2.45-2.31 (br s, -SH), 2.25 (t), 2.00-1.69 (br m), 1.18 (s). IR  $\nu$  ( $\text{cm}^{-1}$ ): 3353 (-OH), 3300 (-OH), 2230 (-SH), 2090 (-SH), 1644 (amide C=O), 819 (ArH bending).

#### 2.4.6 General Disulfide Oxidation (refolding) Procedure:



The unfolded SCNPs (uN1) were dissolved in dry THF under dilute conditions (1 mg/mL) and added to a three neck flask capped with rubber septa. A catalytic amount of FeCl<sub>3</sub> in dry THF and was added via a gas tight syringe. The solution was

stirred at 60 °C for 12 hours. Aliquots were then taken from this solution for direct SEC analysis.

#### 2.4.7 Supplemental Figures

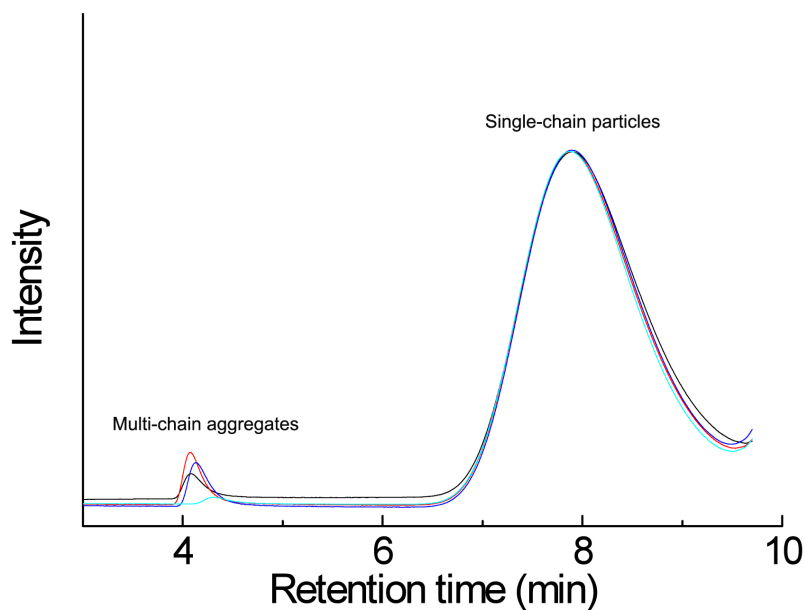


Figure 2.6 Full SEC trace for unfolded chains uN1, showing a small amount of intermolecular particle-particle coupling (see previous text for details).

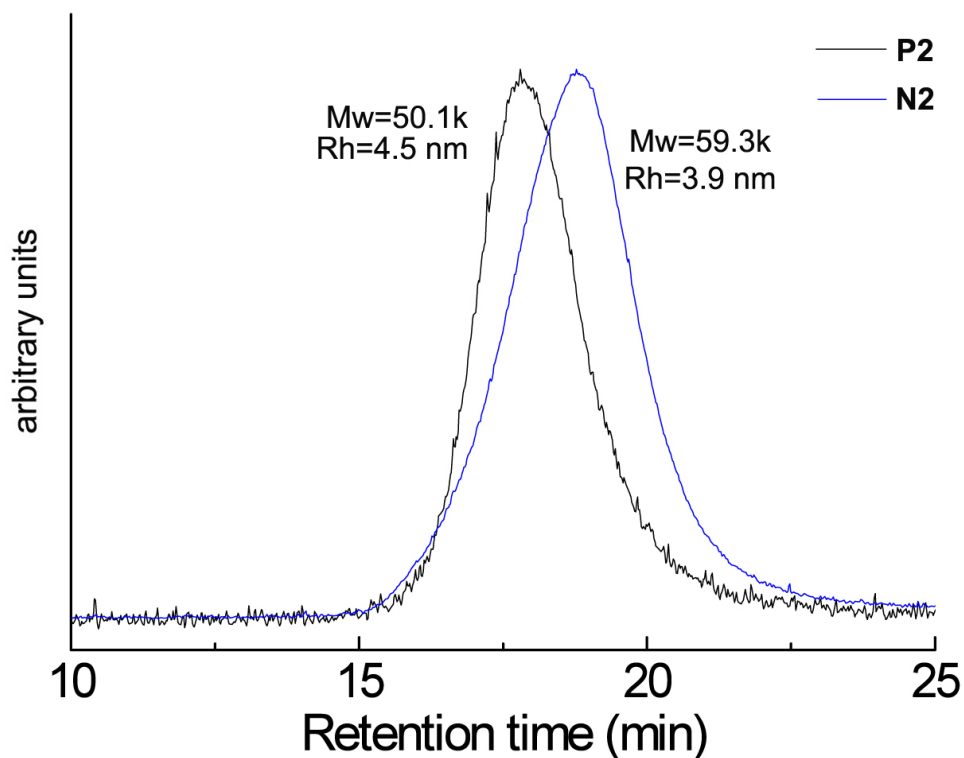


Figure 2.7 SEC overlay of MALS detector trace for N2 and P2 for which data in Table 2.1 MALS and viscometric data for P2 and N2 (see above) was derived.

## 2.4.8 Example Spectra

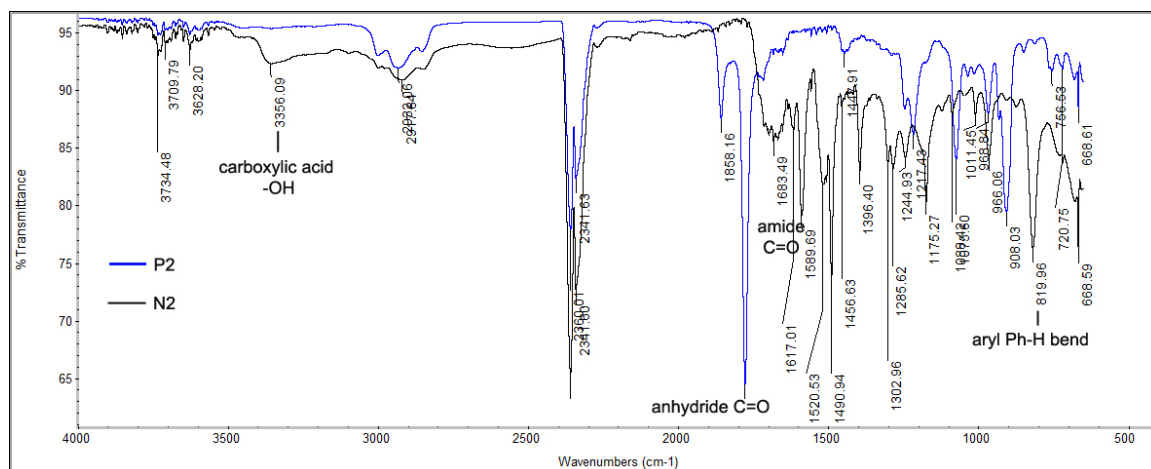


Figure 2.8 IR overlay for P2 and N2. Addition of cross-linker is confirmed by the shift in the anhydride carbonyl stretch to lower wavenumber, as well as the appearance of the Ph-H bend and the carboxylic acid -OH.

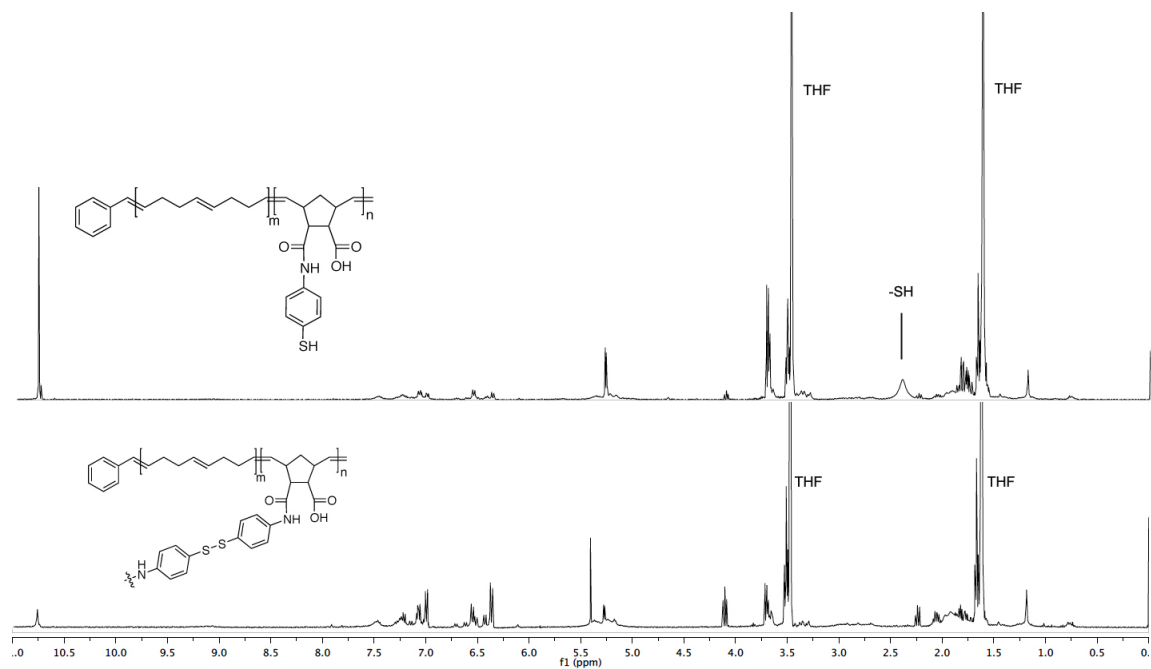
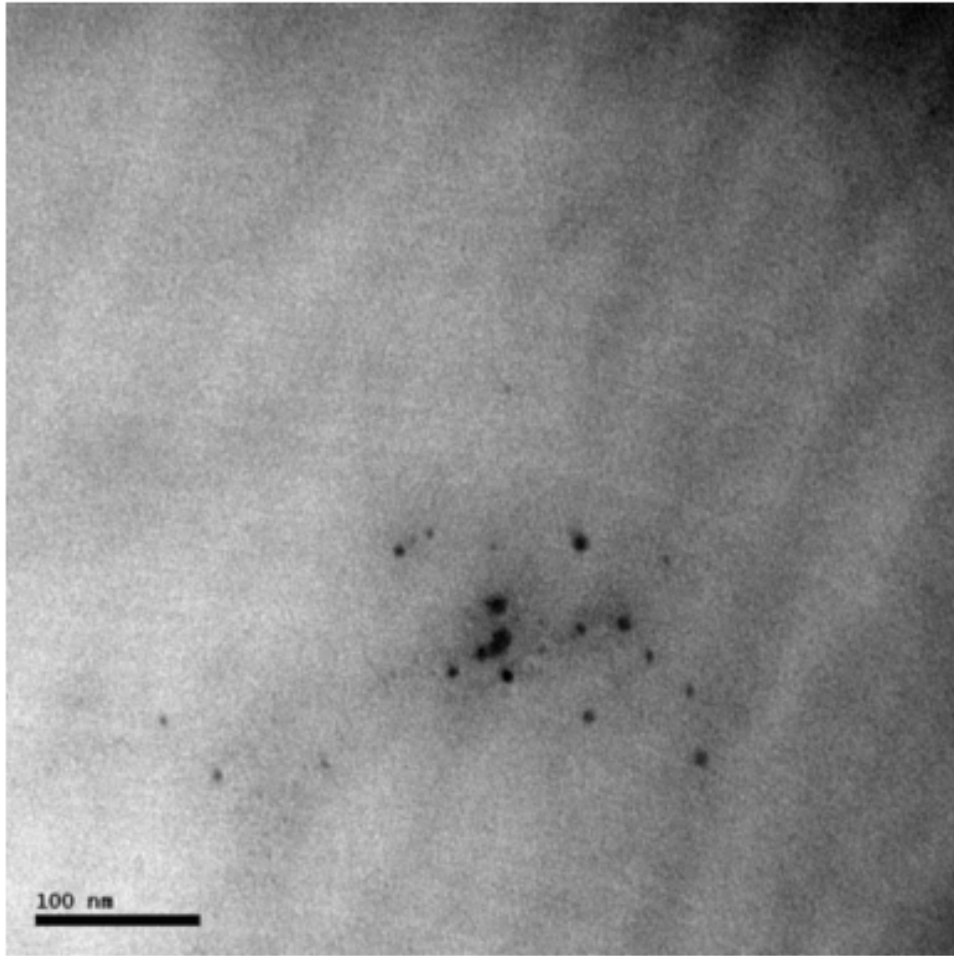


Figure 2.9 NMR overlay of N2 before and after treatment with DTT showing the appearance of the -SH peak confirming disulfide reduction.



*Figure 2.10 Full TEM image of SCNPs N2 from which Figure 2.4 was taken.*

## CHAPTER 3

### MODULAR DESIGN FOR HIERARCHICAL POLYMERIC MATERIALS

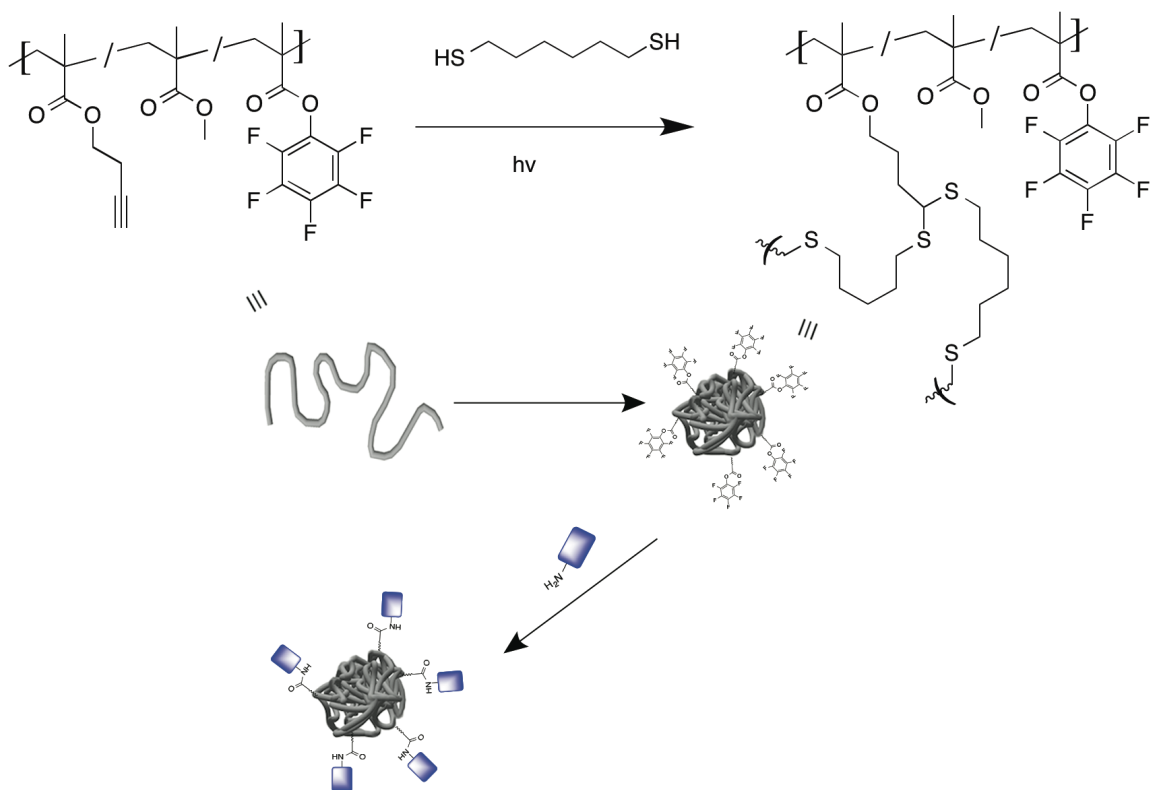
#### 3.1 Introduction

Nature's precise hierarchical self-assembly is precisely why life, as we know it, exists. Starting from atoms and building up to peptides, to proteins, to cells, and so forth, is where all the complexity of life arises. It is in this vein that polymer chemists have often been inspired to create complex supramolecular structures through a wide-range of chemistries and interactions such as intramolecular forces,<sup>94</sup> hydrophobic/hydrophilic interactions,<sup>95</sup> host-guest interactions,<sup>96</sup> and ionic interactions.<sup>97</sup> By creating well-defined, discrete nano-objects with supramolecular interaction moieties precisely placed along the surface of these nano-objects, a nano-sized self-assembly building block is created. SCNPs provide an ideal scaffold for such an application. Creating compact SCNPs imbued with an ability to assemble in pseudo-linear, pseudo-trigonal planar, and pseudo-tetrahedral would be a leap forward in the field of hierarchical self-assembly. In order to create these building blocks, designing a SCNPs that has two different functional handles is needed, the first to fold the linear polymer into the SCNPs and the second to build off of the surface of the SCNPs.

Thiol-yne "click" reactions, pentafluorophenyl activated esters, and the ring-opening of epoxides have been proven as powerful tools in post-polymerization modification.<sup>98-100</sup> Utilizing these chemistries would provide a facile route to both SCNPs and their subsequent modification. On top of the standard advantages that "click" chemistry provide,<sup>101</sup> another advantage of thiol-yne chemistry, as it pertains to SCNPs,



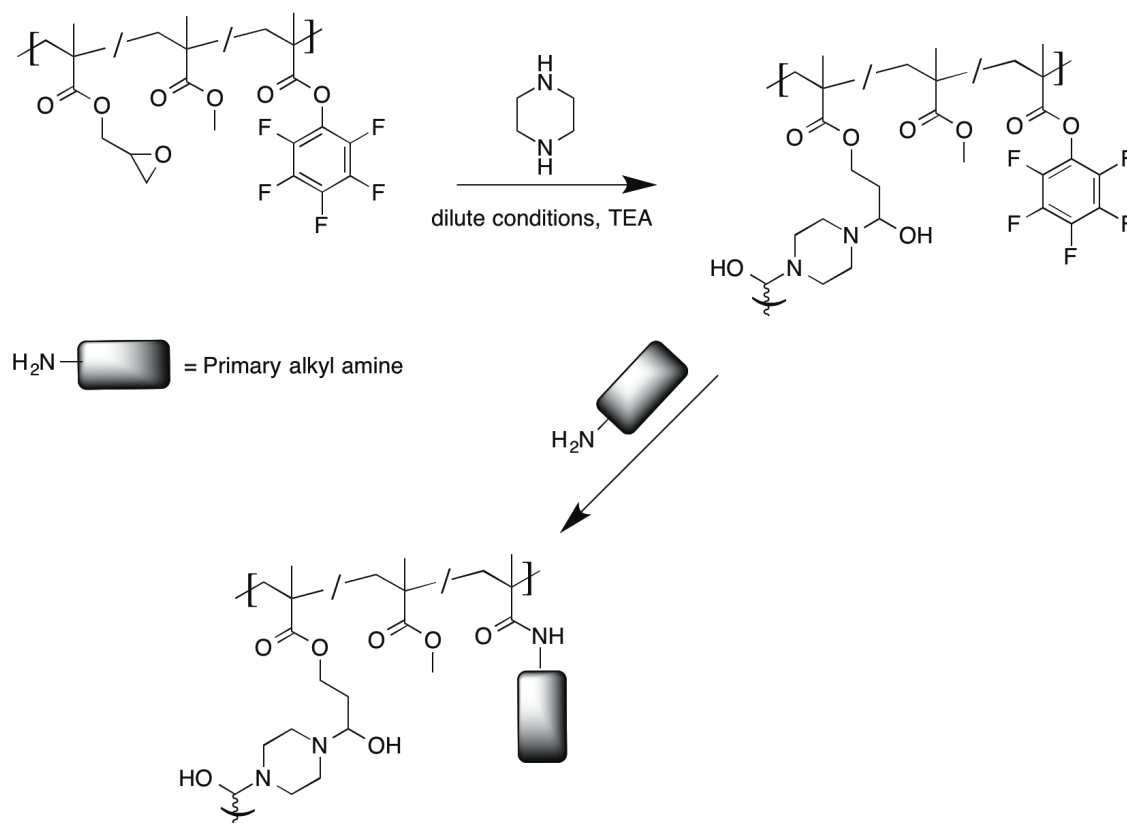
is that two thiols can be added to the pendant alkyne unit, as opposed to a single thiol in thiol-ene “click” chemistry. Having the ability to form subsequent cross-linking has been shown in our group to increase the degree of compaction in an SCNP.<sup>62</sup> Therefore, thiol-yne “click” chemistry provides us with a route to add double the external cross-linker as is normally used in the folding of SCNPs (Scheme 3.1). Once the compact SCNPs are created, the remaining activated esters can be utilized to attach moieties to the surface of the SCNP that will dictate how the nano-object can assemble.



*Scheme 3.1 Example of post-polymerization modification of SCNPs*

## 3.2 Results/Discussion:

### 3.2.1 Modularity via glycidyl methacrylate and pentafluorophenyl methacrylate



*Scheme 3.2 SCNP formation with secondary amine, then SCNP functionalization with primary alkyl amine*

Building off of previous work in the field of post-polymerization modification<sup>102,103</sup> a methacrylate-based backbone was chosen to attempt these hierarchical, orthogonal, macromolecular building blocks. Starting first with commercially available monomers, a set of experiments to synthesize polymers with the monomers MMA and glycidyl methacrylate (GMA) were performed. The idea in using GMA as a base monomer lies in its ability to react with both primary and secondary amines as well as being commercially available. If a polymer using GMA and the activated ester monomer, pentafluorophenyl methacrylate (PFMA), were copolymerized

together then a di-secondary amine (such as piperazine) could collapse the polymer chain while a primary amine could decorate the surface. The nature of these activated ester moieties, such as PFMA, are such that they are quite selective to primary alkyl amines. Since the epoxy moiety at the end of GMA is both reactive to primary and secondary amines, a collapse of single polymer chains with only di-secondary amines will leave the activated ester functional groups undisturbed.

A mixture of varying feed ratios, as can be seen in Table 3.1 Varying comonomer parent polymers, **P**, and their subsequent cross-linking with piperazine was prepared using RAFT conditions. By controlling the amount of GMA incorporated into the parent polymer it was thought that the cross-linking density and compactness of the SNCPs could be manipulated.

*Table 3.1 Varying comonomer parent polymers, **P**, and their subsequent cross-linking with piperazine, **N**.*

	mol% GMA	mol% MMA	mol% PFMA	Mw <sup>a</sup> (KDa)	PDI <sup>a</sup>	R <sub>h</sub> <sup>b</sup> (nm)	[η] <sup>b</sup> mL g <sup>-1</sup>	MHS a-value <sup>b</sup>
<b>P3.1</b>	10	80	10	89.7	1.1	4.9	8.86	0.672
<b>N3.1</b>	10	80	10	59.7	1.21	4.39	9.33	0.584
<b>P3.2</b>	20	60	20	164	1.15	4.7	4.09	0.602
<b>N3.2</b>	20	60	20	194	1.09	5.08	4.38	0.782
<b>P3.3</b>	30	40	30	155	1.47	3.92	2.62	0.189
<b>N3.3</b>	30	40	30	188	1.58	4.56	3.56	0.578

<sup>a</sup> SEC data collected at 30 °C in THF with MALS. <sup>b</sup> SEC data collected at 30 °C in THF with viscometer.

The initial results of using piperazine to collapse the polymers proved challenging. Due to a hydroxy group as well as a tertiary amine resulting from the ring opening of the glycidyl groups this made the precipitation of the polymers into methanol difficult. Hexanes showed promise, however, due to the highly reactive nature of glycidyl groups in the presence of amines, the polymers would rapidly undergo inter-chain cross-linking when precipitated. It was then devised that a pseudo-“quenching” chemical be used in order to react any remaining glycidyl moieties in the polymer chains, in this case piperidine. This pseudo-quench using piperidine solved the issue of gelation, however intra-chain collapse of the parent polymers was never observed. As can be seen in Table 3.1 and Figure 3.1 the degree of intra-chain collapse is negligible. In fact it is noticed that with the increased amount of GMA incorporation into the parent polymer that inter-chain cross-linking begins to take place as can be seen in the MALS trace in Figure 3.2.

Possible reasons for the lack in collapse could lie in the varying reactivities of the nitrogens in piperazine once they begin to ring open the glycidyl moieties. This could lead to rapid mono-addition to half of the glycidyl groups while taking much longer for the second nitrogen in the piperazine molecule to react with the remaining glycidyl functional handles. Another possibility is that piperazine is a relatively short molecule, thus leading to lower probabilities of it finding and ring opening a second glycidyl group. Furthermore, ring opening the epoxy group on GMA leaves a residual hydroxy group as well as a tertiary nitrogen, drastically increasing the polymers overall polarity. This increase in polarity could give rise to the polymer behaving much differently in standard organic solvents such as THF. As can be seen in the work of our colleagues the nature of intra- and inter-chain polymer cross-linking is not a trivial issue and has been studied computationally as well as experimentally.<sup>104</sup> With these initial attempts at creating compact SCNPs by way of a di-secondary amine proving to be difficult, an alternative

approach was devised. Thiol-yne “click”-chemistry was chosen because it is a powerful and versatile tool well-documented in the field of polymer chemistry. Unique to thiol-yne “click”-chemistry is that the terminal alkyne moiety can have not one but two thiols add to it. It was postulated that the increased amount of available cross-linking locations as well as negligible changes to the polymers’ polarity would be a promising route to creating SCNPs with the ability to be orthogonally decorated.

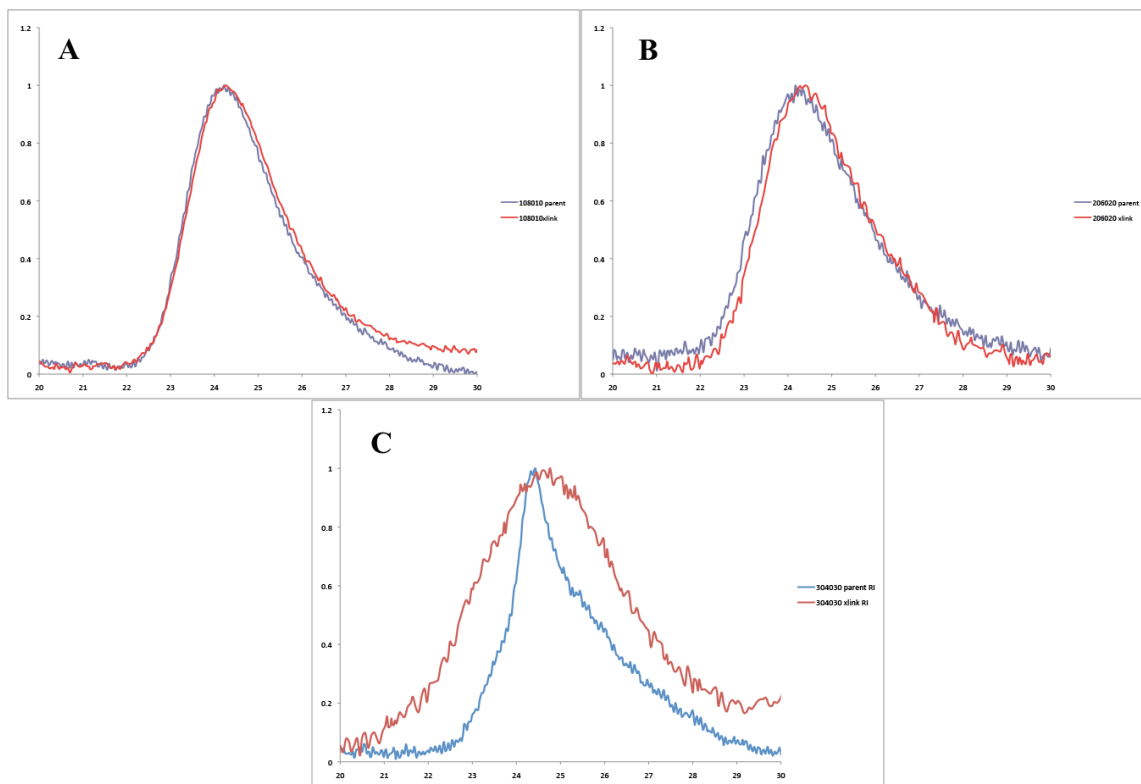


*Figure 3.1 Refractive Index SEC traces of before (blue) and after (red) of cross-linking with piperazine. SEC traces of A) P3.1, B) P3.2 and C) P3.3. Little, to no shift in retention time is observed using piperazine as a cross-linker.*

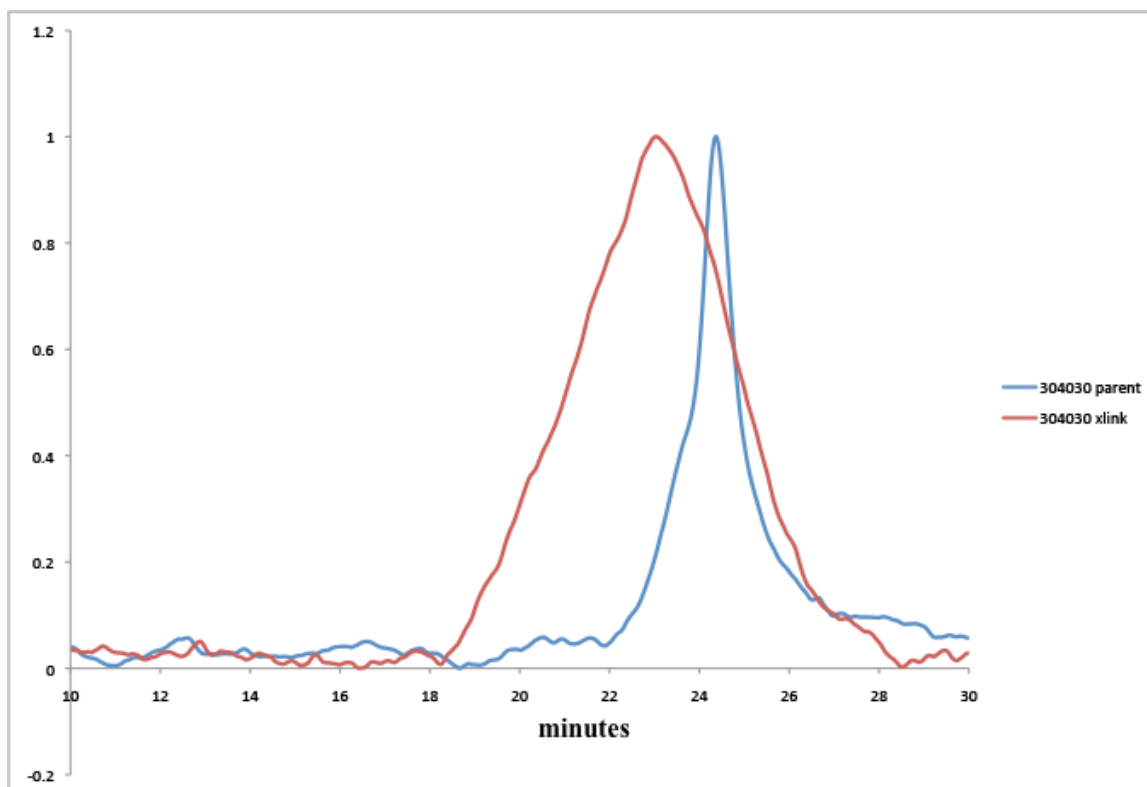


Figure 3.2 MALS trace of P3.3 showing large amounts of inter-chain crosslinking

### **3.2.2 Modularity via propargyl methacrylate and pentafluorophenyl methacrylate**

As an initial proof-of-concept, a random copolymer of methyl methacrylate (MMA) and propargyl methacrylate (PgMA), with varying feed ratios, were used. These polymers were then used to test the ability of a polymer with a terminal alkyne to tightly compact either with thermally initiated or light induced thiol-yne photochemistry. However, due to the alkyne's unsaturation, the monomer was first protected with trimethylsilyl (TMS) protecting group so that the radical-based polymerization would not induce covalent cross-linking prematurely. After polymerization the polymer was de-protected and then subjected to thiol-yne conditions via external thiol-based cross-linkers.

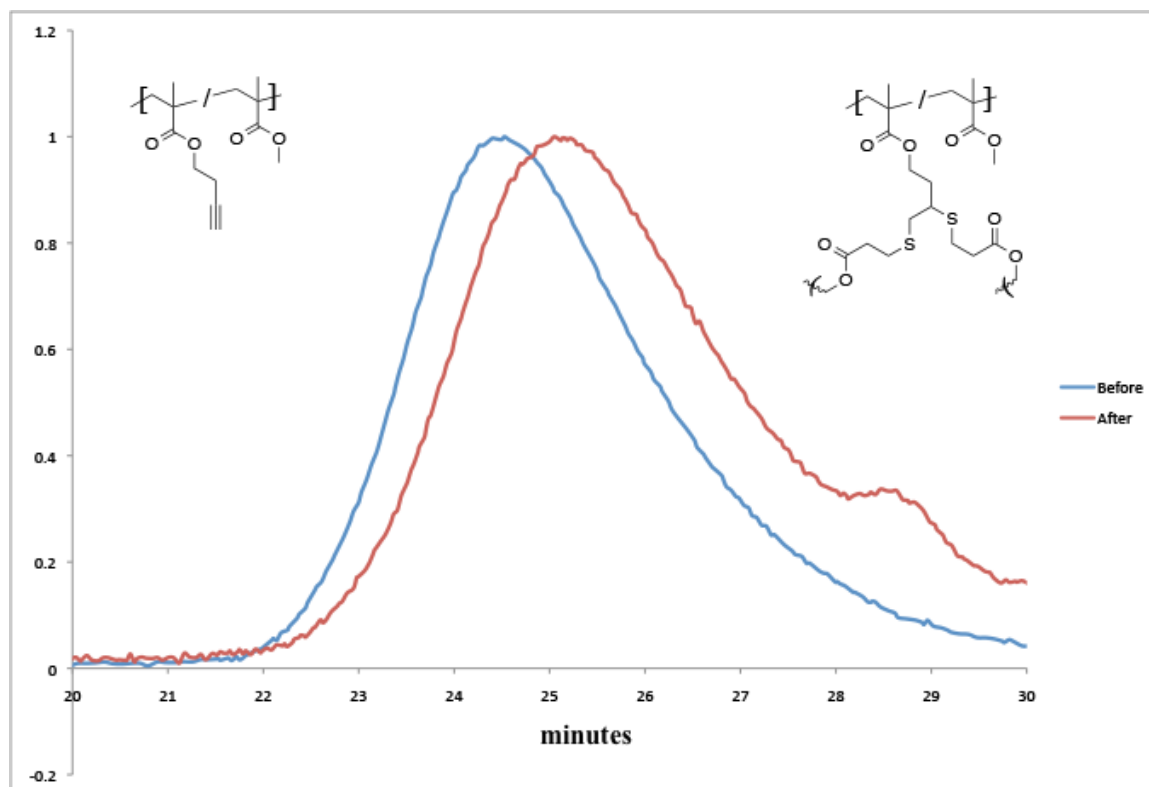


Figure 3.3 Thermally initiated thiol-yne click-chemistry of P3.4 to form SCNPs.

Encouraged by the initial results of the thermally initiated thiol-yne “click”-chemistry as a route to forming SCNPs, polymers containing not only PgMA comonomers but also pentafluorophenyl methacrylate comonomers as well. The feed ratios for the polymers used in the thiol-yne “click”-chemistry experiments can be see in Table 3.2.

Table 3.2 Initial results with thiol-yne polymers, **P**, and SCNP formation, **N**.

	mol% PgMA	mol% MMA	mol% PFMA	Mw <sup>a</sup> (kDa)	PDI <sup>a</sup>	R <sub>h</sub> <sup>b</sup> (nm)	[η] <sup>b</sup> mL g <sup>-1</sup>	MHS a-value <sup>b</sup>
<b>P3.4</b>	20	80	0	22.6	1.11	3.91	17.15	0.804
<b>N3.4</b>	20	80	0	27.4	1.24	3.77	13.17	0.667
<b>P3.5</b>	20	60	20	89.1	1.27	6.34	19.15	0.69

<sup>a</sup> SEC data collected at 30 °C in THF with MALS. <sup>b</sup> SEC data collected at 30 °C in THF with viscometer.

During the process of optimizing the thiol-yne conditions to create SCNPs, a wonderful study on SCNPs and their ability to compact tightly *via* thiol-yne click chemistry was published by Pomposo and co-workers.<sup>105</sup> In this work, Pomposo and coworkers demonstrated through an array of characterization techniques and MD simulations that the key to tight, globular compaction is dependant on the terminal alkyne moiety incorporated into their polymer backbone, capable of two photo-mediated thiol additions and sufficient length in the cross-linking moiety. Due to the large amount of intellectual overlap with this work, research from a methacrylate-based thiol-yne SCNP scheme was changed to a ROMP based system where the length of the side-chain functional group could be precisely controlled and incorporated directly into the polymer backbone. This work, and its subsequent foray into the unexpected doping effects of fluorinated aromatic hydrocarbons is explored further in chapter four.



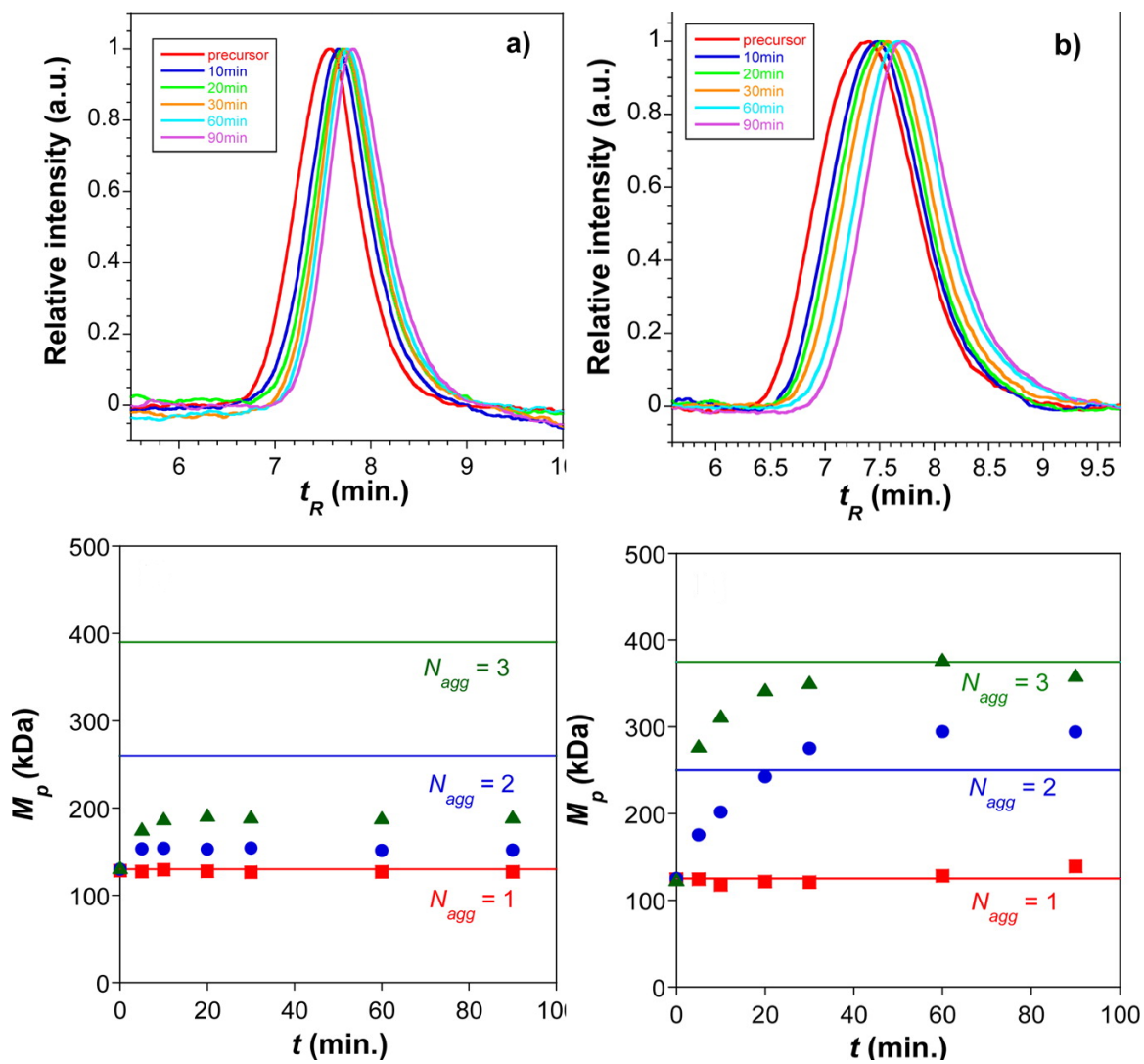


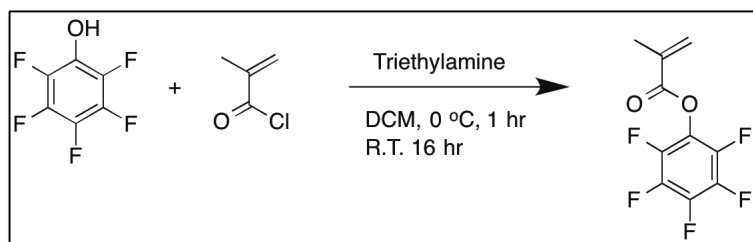
Figure 3.4 Compaction studies performed by Pomposo and coworkers. Column a) are SCNPs formed via thiol-ene click-chemistry analyzed by SEC and SAXS and column b) are SCNPs formed via thiol-yne click chemistry analyzed by SEC and SAXS. See reference<sup>105</sup> for further details.

### **3.3 Experimental:**

#### **3.3.1 General Methods**

Reagents were purchased from Aldrich and used as received. Size exclusion chromatography (SEC) was performed on a Tosoh EcoSEC dual detection (RI and UV) GPC system coupled to an external Wyatt Technologies miniDAWN Treos multi angle light scattering (MALS) detector and a Wyatt Technologies ViscoStarII differential viscometer. Samples were run in THF at 40 °C at a flow rate of 0.35 mL/min. The column set was two Tosoh TSKgel SuperMultipore HZ-M columns (4.6x150 mm), one Tosoh TSKgel SuperH3000 column (6x150mm) and one Tosoh TSKgel SuperH4000 column (6x150mm). Increment refractive index values (dn/dc) were calculated online assuming 100% mass recovery (RI as the concentration detector) using the Astra 6 software package (Wyatt Technologies) by selecting the entire trace from analyte peak onset to the onset of the solvent peak or flow marker. Absolute molecular weights and molecular weight distributions were calculated using the Astra 6 software package. Relative molecular weights were obtained vs. polystyrene standards (PStQuick MP-M, Tosoh) and calculated using the EcoSEC software package (Tosoh). Intrinsic viscosity ( $[\eta]$ ) and viscometric hydrodynamic radii ( $R_h$ ) were calculated from the differential viscometer detector trace and processed using the Astra 6 software.  $^1\text{H}$  NMR (400 MHz) spectra were recorded on a Varian Associates Mercury 400 spectrometer. Solvents ( $\text{CDCl}_3$  or  $d_8\text{-THF}$ ) contained 0.03% v/v TMS as an internal reference, chemical shifts ( $\delta$ ) are reported in ppm relative to TMS. Peak abbreviations are used as follows: s=singlet, d=doublet, t=triplet, m=multiplet, br=broad.

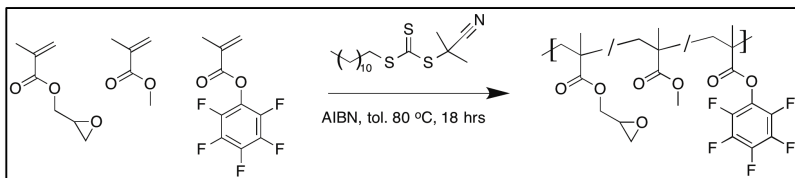
### 3.3.2 Synthesis of pentafluorophenyl methacrylate:



2.5 g of pentafluorophenol (0.014 mol) was added to a RBF and dissolved in 5 mL of

dry DCM. The RBF was sealed with a rubber septum and degassed for 25 minutes with nitrogen. The RBF was then placed in an ice bath and then 2.08 mL of triethylamine (0.015 mol) was added via syringe. Next 1.44 mL of methacryloyl chloride was added dropwise to the RBF via gas-tight syringe. The solution was allowed to stir at 0 °C for one hour, then gradually warmed to room temperature and allowed to stir for 16 hours. The organic layer was washed twice with DI water, twice with 1M HCl, twice with saturated sodium bicarbonate, and twice with brine. Organic layer was dried with anhydrous sodium sulfate and evaporated to dryness under reduced pressure to yield 2.94 g of a pale yellow oil. 78% yield. (<sup>1</sup>H NMR 400 MHz, CDCl<sub>3</sub>): δ ppm 6.49 (s), 5.8 (s), 2.1 (tr). (<sup>19</sup>F NMR 400 MHz, CDCl<sub>3</sub>): δ ppm -153.4 (d), -158.9 (tr), -163.2 (tr).

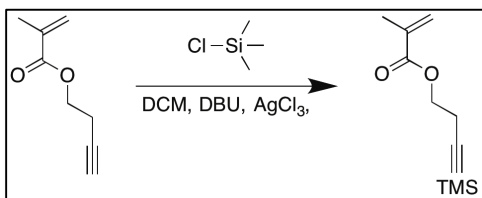
### 3.3.3 Example polymerization for methyl methacrylate, glycidyl methacrylate, and pentafluorophenyl methacrylate.



0.4 g of uninhibited methyl methacrylate (4.0 mmol), 0.071 g of uninhibited glycidyl

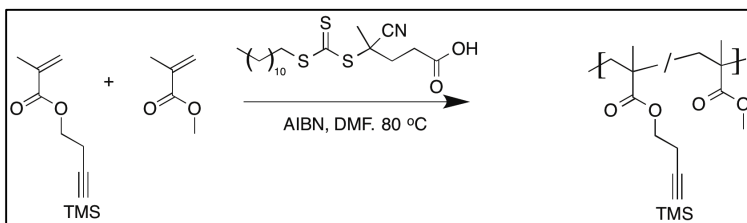
methacrylate (0.5 mmol), and 0.126 g of pentafluorophenyl methacrylate (0.5 mmol) were added into a RBF. Next, 3.5 mg of 2-cyano-2-propyl dodecyl trithiocarbonate (0.01 mmol), acting as a chain transfer agent, was added to the RBF followed by 0.33 mg of azoisobutyronitrile (0.002 mmol), acting as a radical source, were added to the RBF. Finally, 2 mL of dry toluene was added into the RBF. The RBF was then sealed with a rubber septum and degassed with nitrogen for a half hour. After degassing, the RBF was plunged into an 80 °C oil bath to initiate polymerization. Polymerization was allowed to run for 18 hours and was quenched by removing RBF from heat and exposing solution to air. The solution was diluted with about 5 mL of dichloromethane (DCM) and then precipitated into cold hexanes to yield an off-white gummy polymer. Polymer was redissolved in about 5 mL of DCM and then precipitated into cold methanol to yield a white powder. 0.86 g of polymer was recovered, 75% conversion.  $^1\text{H}$  NMR (400 MHz,  $\text{CDCl}_3$ ):  $\delta$  ppm 4.40 (br s), 3.80 (br s), 3.65 (br s), 3.27 (br s), 3.85 (br s), 3.65 (br s), 2.37-1.68 (br m), 1.52-0.77 (br m),  $^{19}\text{F}$  NMR (400 MHz,  $\text{CDCl}_3$ ):  $\delta$  ppm -149.9- -152.4 (br m), -157.9 (br s), -161.9- -162.8 (br s). SEC (THF) **P3.1**:  $M_w = 89.7$  kDa, PDI = 1.1. **P3.2**  $M_w = 164$  kDa, PDI = 1.15. **P3.3**  $M_w = 155$  kDa, PDI = 1.47.

### 3.3.4 TMS-Monomer synthesis



To a suspension of silver chloride (0.30 g, 2.1 mmol) in 50 mL of dry dichloromethane was added propargylmethacrylate (2.8 g, 0.02 mol) and 1,8-diazabicyclo[5.4.0] undec-7-ene (DBU), (0.44 g, 2.94 mmol). An appearance of dark color was observed. After stirring at room temperature for about 15 minutes, chloromethylsilane (3.15 g, 0.03 mol) was added dropwise and stirred for 24 hrs at 45 °C. The reaction mixture was then diluted with 100 mL of *n*-hexane and the organic phase was washed with saturated aqueous sodium bicarbonate, 1% Hydrochloric acid and water respectively. The extract was dried over magnesium sulfate, filtered and concentrated under reduced pressure to give a yellow liquid. The crude product was further purified by column chromatography eluting with a solvent mixture of 25:1 *n*-Hexane and diethyl ether to obtain a colorless liquid (75 % yield). <sup>1</sup>H NMR (400 MHz, CDCl<sub>3</sub>, δ): 6.18 (s, 1H, CH), 5.62 (s, 1H, CH), 4.76 (s, 2H, CH<sub>2</sub>), 1.97 (s, 3H, CH<sub>3</sub>), 0.19 (s, 9H, Si(CH<sub>3</sub>)<sub>3</sub>). <sup>13</sup>C NMR (400 MHz, CDCl<sub>3</sub>, δ): 166.96, 136.14, 126.97, 99.55, 92.34, 53.38, 18.10, -0.12.

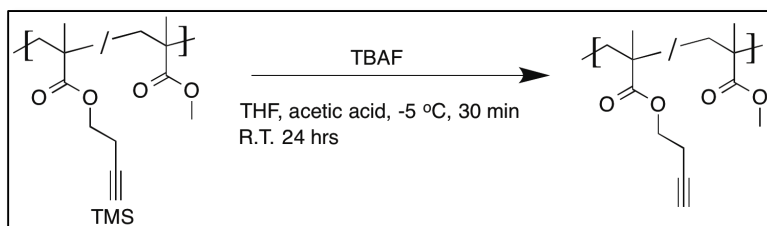
### 3.3.5 TMS Polymer synthesis



An oven dried 10 mL schlenk flask was charged with a mixture of MMA (0.33 g, 3.3 mmol) and TMSPgMA (0.65 g, 3.3 mmol). 4-Cyano-4-[(dodecylsulfanylthiocarbonyl)sulfanyl] pentanoic acid (12 mg, 0.04 mmol) and AIBN

(0.65 mg, 0.004 mmol) were then added, in stock solutions in dimethylformamide with a final volume of 2 mL. The polymerization mixture was degassed by three freeze-pump-thaw cycles. The schlenk flask was then heated in an oil bath at 80 °C for 24 hours. After the polymerization was complete the schlenk flask was opened to air. The resulting viscous polymer was diluted with 3 mL of THF and precipitated in 10 mL of ice-cold water. <sup>1</sup>H NMR (400 MHz, CDCl<sub>3</sub>, δ): 4.50-4.70 (s, CH<sub>2</sub> -C, TMSPgMA), 3.54-3.67 (s, CH<sub>3</sub>-O-(O)C, MMA,), 1.60-1.41(br, (CH<sub>2</sub>-C(CH<sub>3</sub>), MMA, TMSPgMA), 0.84-1.02 (br, (CH<sub>3</sub>(C), MMA, TMSPgMA), 0.16 (s, (CH<sub>3</sub>)<sub>3</sub>Si-) TMSPgMA).

### **3.3.6 Polymer deprotection:**

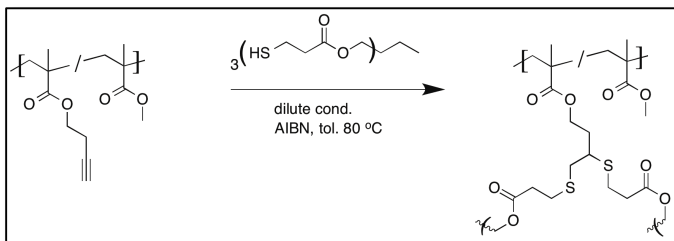


The copolymer **P 2.1-TMS** (865 mg, 0.049 mmol) containing 45 %

(0.022 mmol) of the trimethylsilyl protected alkyne was dissolved in argon purged 100 mL THF. Acetic acid (0.002 mL, 0.033 mmol) was added to the solution. Argon was bubbled to the solution (~ 30 min) and the solution was cooled to -5 °C in an ice-salt-water bath. A 1M solution of tetrabutylammoniumfluoride (TBAF) (0.033 mL, 0.033 mmol) was added slowly via a syringe (~ 5 min). The resulting mixture was stirred at this temperature for 30 minutes and then warmed to ambient temperature followed by stirring for 24 hours. The solution was passed through a short silica column to remove the excess of TBAF, followed by washing with additional THF. The resulting solution was then concentrated under a reduced pressure to a small volume, which was then precipitated in to cold water. The precipitate was then filtered and dried under vacuum to give a P 2.1 as a white powder. <sup>1</sup>H NMR (400 MHz, CDCl<sub>3</sub>, δ): 4.50-4.70 (s, CH<sub>2</sub> -C, PgMA), 3.54-3.67

(s, CH<sub>3</sub>-O(O)C), MMA, 2.47 (S, (CH, PgMA), 1.60-1.41(br, (CH<sub>2</sub>-C(CH<sub>3</sub>), MMA, PgMA), 0.84-1.02 (br, (CH<sub>3</sub>(C), MMA, PgMA). SEC (THF) Mw = 22.6 kDa, PDI = 1.11

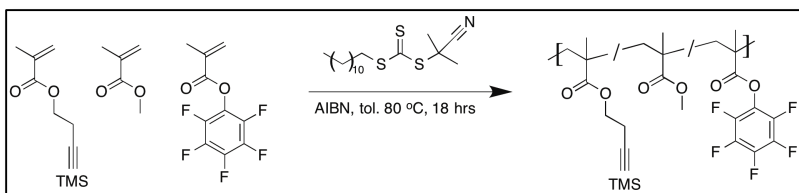
### 3.3.7 SCNP formation via thermally initiated thiol-yne click chemistry:



20 mg of deprotected poly(propargyl methacrylate-co-methyl methacrylate) was dissolved in 20 mL of dry toluene

and added to a RBF. Next, 0.078 mg (0.00002 mmol) of trimethylolpropane tris(3-mercaptopropionate) was added into the RBF. Finally 6 mg (0.037 mmol) of AIBN was added into the RBF which was then sealed with a rubber septum and degassed for 30 minutes with nitrogen. Then, all at once, the RBF was submerged into an 80 C oil bath and stirred for 16 hours. Toluene was removed under reduced pressure and the polymer was redissolved in THF for SEC analysis. SEC (THF) Mw = 27.4 kDa, PDI = 1.24

### 3.3.8 Synthesis of poly(propargyl methacrylate-co-methyl methacrylate-co-pentafluorophenyl methacrylate):



To a RBF, 0.3 g of MMA (0.003 mol), 0.252 g of PFMA

(0.001 mol), and 0.164 g of PgMA (0.001 mol) were added and dissolved in 2 mL of dry toluene. Next 2.1 mg of 2-cyano-2-propyl dodecyl trithiocarbonate (0.00625 mmol) and 0.2 mg of AIBN (6.25E-3 mmol) were added to the RBF. The RBF was then sealed with a rubber septum and then degassed with nitrogen for 30 minutes. The polymerization was then initiated by submerging the RBF into an 80 °C oil bath and left to stir for 18

hours. The polymerization was quenched by removing the RBF from the oil bath and exposing the solution to atmosphere. The solution was the precipitated into cold methanol to yield 0.53 g of a white powder. 74% conversion. SEC (THF)  $M_w = 89.1$  kDa, PDI = 1.27.



## CHAPTER 4

### 4.1 Pentafluorophenyl activated esters and their doping effects on second and third generation Grubbs' catalyst

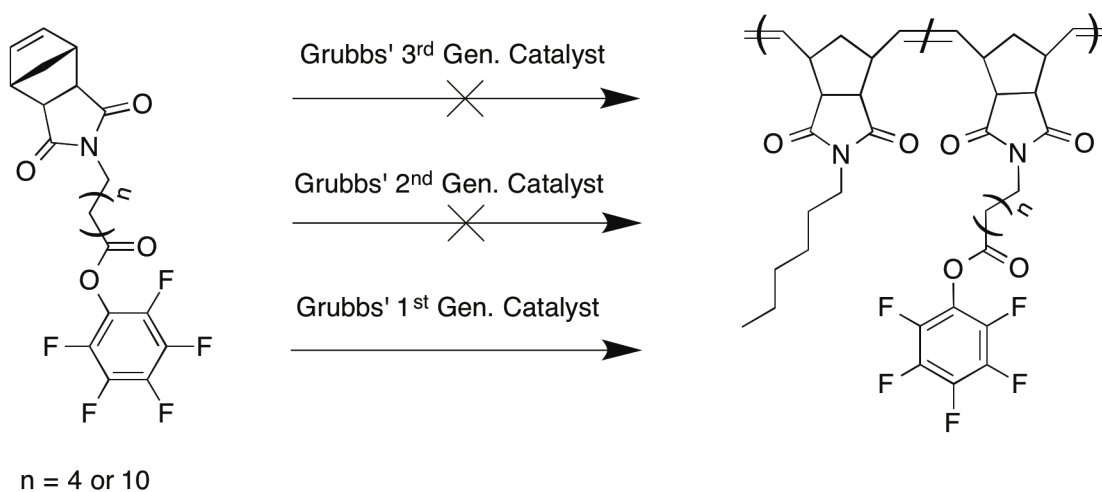
#### 4.1.1 Introduction:

The exciting growth and expansion in the field of single chain polymer nanoparticles (SCNPs) has led to fascinating work in the chemistry and applications of these nanodevices. From discrete, intra-molecularly cross-linked polymers,<sup>24,106</sup> the field has begun to blossom with the creation of useful materials in the fields of sensors,<sup>6</sup> catalysis,<sup>1-5</sup> nanomedicine,<sup>8-11</sup> and nanoreactors.<sup>7</sup> Looking to expand on the usefulness of SCNPs, an intra-molecular cross-linking methodology utilizing pentafluorophenyl activated esters was designed. Activated esters, particularly pentafluorophenyl esters, have gained notoriety in the field of post-polymerization modification<sup>23,102</sup> as they show an affinity to primary alkyl amines,<sup>107,108</sup> are very hydrolytically stable,<sup>109</sup> and can be incorporated into polymers via RAFT,<sup>109</sup> ATRP,<sup>103</sup> and ROMP.<sup>110</sup> This makes them useful handles for creating polymer brushes,<sup>111</sup> hyper-branched polymers,<sup>112</sup> polymer amphiphiles,<sup>113</sup> as well as a site to attach peptides.<sup>103</sup>

By utilizing the versatility of pentafluorophenyl activated esters, coupled with an olefin-based backbone, a system in which multiple avenues of collapse and

functionalization is created whether through utilizing a thiol-ene click-chemistry with the olefin backbone<sup>114</sup> or through a dialkyl amine and the activated pentafluorophenyl esters.<sup>108</sup>

It is here that we made an unexpected discovery. After successfully synthesizing different activated ester monomers with varying numbers of methylene units from the polymerizable moiety an as of yet unreported phenomenon in the field of polymer chemistry was discovered. We have shown that a fluorinated aromatic hydrocarbon (FAH) moiety attached to a sufficiently long spacer unit on a ROMP active monomer demonstrates extremely fast and uncontrolled rates of propagation when using second and third generation Grubbs' catalysts.



*Scheme 4.1 Attempted polymerizations of FAH-containing polymers with different Grubbs' catalysts*

Examples of the doping effect that FAHs have on second and third generation Grubbs' catalyst have been documented in a few synthetic organic chemistry reactions such as ring-closing metathesis and cross-metathesis reactions.<sup>115,116</sup> What Samojowicz and co-workers noted is that the mesityl groups on second and third generation Grubbs' catalyst formed strong  $\pi$ - $\pi$  interactions that drastically increased the catalyst's ability to

complete otherwise difficult ring closing reactions such as the formation of tetra-substituted double bonds and “ene-yne” reactions.<sup>115</sup> There is still some debate as to the actual mechanism of FAH’s doping effects on ruthenium, such as fluorine-ruthenium interactions,<sup>117</sup> however, the consensus seems to be it is caused by strong, stabilizing  $\pi$ - $\pi$  interactions<sup>118-121</sup>. Although monomers containing fluorinated esters being successfully polymerized have been reported in the literature<sup>122-124</sup> few examples exist where the authors report using second or third generation Grubbs’ catalysts,<sup>125</sup> instead preferring to use first generation Grubbs’. Demonstrating some very fascinating polymer architectures, the Tew lab reported the successful polymerization of cyclic polymers containing pentafluorophenyl activated esters by way of a modified second generation Grubbs’ catalyst.<sup>126,127</sup> What is different in this work, however, is that in order to create a catalyst that would directly polymerize cyclic polymers Zhang and Tew had to replace one of the mesityl sites with a methylene bridge, thus reducing the ability for the FAH moiety to form  $\pi$ - $\pi$  interactions with the catalyst.

Santiago and co-workers showed that oxanorbornenes and norbornenes with a pentafluorophenyl group attached directly to the nitrogen imide could be synthesized with second generation Grubbs’ catalyst, however, often times these polymers were of very high molecular weight and displayed broad molecular weight distributions.<sup>128</sup> Whether or not the FAH moiety in their monomers contributed to these high molecular weights and broad molecular weight distributions was not commented on.

When it became apparent that there was potential for FAHs to cause rapid, uncontrolled propagation during ROMP, we decided to study the effects of methylene spacer units between the pentafluorophenyl ester and the norbornene imide monomer. The logical first step was creating a grid of various feed ratios and also methylene spacer units in the monomer and polymerizing them with Grubbs’ first, second, and third

generation catalysts. Often times within 90 seconds a complete insoluble mass was observed in the round bottom flask with second and third generation Grubbs' catalysts. A complete summary of the results can be seen below in Table 4.1. Interestingly, this phenomenon is not seen when the monomers are initiated with first generation Grubbs' catalyst, suggesting that the pentafluorophenyl ester moieties do not have a doping effect, or otherwise alter the rate of propagation because there are no mesityl moieties to form  $\pi$ - $\pi$  interactions with the Grubbs' catalyst.

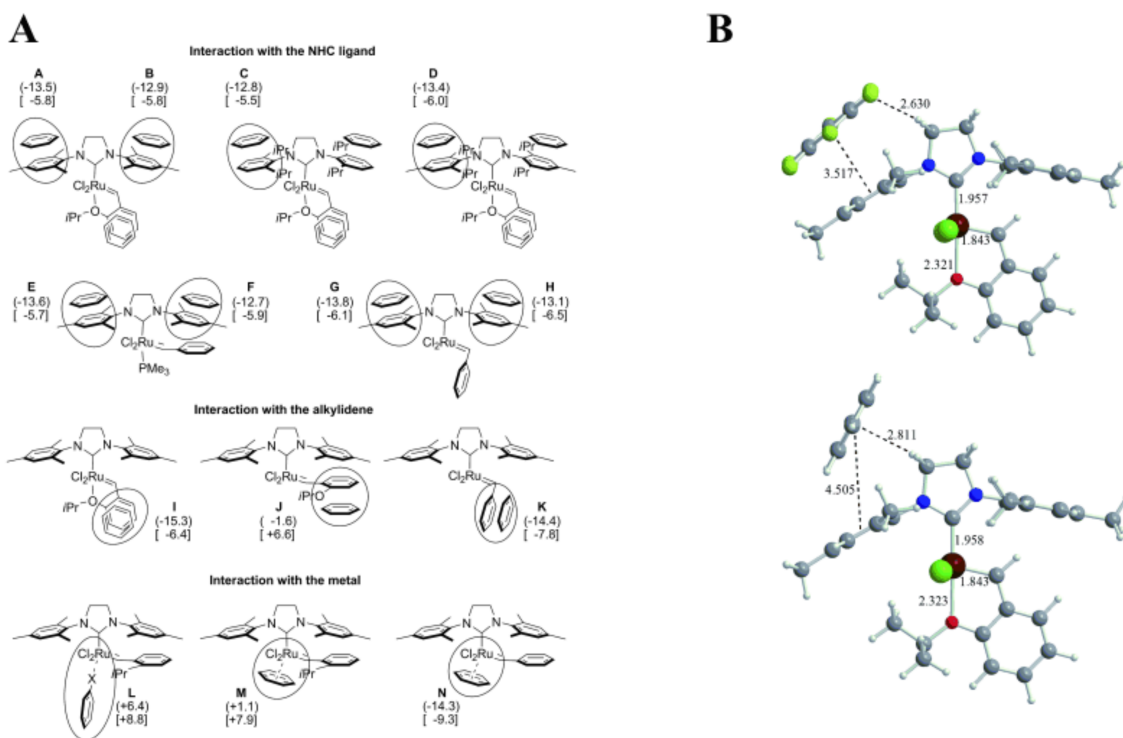


Figure 4.1 A) A basic scheme for possible FAH interactions with Grubbs' catalyst. B) DFT optimized MD simulations for hexafluorobenzene (top) and benzene (bottom). See reference <sup>115</sup> for further details.

## 4.2 Results and discussion:

Following standard, previously reported procedures for creating functional polymers via ROMP,<sup>75,129</sup> catalyst solutions were added all at once to monomer solutions.

When using this method with Grubbs' 2<sup>nd</sup> and Grubbs' 3<sup>rd</sup> the solutions would crash out of solution, forming insoluble gelatinous masses in the round bottom flasks. It was then decided that a slow, "starve-feed" method to polymerizing these functional polymers would be attempted. It was here, that we hoped that the slow addition of monomer would limit the doped ruthenium catalyst's ability to have a "run away" effect on the polymerization. When the monomer solutions were added dropwise to catalyst solutions over the course of 5 minutes there was no gelation in the round bottom flask. The polymers were then precipitated into room temperature methanol yielding a gummy, off-white solid. When the polymers were redissolved in THF, there was some large particulate that would not dissolve completely into solution. Furthermore, when these solutions were sufficiently filtered and analyzed by GPC there was very large shouldering in the chromatographs, suggesting that there was still very little control over the polymerization of the FAH containing polymers.

Table 4.1 Matrix of varying FAH containing ROMP monomers

	mol%	mol%	mol%	Gen. of	Mw <sup>a</sup>	PDI <sup>a</sup>
	6NBIE	12NBIE	hexylNBI	Grubbs' Cat.	(KDa)	
<b>P4.1</b>	30	0	70	3	412	1.39*
<b>P4.2</b>	25	0	75	3	140	1.04*
<b>P4.3</b>	50	0	50	3	gel	gel
<b>P4.4</b>	0	30	70	3	gel	gel
<b>P4.5</b>	0	100	0	3	gel	gel
<b>P4.6</b>	0	100	0	2	gel	gel
<b>P4.7</b>	0	50	50	1	91.6	1.28
<b>P4.8</b>	100	0	0	2	gel	gel

<sup>a</sup> SEC data collected at 30 °C in THF with MALS. <sup>b</sup> SEC data collected at 30 °C in THF with viscometer. \*SEC chromatograph multi-modal, see Figure 4.2

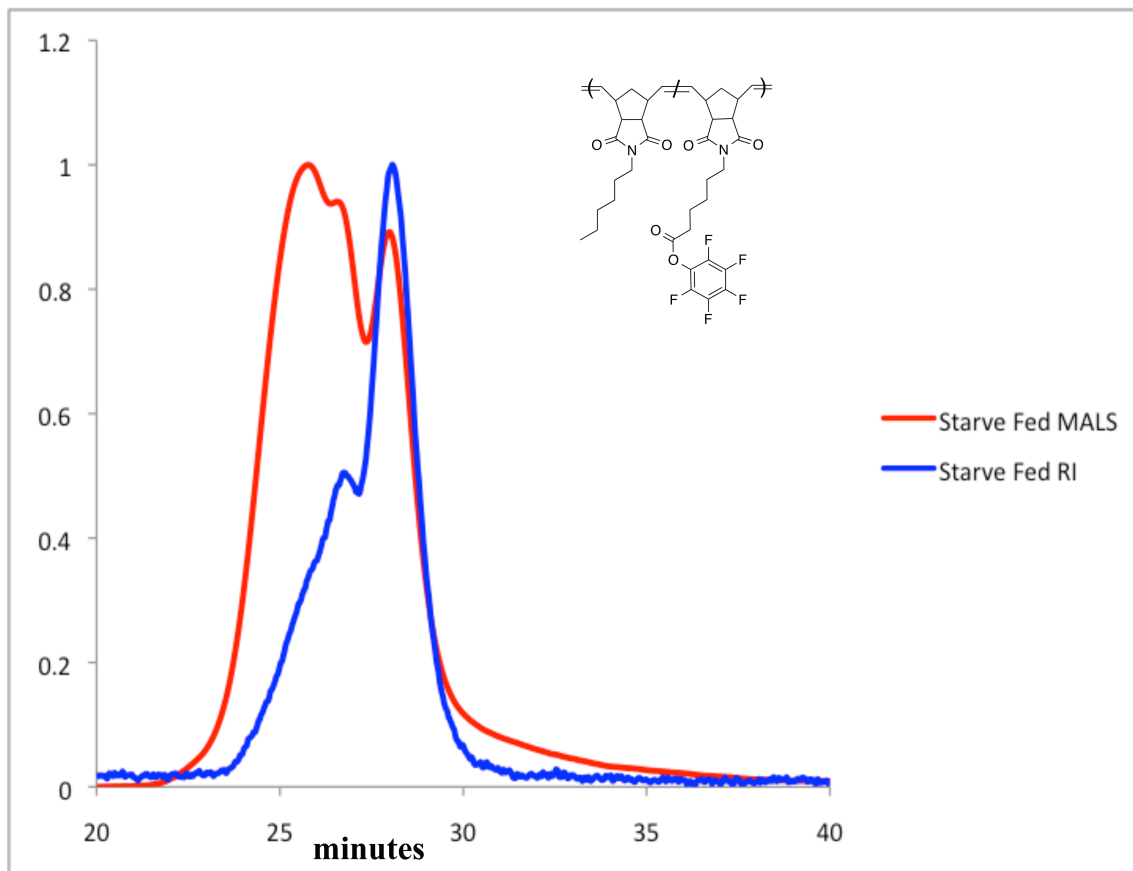


Figure 4.2 MALS trace (red) and RI trace (blue) of “starve-fed” polymerizations showing poor control over dispersity.

What is fascinating is that once the catalyst is changed to Grubbs’ first generation, the issue of rapid polymerization seems to disappear. When using Grubbs’ first generation, the polymers can be precipitated, redissolved, and analyzed with all standard polymer analyzation techniques. We can also see in the SEC chromatographs that relatively monodisperse polymers are formed.

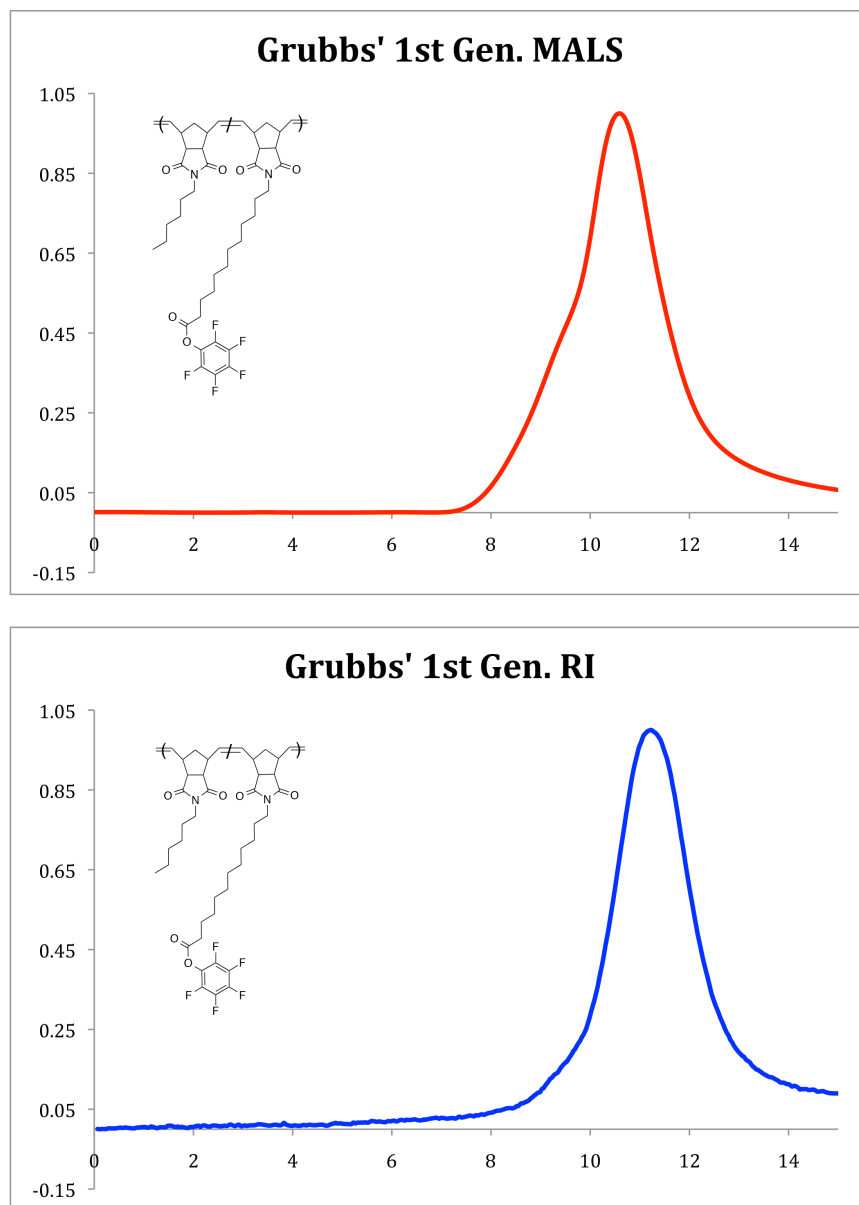


Figure 4.3 MALS (top) and RI (bottom) traces of FAH containing polymer using Grubbs' 1<sup>st</sup> generation catalyst showing low polydispersity.

A further test to confirm the doping effects of FAHs on the rate of polymerization was performed while carrying out homopolymerizations of just the hexyl norbornene imide monomers in hexafluorobenzene as well as pentafluorophenol with second generation Grubbs' catalyst. In these reactions the amount of FAH chosen was meant to mimic the molar amount of FAH present in a 50:50 molar feed ratio of the pentafluorophenyl ester monomers. In these tests, both fluorinated benzene and



pentafluorophenol showed rapid gelation and poor molecular weight control. Both of the doped polymerizations, after considerable sonication and stirring overnight, could be redissolved, however, they showed extremely high molecular weights.

As this particular project continues to evolve it has become apparent that a multidisciplinary approach to elucidating the mechanism of this FAH doping effect would be required. Future work would require intensive MD simulations, a greater knowledge in catalyst design and synthesis, as well as a more careful study and analysis of the propagation kinetics of this polymerization i.e. is this a phenomenon that can be manipulated or controlled to become a useful tool in ROMP chemistry? If the doping effects can be fully understood this chemistry could have potential in increasing the reactivity of Grubbs' second and third generation catalysts in order to polymerize endo-norbornene isomers or maybe the living polymerization of cyclooctene. Unfortunately there is not enough time remaining in this dissertation to explore these possibilities.

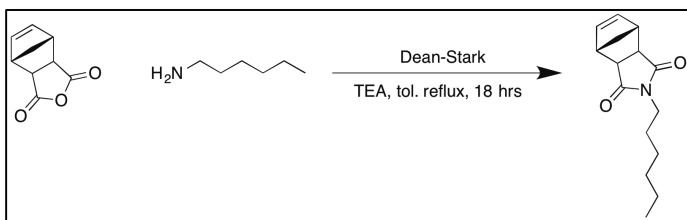
### **4.3 Experimental:**

#### **4.3.1 General Methods.**

Reagents were purchased from Aldrich and used as received. Size exclusion chromatography (SEC) was performed on a Tosoh EcoSEC dual detection (RI and UV) GPC system coupled to an external Wyatt Technologies miniDAWN Treos multi angle light scattering (MALS) detector and a Wyatt Technologies ViscoStarII differential viscometer. Samples were run in THF at 30 °C at a flow rate of 0.35 mL/min. The column set was two Tosoh TSKgel SuperMultipore HZ-M columns (4.6x150 mm), one Tosoh TSKgel SuperH3000 column (6x150mm) and one Tosoh TSKgel SuperH4000 column (6x150mm). Increment refractive index values (dn/dc) were calculated online

assuming 100% mass recovery (RI as the concentration detector) using the Astra 6 software package (Wyatt Technologies) by selecting the entire trace from analyte peak onset to the onset of the solvent peak or flow marker. Absolute molecular weights and molecular weight distributions were calculated using the Astra 6 software package. Intrinsic viscosity ( $[\eta]$ ) and viscometric hydrodynamic radii ( $R_h$ ) were calculated from the differential viscometer detector trace and processed using the Astra 6 software.  $^1\text{H}$  NMR (400 MHz) spectra were recorded on a Varian Associates Mercury 400 spectrometer. Solvents ( $\text{CDCl}_3$  or  $d_8$ -THF) contained 0.03% v/v TMS as an internal reference, chemical shifts ( $\delta$ ) are reported in ppm relative to TMS. Peak abbreviations are used as follows: s=singlet, d=doublet, t=triplet, m=multiplet, br=broad.

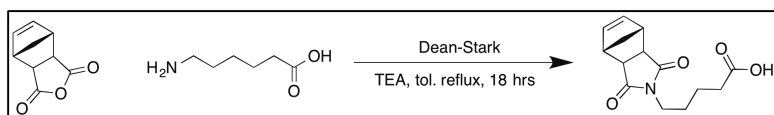
#### **4.3.2 Synthesis of norbornene hexyl imide:**



3 g of exo-norbornene anhydride (0.018 mol) was added to a round-bottom flask (RBF) and dissolved in 10 mL of dry toluene. Then 2.64 mL of hexylamine (0.020 mol) was added to the RBF followed by 2.92 mL of triethylamine (0.020 mol). The RBF was then attached to a Dean-Stark apparatus and heated to reflux overnight. Reaction mixture was washed two times with DI water, followed by two washes with 1M HCl, followed by two washes with saturated sodium bicarbonate, followed by two washes of a saturated brine solution. Organic layer was then dried over anhydrous sodium sulfate and gravity filtered into 20 mL scintillation vial. Product was evaporated to dryness under reduced pressure to afford a free-flowing pale colored oil. 72% yield.  $^1\text{H}$  NMR (400 MHz,  $\text{CDCl}_3$ ):  $\delta$  ppm 6.29 (t, 2H), 3.50-3.42

(m, 2H), 3.29-3.26 (m, 2H), 2.67 (d, 2H), 1.60-1.48 (m, 2H), 1.35-1.20 (m, 8H), 0.92-0.82 (m, 3H).

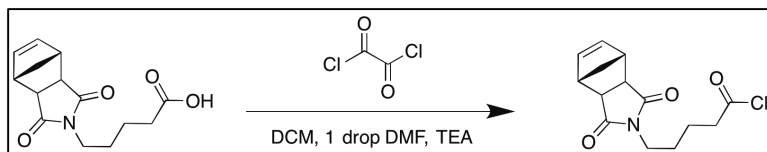
### **4.3.3 Synthesis of exo-norbornene hexanoic acid:**



5 g of exo-carbic anhydride (0.0305 mol)

was added to a RBF. Then 4.4 g of hexanoic acid (0.0335 mol) was added to the RBF. 10 mL of dry toluene was then added to the RBF, partially dissolving the solids. Then 4.76 mL of triethylamine was added to the solution. The RBF was then attached to a Dean-Stark apparatus and heated to 130 °C overnight. Organic layer was washed with two washes of DI water, two washes with 1M HCl, two washes with saturated sodium bicarbonate, and two washes with brine solution. The organic layer was then dried over anhydrous sodium sulfate and filtered into a 20 mL scintillation vial and evaporated to dryness under reduced pressure to afford a thick, viscous oil which slowly crystallized overnight. 74% yield. <sup>1</sup>H NMR (400 MHz, CDCl<sub>3</sub>): δ ppm 6.28 (s), 3.49 (tr), 3.31 (s), 2.42 (tr), 1.68-1.27 (m), 1.18 (d),

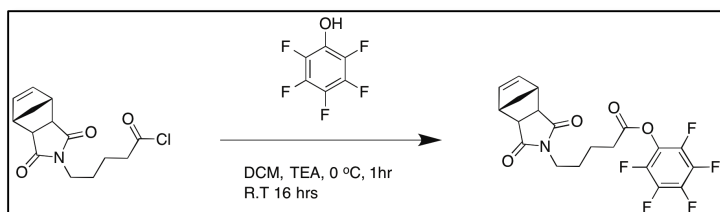
#### **4.3.4 Synthesis of exo-norbornene hexanoic acid chloride:**



0.915 g (3.3 mmol) was dissolved in 4 mL of dichloromethane (DCM)

and then added to a RBF. Then a catalytic amount of dimethylformamide (DMF) (one drop) was added to the solution. The RBF was sealed with a rubber septum and the solution was sparged with nitrogen for 10 minutes. Then 0.314 mL of oxalyl chloride (3.6 mmol) was syringed, dropwise, into the RBF. Finally, 0.26 mL of triethylamine (3.6 mmol) was added to dropwise, via syringe into the RBF. Rapid bubbling ensued upon addition of triethylamine and the solution turned a bright orange/pink color. Solution was allowed to stir overnight, turning into a dark orange/brown colored solution. The product was immediately used in the following step to synthesize exo-norbornene hexanoic pentafluorophenyl ester.

#### **4.3.5 Synthesis of exo-norbornene hexanoic pentafluorophenyl ester:**

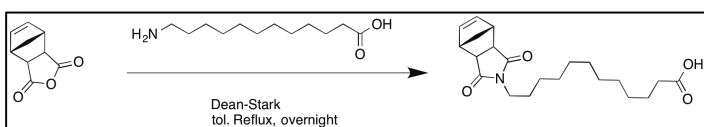


Immediately using the exo-norbornene hexanoic acid chloride from the previous step, and assuming

quantitative yields, the RBF was placed in an ice bath. 0.607 g of pentafluorophenol (3.3 mmol) was dissolved in 1 mL of DCM and then syringed into the RBF. Then 0.24 mL of triethylamine was syringed into the flask dropwise, via syringe. Rapid bubbling and gas evolution ensued. Product was allowed to warm to room temperature after 15 minutes, then left to stir overnight. Organic layer was washed twice with DI water, two times with

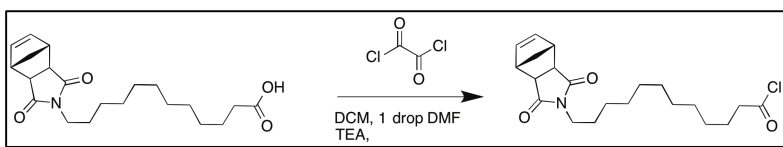
1M HCl, two times with saturated sodium bicarbonate, then two times with brine solution. The organic layer was then dried over anhydrous sodium sulfate and filtered into a 20 mL scintillation vial and evaporated to dryness under reduced pressure to afford a dark orange, viscous oil. 58% yield.  $^1\text{H}$  NMR (400 MHz,  $\text{CDCl}_3$ ):  $\delta$  ppm 6.28 (s), 3.49 (tr), 3.31 (s), 2.42 (tr), 1.68-1.27 (m), 1.18 (d).  $^{19}\text{F}$  NMR (400 MHz,  $\text{CDCl}_3$ ):  $\delta$  ppm -152.75 (d), -158.76 (tr), -162.9 (tr).

#### **4.3.6 Synthesis of exo-norbornene dodecanoic acid:**



2 g of exo-norbornene anhydride (0.012 mol) was added to a RBF. Then 2.89 g of dodecanoic acid (0.013 mol) was added to the RBF. Then 5 mL of dry toluene was added to the RBF, partially dissolving the solids. Then 1.83 mL of triethylamine was added to the RBF (0.013 mol). The RBF was attached to a Dean-Stark apparatus and heated to 126 oC overnight. The organic layer was washed twice with DI water, twice with 1M HCl, twice with saturated sodium bicarbonate, and twice with brine. The organic layer was then dried over anhydrous sodium sulfate and filtered into a 20 mL scintillation vial and evaporated to dryness under reduced pressure to afford an extremely thick oil. 77% yield.

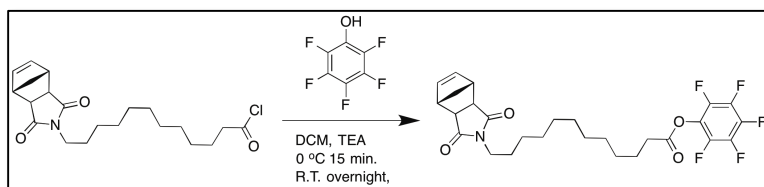
#### **4.3.7 Synthesis of exo-norbornene dodecanoic acid chloride:**



2 g of exo-norbornene dodecanoic acid (5.5 mmol) was dissolved in 4 mL of dry DCM and then added to a RBF followed by a catalytic amount of DMF (1

drop). The RBF was then sealed with a rubber septum and sparged with nitrogen for 10 minutes. 0.57 mL of oxalyl chloride (6.6 mmol) was syringed, dropwise, into the RBF where slight bubbling was observed. After the effervescence ceased, 0.927 mL of triethylamine (6.6 mmol) was syringed dropwise into the RBF. The reaction proceeded to bubble rapidly and turn a bright orange/pink color. The solution was allowed to stir overnight turning into a dark orange/brown color. This solution was used immediately in the following step to synthesize the *exo*-norbornene dodecanoic pentafluorophenyl ester without further purification.

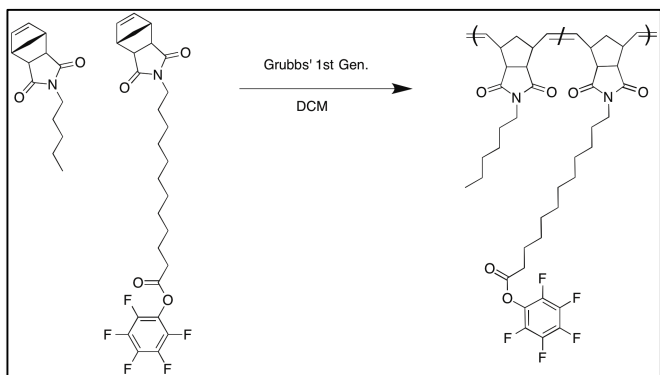
#### **4.3.8 Synthesis of *exo*-norbornene dodecanoic pentafluorophenyl ester:**



Assuming quantitative yield from previous step, the RBF was then

submerged in an ice bath. While RBF cooled to 0 °C, 1.21 g of pentafluorophenol (6.6 mmol) was dissolved in 2 mL of DCM then syringed into the RBF dropwise. Finally 0.927 mL of triethylamine (6.6 mmol) was syringed, dropwise, into the RBF. Rapid bubbling ensued. After 15 minutes the reaction was allowed to warm to room temperature and stir overnight. Organic layer was washed twice with DI water, twice with 1M HCl, twice with saturated sodium bicarbonate, and twice with brine. The organic layer was then dried over anhydrous sodium sulfate and filtered into a 20 mL scintillation vial and evaporated to dryness under reduced pressure to afford a thick, dark orange oil. 74% yield. <sup>1</sup>H NMR (400 MHz, CDCl<sub>3</sub>): δ ppm 6.15 (s), 3.45-3.21 (m), 2.68 (tr), 1.84-1.15 (br m). <sup>19</sup>F NMR (400 MHz, CDCl<sub>3</sub>): δ ppm -153.3 (d), -158.9 (tr), -163.1 (tr).

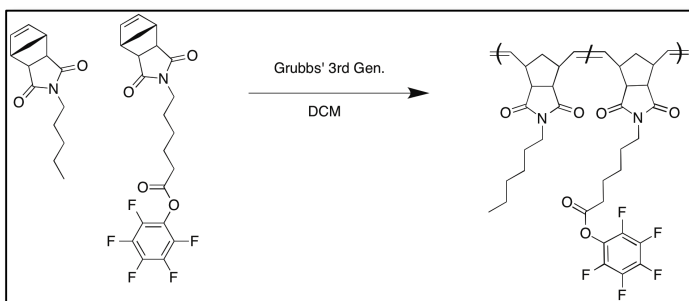
### 4.3.9 An example procedure for ROMP (catalyst added last):



0.16 g of of the monomers exo-norbornene hexyl imide (0.65 mmol) and 0.34 g of exo-norbornene dodecanoic pentafluorophenyl ester (0.66 mmol) were added to RBF . Then

the monomers were dissolved in 5 mL of dry DCM. The RBF was then sealed with a rubber septum and the monomer solution was sparged with nitrogen for 10 minutes. After sparging, 8.22 mg of Grubbs' 1st generation catalyst (0.01 mmol) dissolved in 1 mL of dry DCM was syringed into the RBF all at once. The reaction underwent vigorous stirring for 20 minutes then was quenched with a large excess of ethyl vinyl ether and stirred for 2 hours. The polymer solution was then precipitated into room temperature methanol to afford 0.228 g of a tacky, dark gray/tan polymer. 46% yield. Polymer was characterized via triple detection.  $^1\text{H}$  NMR (400 MHz,  $\text{CDCl}_3$ ):  $\delta$  ppm 5.78-5.45 (br d), 3.50-2.63 (br m), 2.37-0.88 (br m).  $^{19}\text{F}$  NMR (400 MHz,  $\text{CDCl}_3$ );  $\delta$  ppm -153.2 (br s), -158.5 (br s), -162.8 (br s). SEC (THF)  $M_w = 91.6$  kDa, PDI = 1.28

### 4.3.10 An example procedure for a “starve-fed” ROMP:



Due to the propensity of ROMP monomers containing FAH moieties to gel with Grubbs' 2nd and 3rd generation catalyst, an attempt to “starve-feed” the

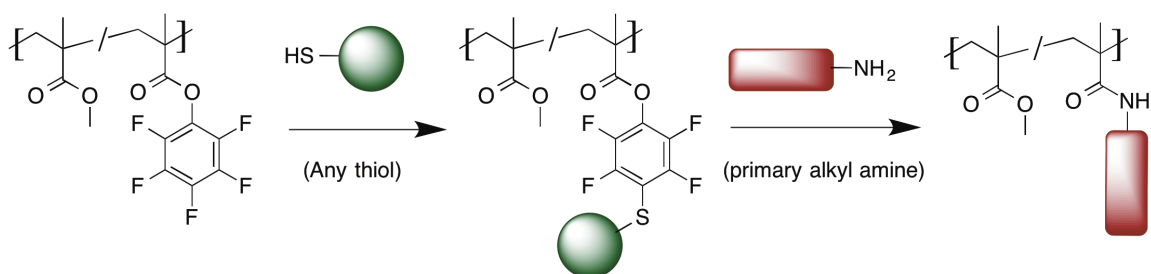
polymerization in order to control the degree of polymerization was performed. 11.1 mg of Grubbs' 3rd generation catalyst (0.013 mmol) was dissolved in 0.4 mL of dry tetrahydrofuran and added to a RBF and sealed with a rubber septum. The RBF was then degassed with nitrogen for 10 minutes. Then 0.44 g of exo-norbornene hexyl imide (1.78 mmol), and 0.80 g of exo-norbornene hexanoic pentafluorophenyl ester (1.8 mmol) was dissolved in 10 mL of dry THF in a 20 mL scintillation vial. The monomer solution was then added dropwise over 5 minutes. After the last drop of monomer solution was added the reaction was allowed to stir for one minute and was then quenched with a large excess of ethyl vinyl ether and allowed to stir for two hours. The polymer was then precipitated into room temperature methanol to yield a dark tan/gray gummy solid. Quantitative yield. Polymers did not fully redissolve in THF after precipitation. The solution was filtered twice through 0.45  $\mu$ m PTFE luer lock filters. SEC traces displayed very large shoulder in the high molecular weight region.  $^1\text{H}$  NMR (400 MHz,  $\text{CDCl}_3$ ):  $\delta$  ppm 5.79-5.47 (br d), 3.51-2.62 (br m), 2.37-0.95 (br m).  $^{19}\text{F}$  NMR (400 MHz,  $\text{CDCl}_3$ );  $\delta$  ppm -153.2 (br s), -158.5 (br s), -162.8 (br s). SEC (THF)  $M_w = 140$  kDa, PDI = 1.04\*. \* see Figure 4.2.



## CHAPTER 5

### NEW ROUTES IN POST-POLYMERIZATION MODIFICATION WITH PENTAFLUOROPHENYL ACTIVATED ESTERS

#### 5.1 Introduction



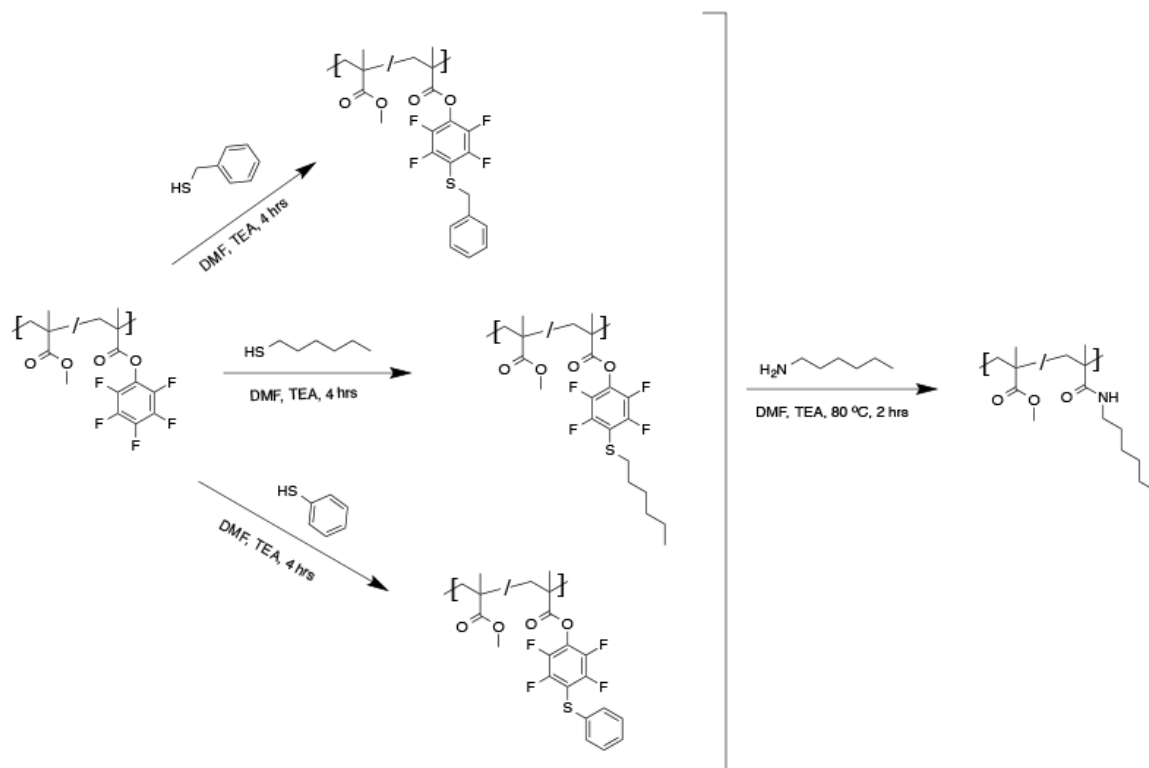
*Scheme 5.1 Sequential post-polymerization modifications with pentafluorophenyl activated esters*

Post-polymerization modification is one of the most powerful tools available to polymer chemists. By imbuing specific functional moieties into polymer backbones that are unreactive to various polymerization chemistries such as ATRP,<sup>100</sup> RAFT,<sup>130</sup> ROMP,<sup>131</sup> ADMET<sup>132</sup> and more,<sup>102,133</sup> this allows the scientist to create a vast array of intricate polymeric materials. One of the most powerful tools in post-polymerization modification lies in the use of activated esters.<sup>134</sup> Some of the most well-studied activated esters include N-hydroxysuccinimide activated ester,<sup>135</sup> thiazolidine-2-thione esters,<sup>136</sup> salicylic-acid-derivatives,<sup>137</sup> tetrafluorophenyl esters,<sup>138</sup> and pentafluorophenyl esters.<sup>108,139</sup> All of these activated ester moieties provide a functional handle for a wide range of classic nucleophiles such as hydroxy groups, amines, and more.<sup>134</sup>

Of particular interest to this work is the pentafluorophenyl activated ester moiety, in pentafluorophenyl methacrylate (PFMA). Thanks to PFMA's hydrolytic stability<sup>109</sup> and selectiveness to primary alkyl amines,<sup>108</sup> PFMA has enjoyed success in the fields of [medicine, drug delivery, smart materials, and more]. However, to the best of our knowledge, what has yet to be shown regarding the use of PFMA's pentafluorophenyl activated ester is its ability to undergo thiol-para fluoro "click-like" reactions while still maintaining its reactivity towards primary alkyl amines.

Thiol-para fluoro "click-like" reactions are high yielding, fast, and atom efficient reactions fulfilling most of the requirements for a "click" reaction.<sup>101</sup> These reactions have been used in various post-polymerization modifications such as in the creation of glycopolymers,<sup>140,141</sup> tuning hydrogen bonding capabilities within functional polymers,<sup>142</sup> and post-polymerization modifications of multi-component based monomers.<sup>143</sup> Thiols function as "soft" nucleophiles capable of undergoing nucleophilic aromatic substitution with various aromatic halogens.<sup>144-146</sup> This is critical when working with activated esters, as it selectively substitutes at the para-position, leaving the activated ester moiety unscathed.

## 5.2 Results and Discussion



*Scheme 5.2 Scheme of the different thiols capable of performing thiol-para fluoro click-reactions on pentafluorophenyl-activated esters.*

Due to its simple synthesis, ease of polymerization, selectivity towards primary alkyl amines, and straightforward post-polymerization modification procedure,<sup>108,113</sup> PFMA was chosen for this work. A simple copolymer of methyl methacrylate (MMA) and PFMA were synthesized for this work. Benzyl mercaptan was chosen first as a proof-of-concept reaction for the thiol-para fluoro “click-like” reaction because of the obvious benzylic proton peak, as well as the aromatic proton peaks in <sup>1</sup>H NMR spectroscopy. Further more, <sup>19</sup>F NMR was also employed to first show the disappearance of the para fluorine, and then the complete disappearance of the fluorinated moiety after exposure to a primary alkyl amine, hexylamine in this case. Finally, size-exclusion chromatography was used to show the shifts in molecular weight on the addition of a thiol-containing

molecule, as well as a second shift to longer retention time after the addition of hexylamine. After showing the successful addition of benzyl mercaptan, followed by the addition of hexylamine, an aromatic thiol (thiophenol) and an alkyl thiol (1-hexanethiol) were chosen to show the utility of this new, powerful tool in post-polymerization modification. Further demonstrating the robustness of this methodology, all of the thiol-para fluoro reactions were carried out in scintillation vials in ambient atmosphere, and without the use of dry solvents.

In order to prove the power and utility in this new post-polymerization technique, we have also demonstrated that the thiol-para fluoro click-chemistry, while attached to the ester, can have a range of different thiols used. As can be seen in Figure A 45, Figure A 46, Figure A 47, and Figure A 48 we have demonstrated that this chemistry can be achieved with a broad range of different thiols including a primary alkyl thiol (1-hexanethiol) as well as an aromatic thiol (thiophenol), respectively.

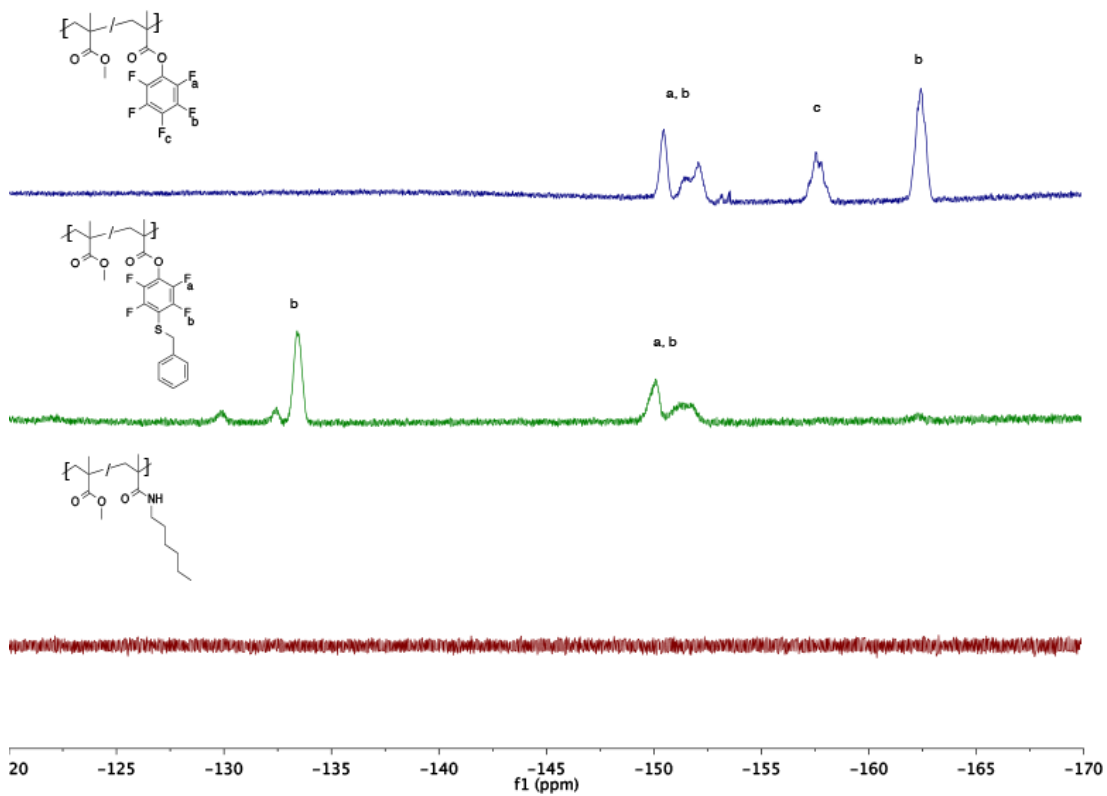


Figure 5.1  $^{19}\text{F}$  NMR of the parent pentafluorophenyl methacrylate polymer (top), the thiol-para fluoro post-polymerization modification (middle), and the post-polymerization of the still activated ester via primary alkyl amine (bottom)

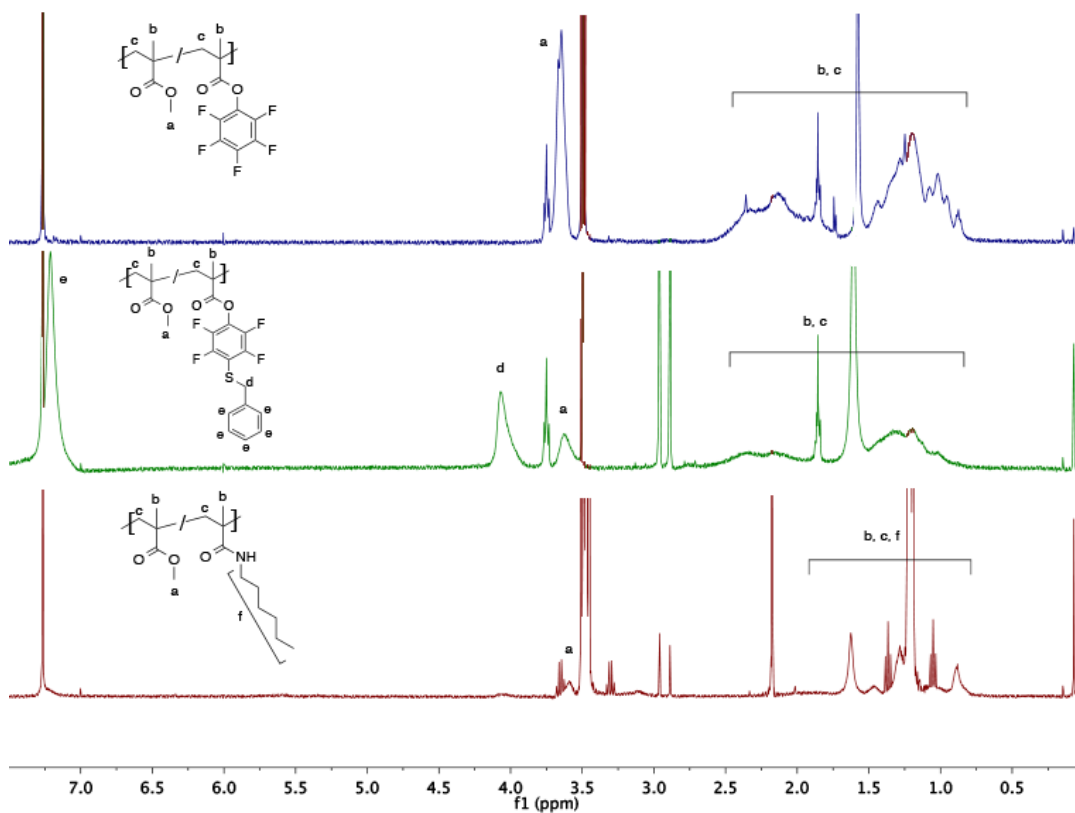


Figure 5.2  $^1\text{H}$  NMR spectra of sequential post-polymerization modifications through the pentafluorophenyl-activated ester.

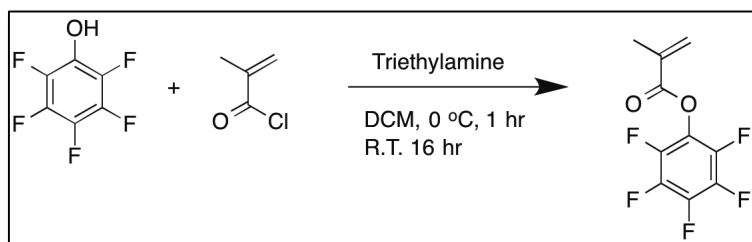
## 5.3 Experimental

### 5.3.1 General Methods

General Methods. Reagents were purchased from Aldrich and used as received. Size exclusion chromatography (SEC) was performed on a Tosoh EcoSEC dual detection (RI and UV) GPC system coupled to an external Wyatt Technologies miniDAWN Treos multi angle light scattering (MALS) detector and a Wyatt Technologies ViscoStarII differential viscometer. Samples were run in THF at 30 °C at a flow rate of 0.35 mL/min. The column set was one SuperH-L guard column, one Tosoh TSKgel SuperH3000 column (6x150mm), and one Tosoh TSKgel SuperH4000 column (6x150mm). Increment refractive index values ( $dn/dc$ ) were calculated online assuming 100% mass recovery (RI

as the concentration detector) using the Astra 6 software package (Wyatt Technologies) by selecting the entire trace from analyte peak onset to the onset of the solvent peak or flow marker. Absolute molecular weights and molecular weight distributions were calculated using the Astra 6 software package. Intrinsic viscosity ( $[\eta]$ ) and viscometric hydrodynamic radii ( $R_h$ ) were calculated from the differential viscometer detector trace and processed using the Astra 6 software.  $^1\text{H}$  NMR (400 MHz) spectra were recorded on a Varian Associates Mercury 400 spectrometer. Solvents ( $\text{CDCl}_3$  or  $d_8$ -THF) contained 0.03% v/v TMS as an internal reference, chemical shifts ( $\delta$ ) are reported in ppm relative to TMS. Peak abbreviations are used as follows: s=singlet, d=doublet, t=triplet, m=multiplet, br=broad.

### **5.3.2 Synthesis of pentafluorophenyl methacrylate**

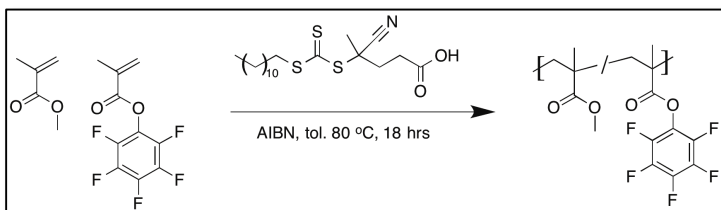


2.5 g of  
pentafluorophenol  
(0.014 mol) was added

to a RBF and dissolved in 5 mL of dry DCM. The RBF was sealed with a rubber septum and degassed for 25 minutes with nitrogen. The RBF was then placed in an ice bath and then 2.08 mL of triethylamine (0.015 mol) was added via syringe. Next 1.44 mL of methacryloyl chloride was added dropwise to the RBF via gas-tight syringe. The solution was allowed to stir at 0 °C for one hour, then gradually warmed to room temperature and allowed to stir for 16 hours. The organic layer was washed twice with DI water, twice with 1M HCl, twice with saturated sodium bicarbonate, and twice with brine. Organic layer was dried with anhydrous sodium sulfate and evaporated to dryness under reduced pressure to yield 2.94 g of a pale yellow oil. 78% yield. ( $^1\text{H}$  NMR 400 MHz,  $\text{CDCl}_3$ ):  $\delta$

ppm 6.49 (s), 5.8 (s), 2.1 (tr). ( $^{19}\text{F}$  NMR 400 MHz,  $\text{CDCl}_3$ ):  $\delta$  ppm -153.4 (d), -158.9 (tr), -163.2 (tr).

### 5.3.3 Polymer synthesis

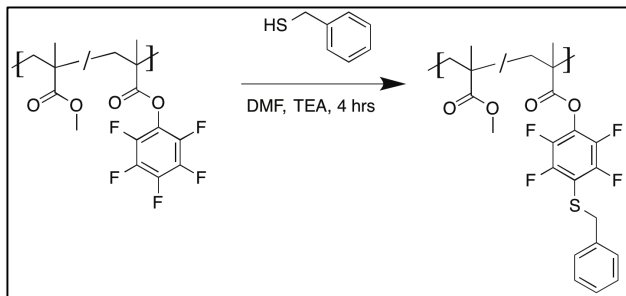


0.28 g of uninhibited methyl methacrylate (2.8 mmol) and 0.71 g of pentafluorophenyl methacrylate (2.8 mmol)

were added into a RBF. Next, 8.0 mg of 4-cyano-4-[(dodecylsulfanylthiocarbonyl)sulfanyl] pentanoic acid (0.02 mmol), acting as a chain transfer agent, was added to the RBF followed by 0.066 mg of azoisobutyronitrile (0.004 mmol), acting as a radical source, were added to the RBF. Finally, 2 mL of dry toluene was added into the RBF. The RBF was then sealed with a rubber septum and degassed with nitrogen for a half hour. After degassing, the RBF was plunged into an 80 °C oil bath to initiate polymerization. Polymerization was allowed to run for 18 hours and was quenched by removing RBF from bath and exposing solution to air. The solution was precipitated into cold methanol to yield a white powder. 0.216 g of polymer was recovered, 21% conversion.  $^1\text{H}$  NMR (400 MHz,  $\text{CDCl}_3$ ):  $\delta$  ppm 3.75-3.55 (br s), 2.64-1.67 (br m), 1.71-0.75 (br m).  $^{19}\text{F}$  NMR (400 MHz,  $\text{CDCl}_3$ ):  $\delta$  ppm -149.9- -152.8 (br m), -156.9- -158.5 (br s), -161.9- -163.1 (br s). SEC (THF)  $M_w$  = 14.0 kDa, PDI 1.09



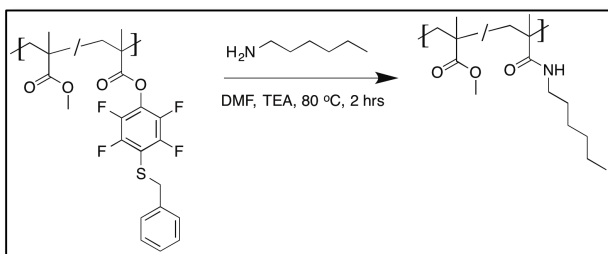
### 5.3.4 Representative thiol-para fluoro post polymerization modification:



0.1 g of poly(methyl methacrylate-co-pentafluorophenyl methacrylate) was added into a 20 mL scintillation vial. The polymer was then dissolved in 1 mL of DMF. Next, a large

excess of benzyl mercaptan (10 drops) and triethylamine (10 drops) was added to the scintillation vial. The reaction was stirred for four hours and then precipitated into room temperature methanol. The polymer solution was then vacuum filtered and subsequently washed numerous times with cold methanol to reduce the unpleasant odor. 0.89 g of a white powder was recovered.  $^1\text{H}$  NMR (400 MHz,  $\text{CDCl}_3$ ):  $\delta$  ppm 7.35-7.05 (br s), 4.21-3.95 (br s), 3.70-3.45 (br s), 2.60-0.75 (br m).  $^{19}\text{F}$  NMR (400 MHz,  $\text{CDCl}_3$ ):  $\delta$  ppm -134.2 (br s), -149.7- -153.3 (br m). SEC (THF) **P5.2**:  $M_w$  = 16.4 kDa, PDI = 1.08. **P5.3**:  $M_w$  = 17.6 kDa, PDI = 1.11. **P5.4**:  $M_w$  = 17.7 kDa, PDI = 1.08.

### 5.3.5 Representative post-polymerization modification of the active ester:



0.05 g of the benzyl mercaptan functionalized polymer was dissolved in 0.5 mL of DMF and added into a 5 mL RBF. Next, a large excess of

hexylamine (10 drops) and triethylamine (10 drops) was added to the RBF. The RBF was then sealed with a rubber septum and degassed with nitrogen for 20 minutes. The RBF was then submerged into a 80 °C oil bath and stirred for 2 hours. The polymer was then precipitated into diethyl ether yielding an off-white sticky solid. 0.021 grams were

recovered.  $^1\text{H}$  NMR (400 MHz,  $\text{CDCl}_3$ ):  $\delta$  ppm 3.67 (br s), 2.73-0.89 (br m). SEC (THF)

$M_w = 9.45$  kDa, PDI = 1.17.

# APPENDIX

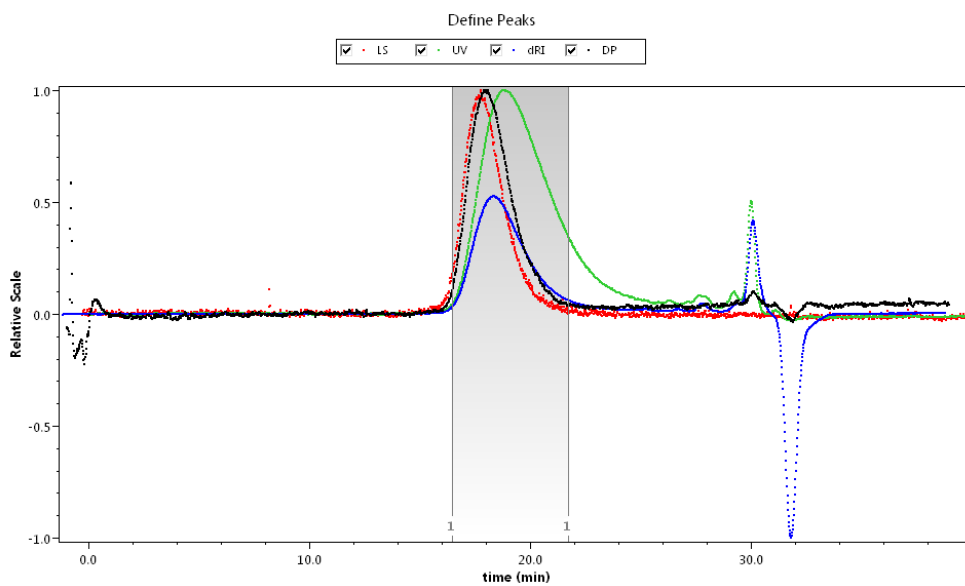


Figure A 1 P1 SEC trace see page 30

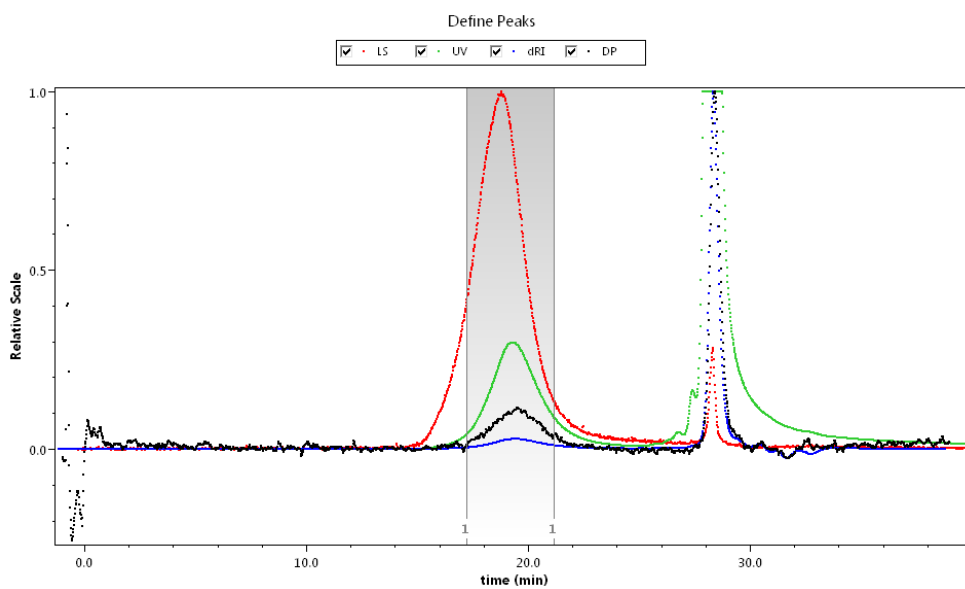


Figure A 2 N1 SEC trace see page 32

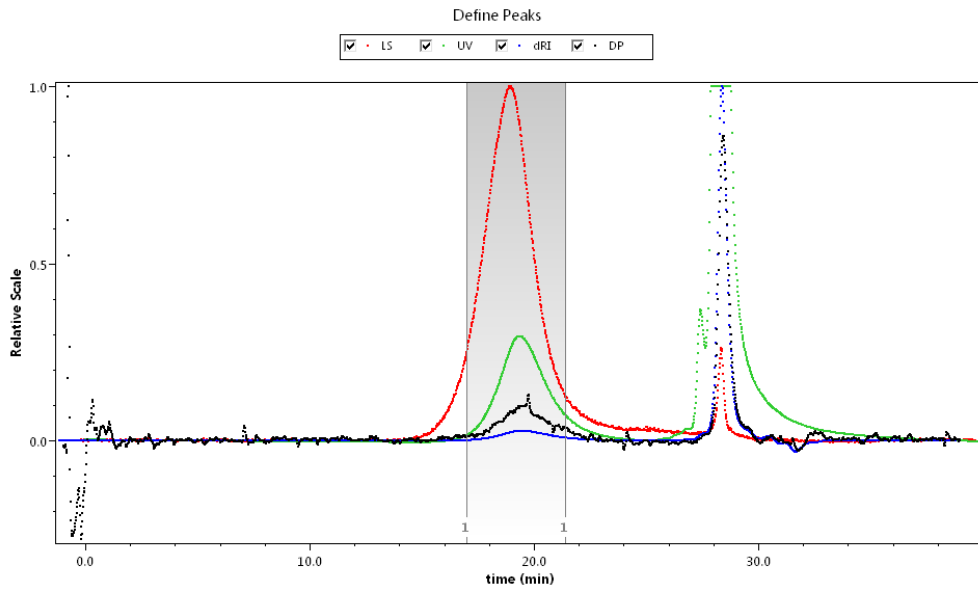


Figure A 3 uN1 SEC trace see page 33

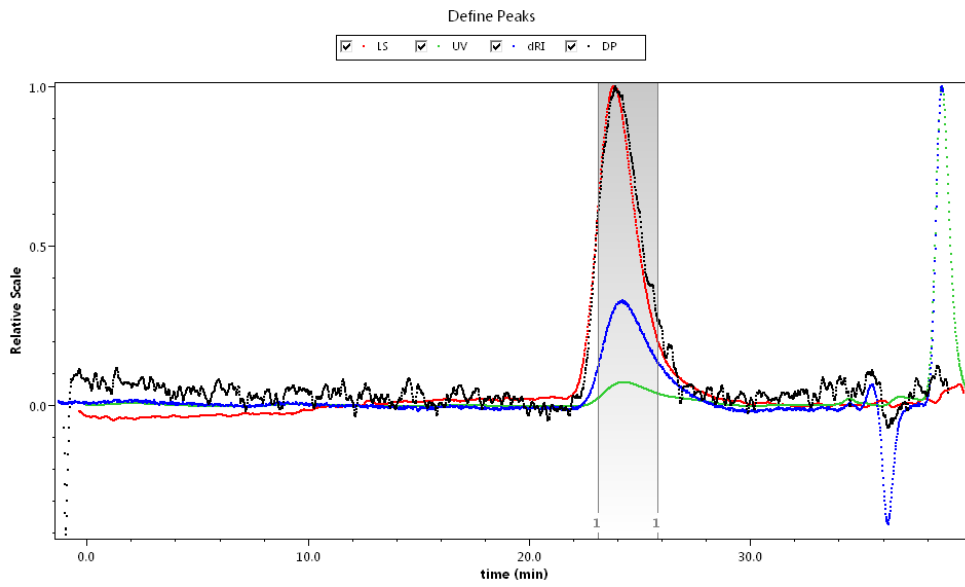


Figure A 4 Oxidized uN1 SEC trace see page 34

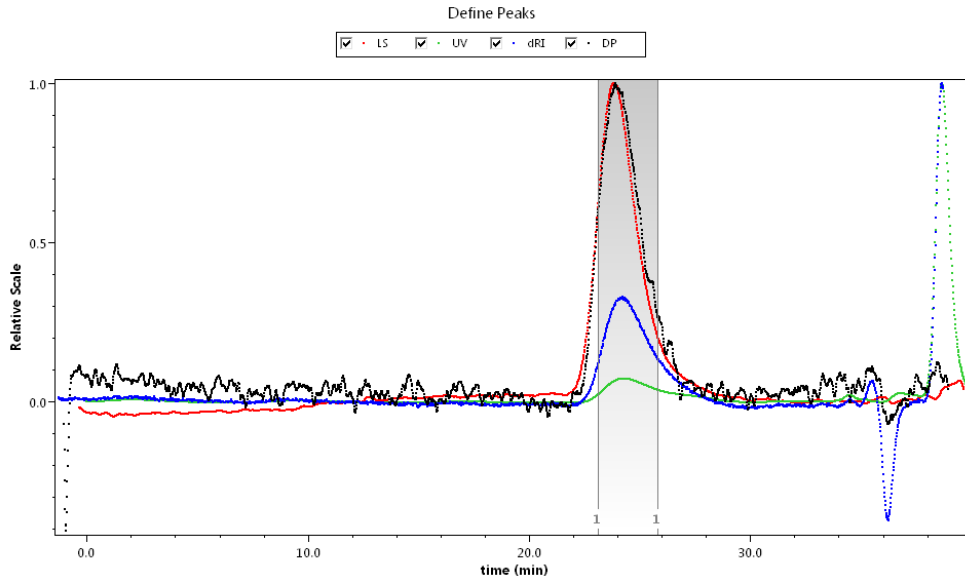


Figure A 5 P3.1 SEC trace see page 50

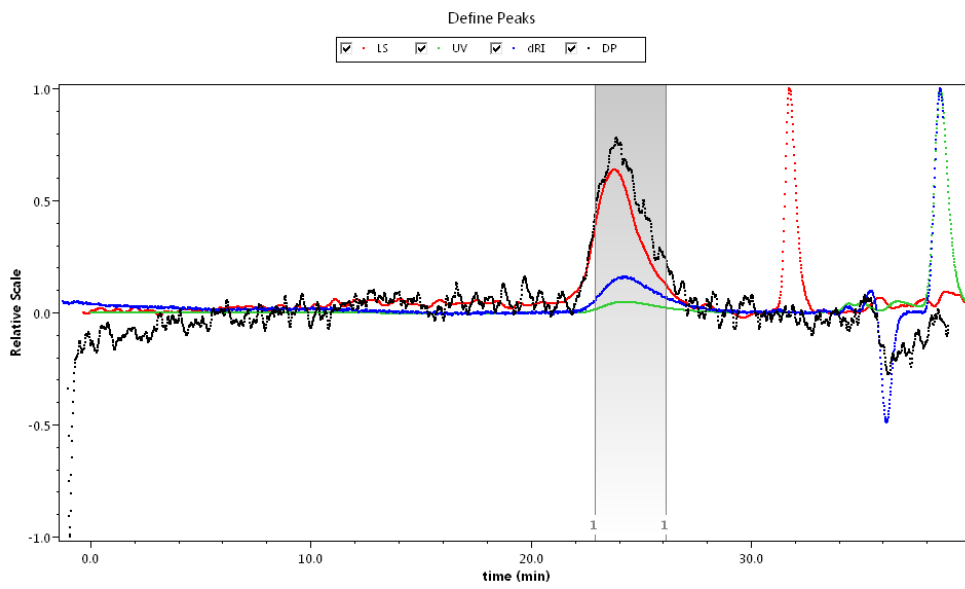


Figure A 6 P3.2 SEC trace see page 50

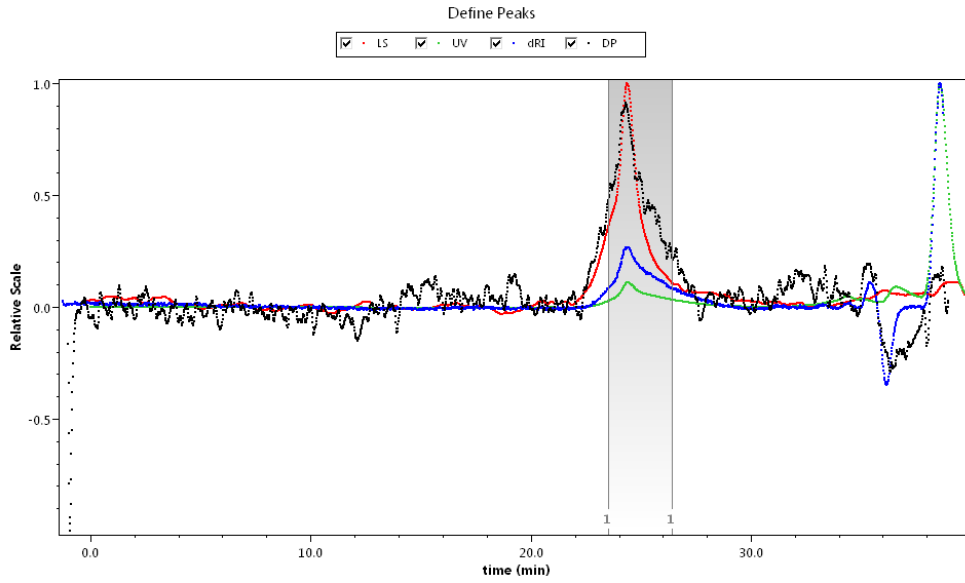


Figure A 7 P3.3 SEC trace see page 50

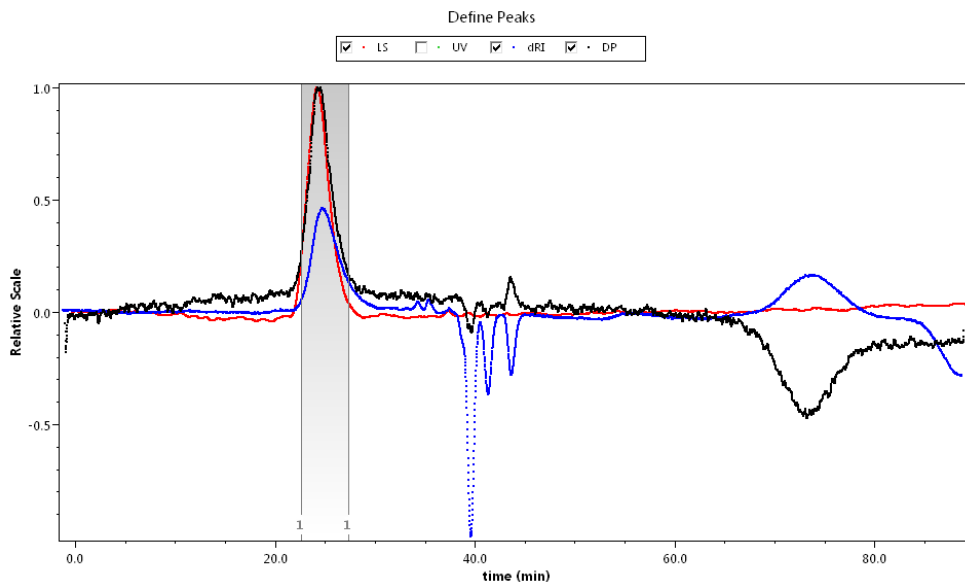


Figure A 8 P3.4 SEC trace see page 52

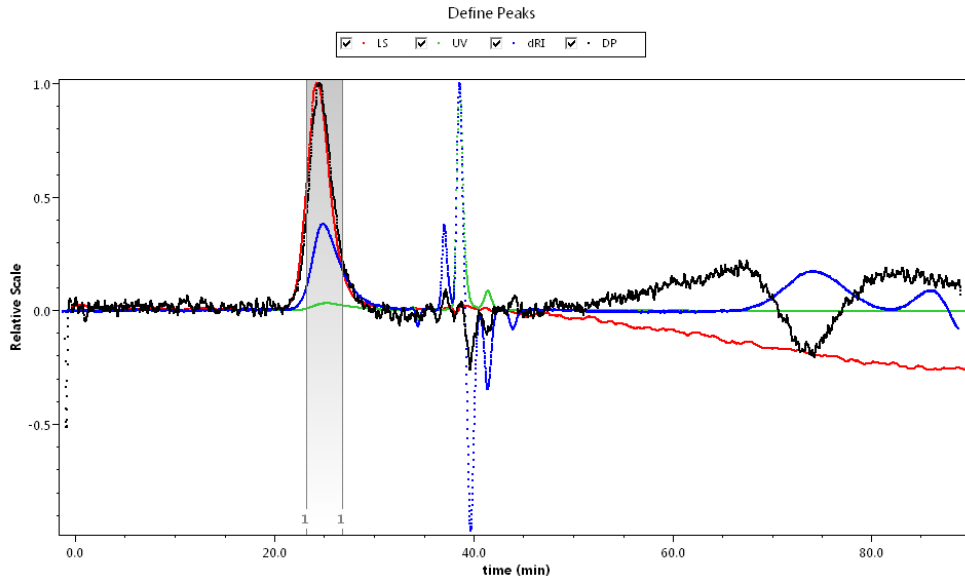


Figure A 9 N3.4 SEC trace see page 53

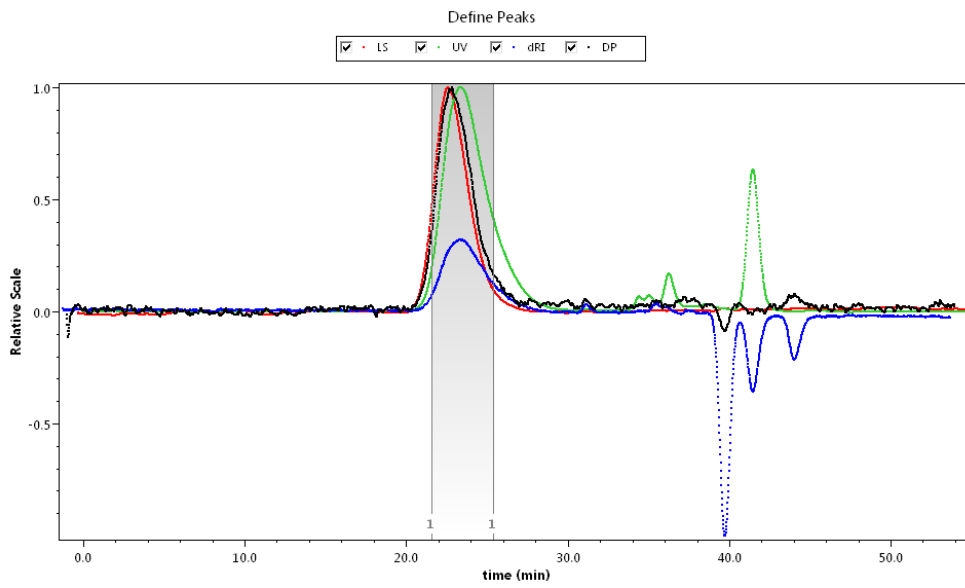


Figure A 10 P3.5 SEC trace see page 53

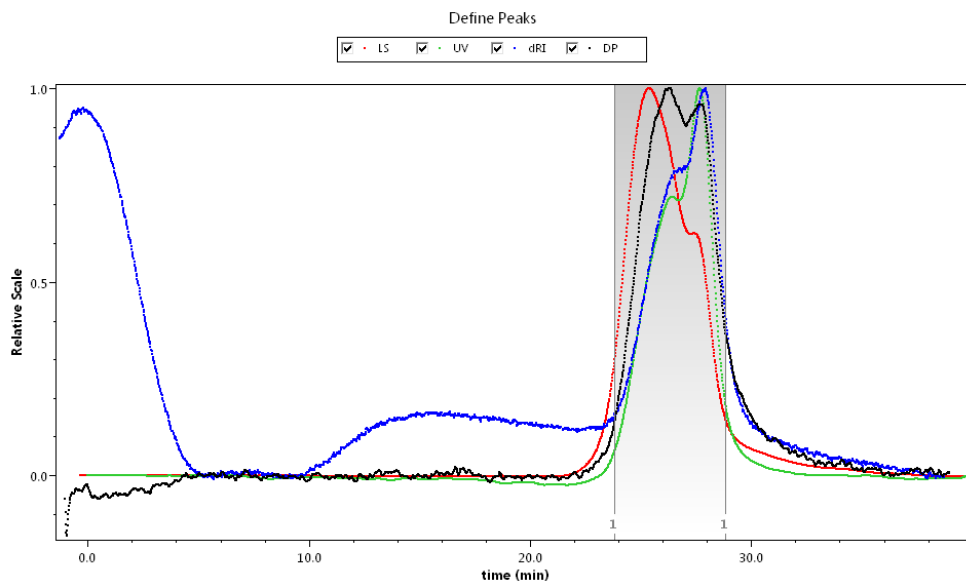


Figure A 11 P4.1 SEC trace see page 69

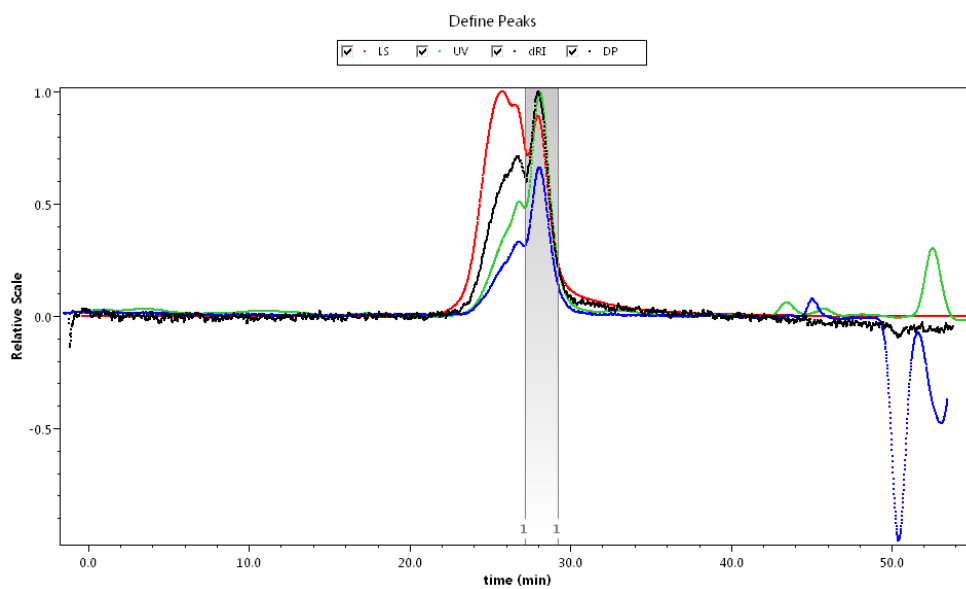


Figure A 12 P4.2 SEC trace see page 69



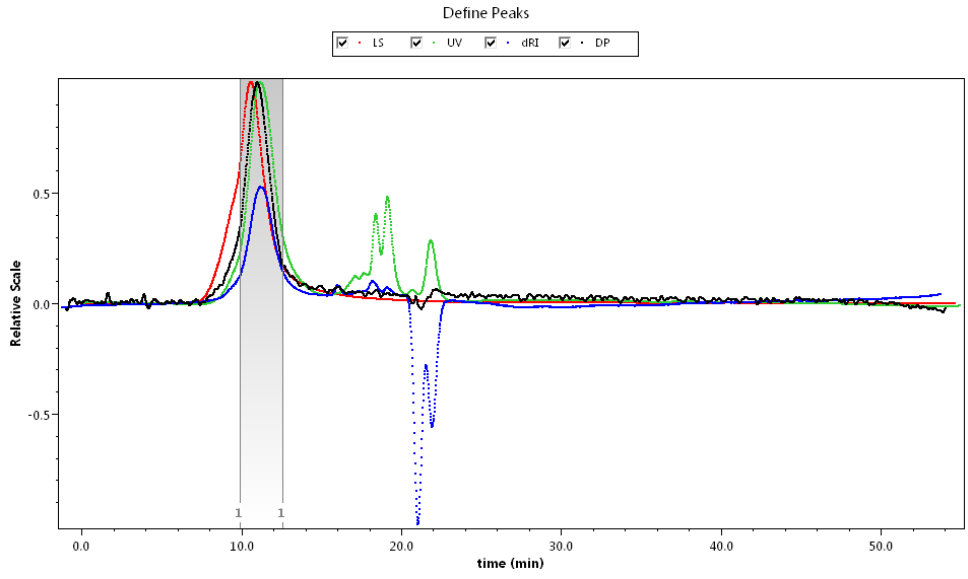


Figure A 13 P4.7 SEC trace see page 69

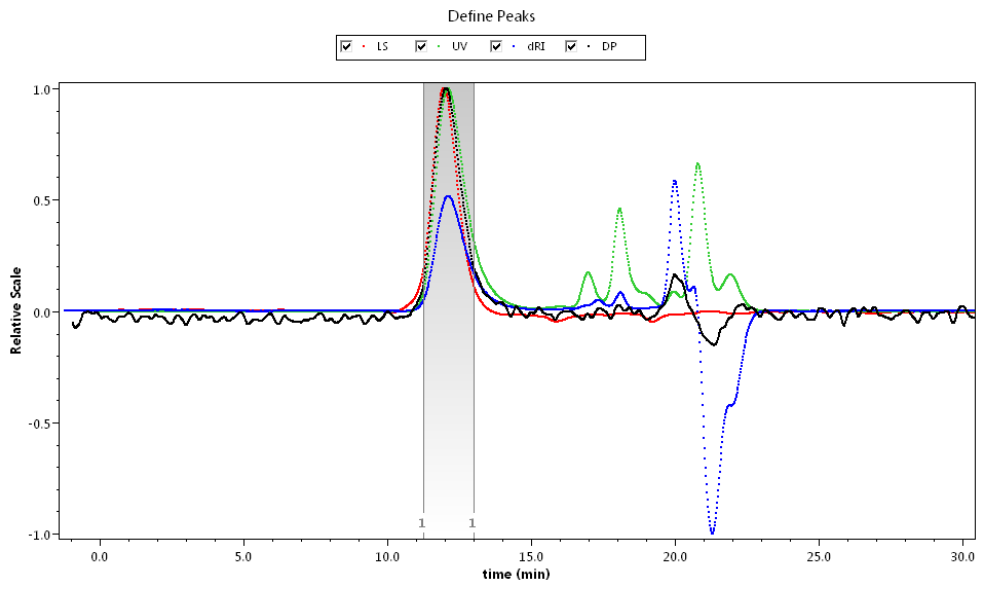


Figure A 14 P5.1 SEC trace see page 78

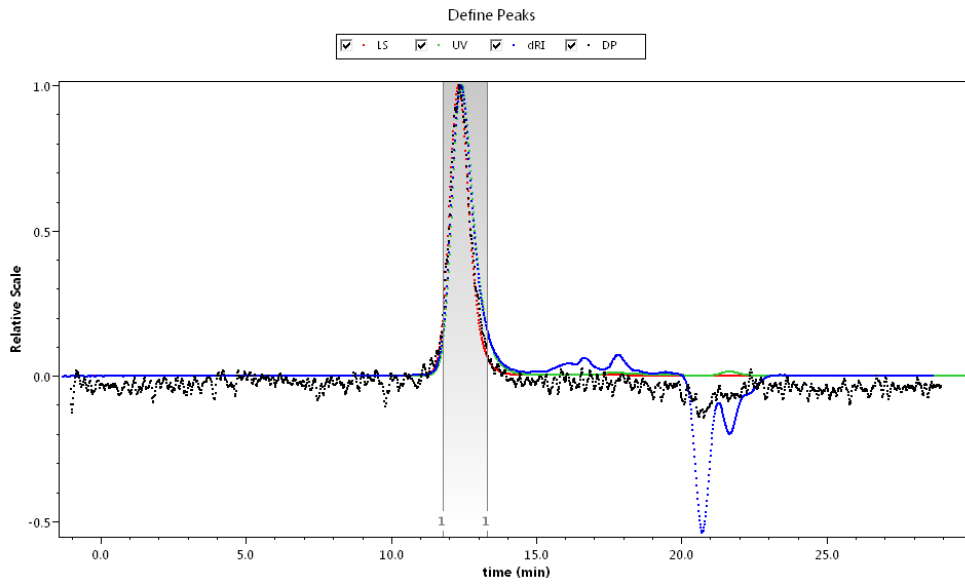


Figure A 15 P5.2 SEC trace see page 79

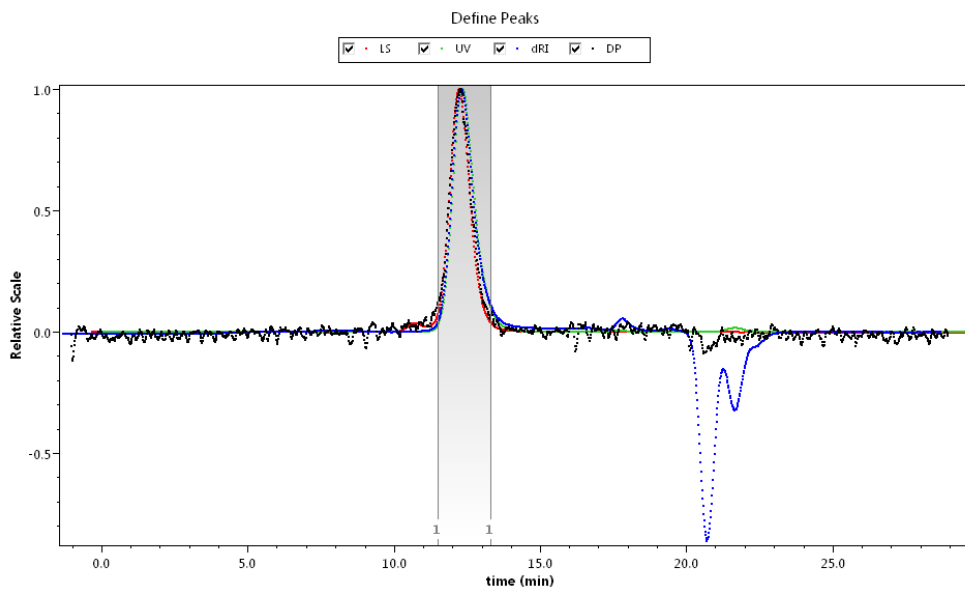


Figure A 16 P5.3 SEC trace see page 79

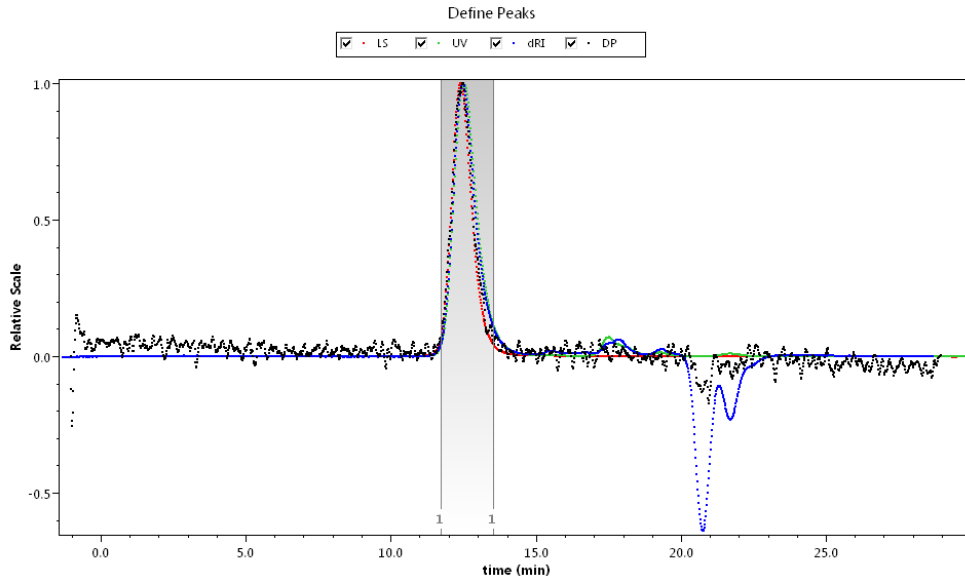


Figure A 17 P5.4 SEC trace see page 79

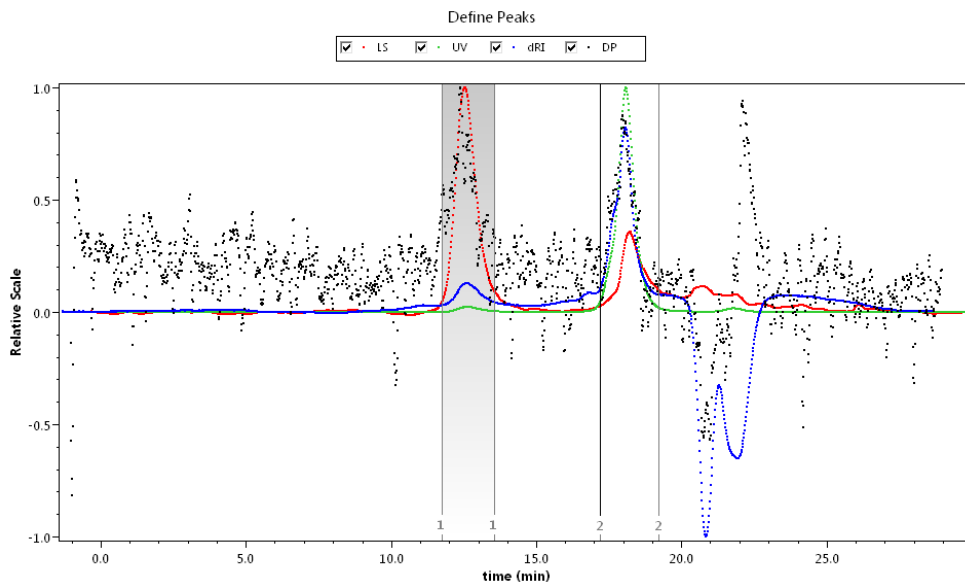


Figure A 18 P5.5 SEC trace see page 79

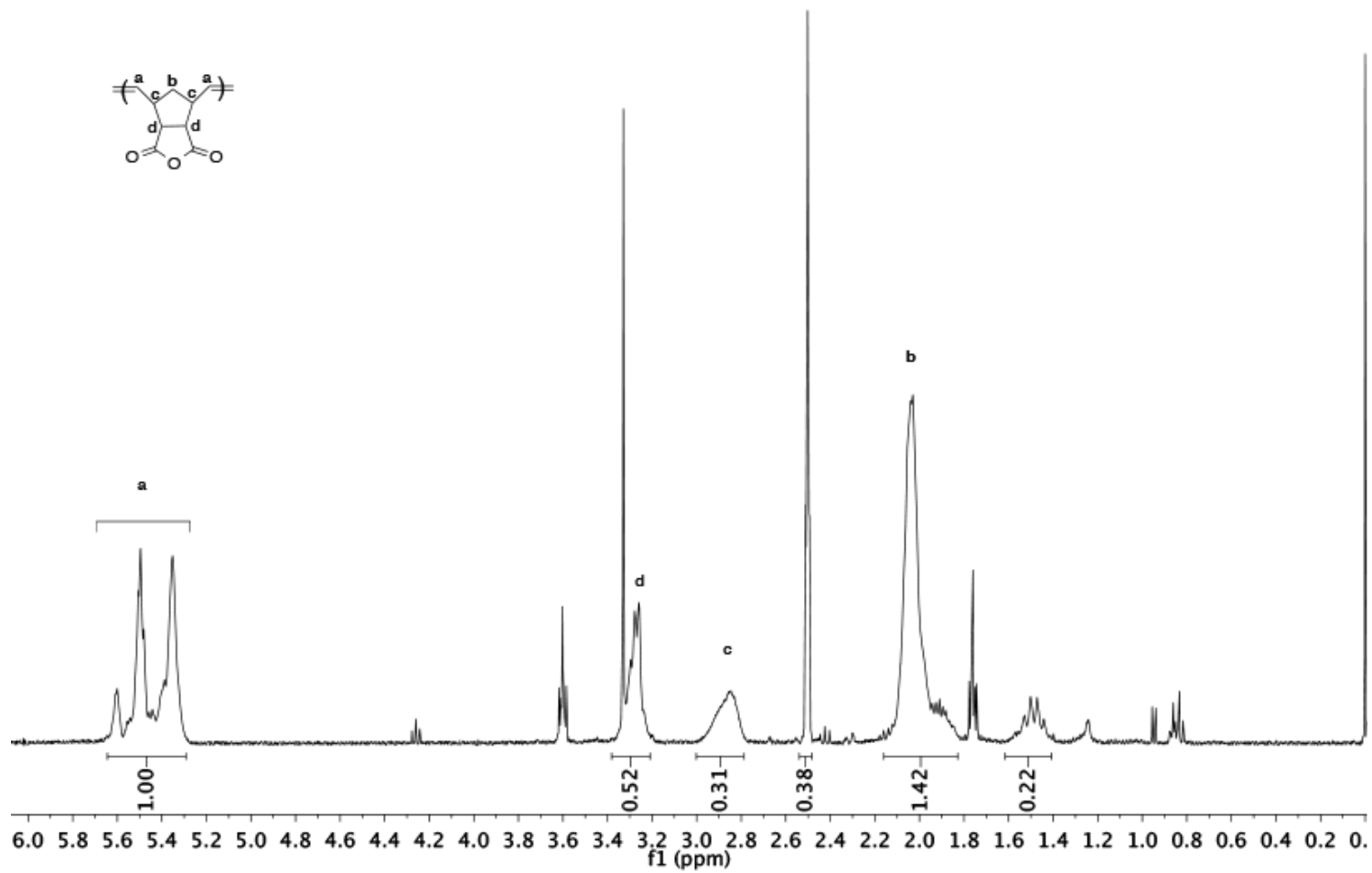


Figure A 19 P1 proton NMR see page 30

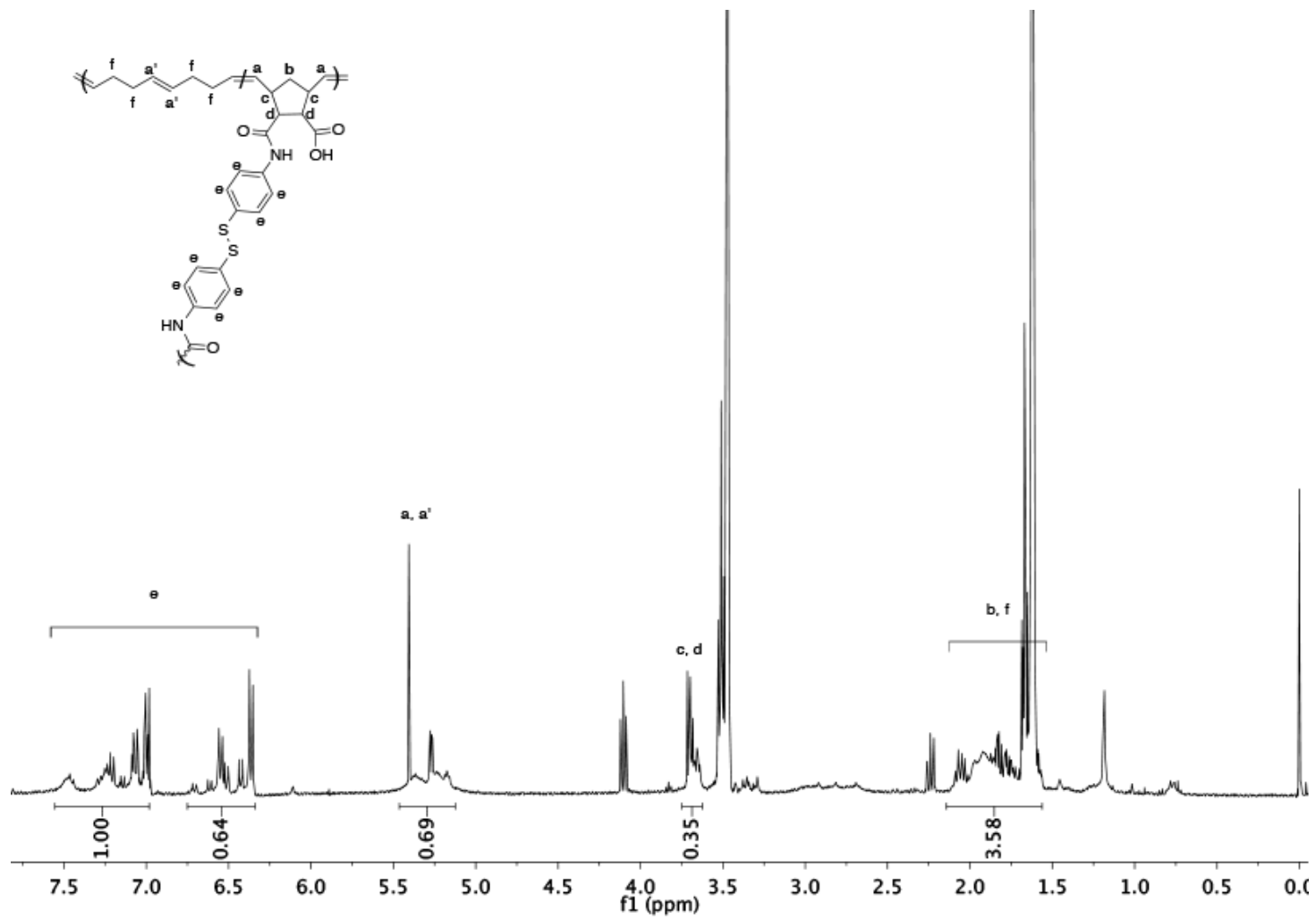


Figure A 20 N2 proton NMR see page 32

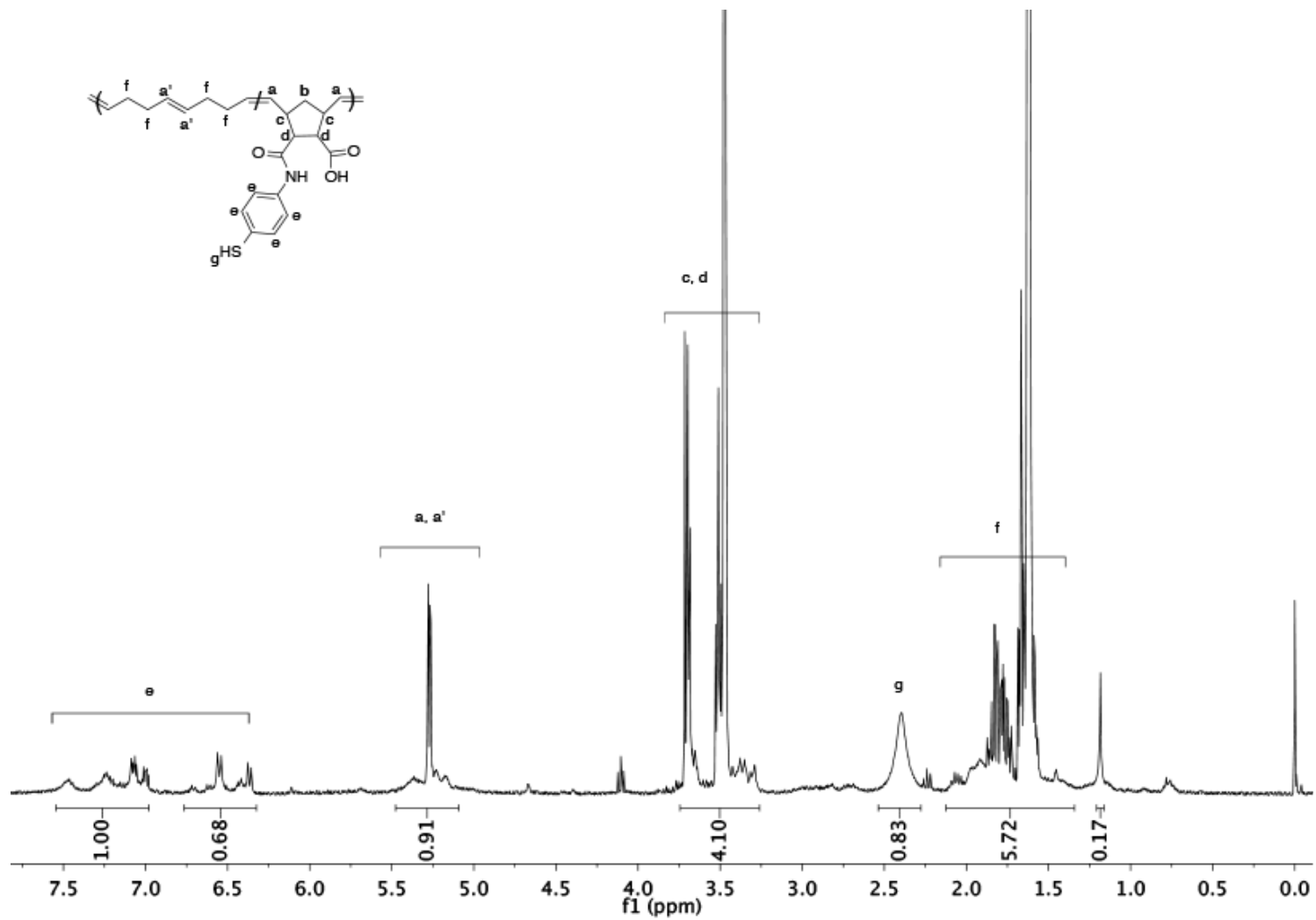


Figure A 21 uN2 proton NMR see page 33

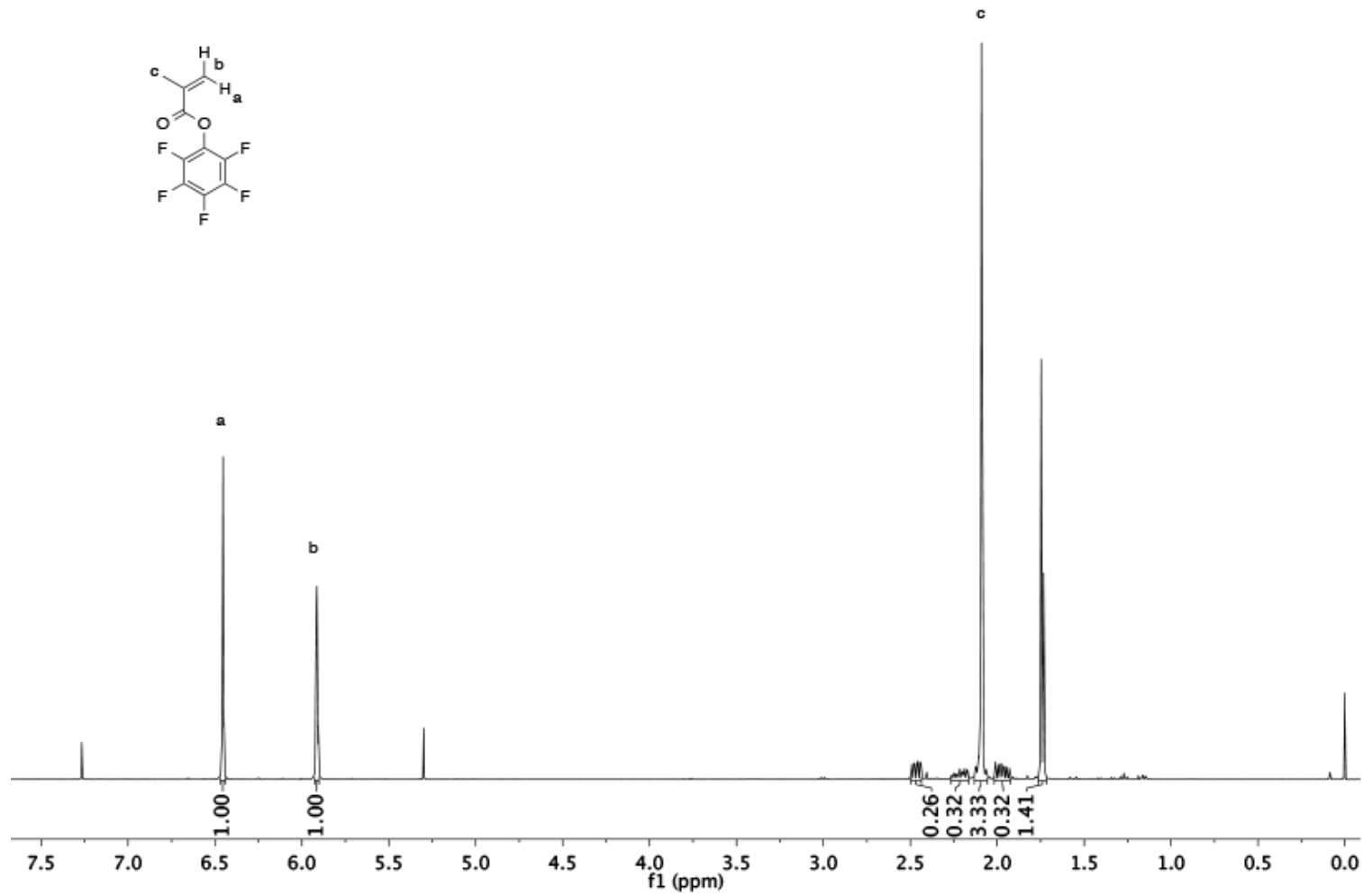


Figure A 22 Pentafluorophenyl methacrylate proton NMR see page 49

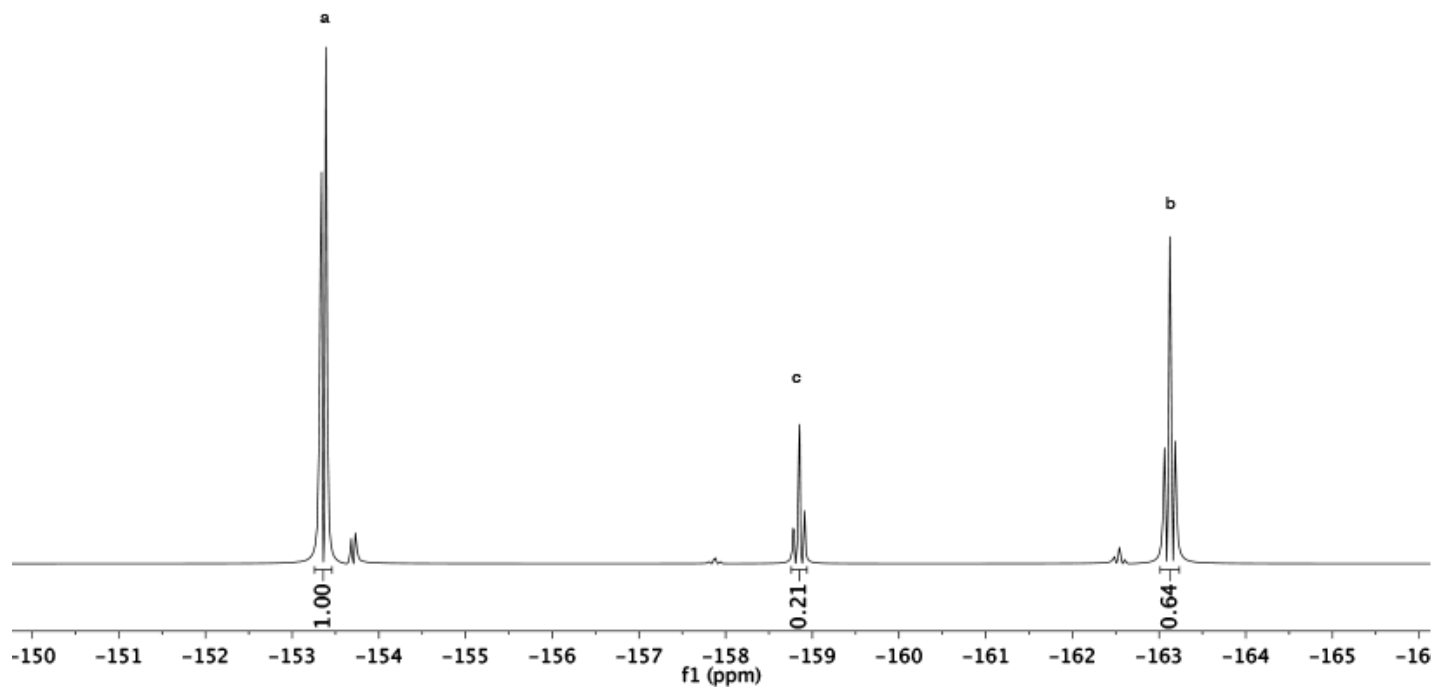
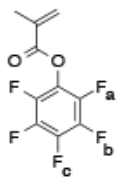
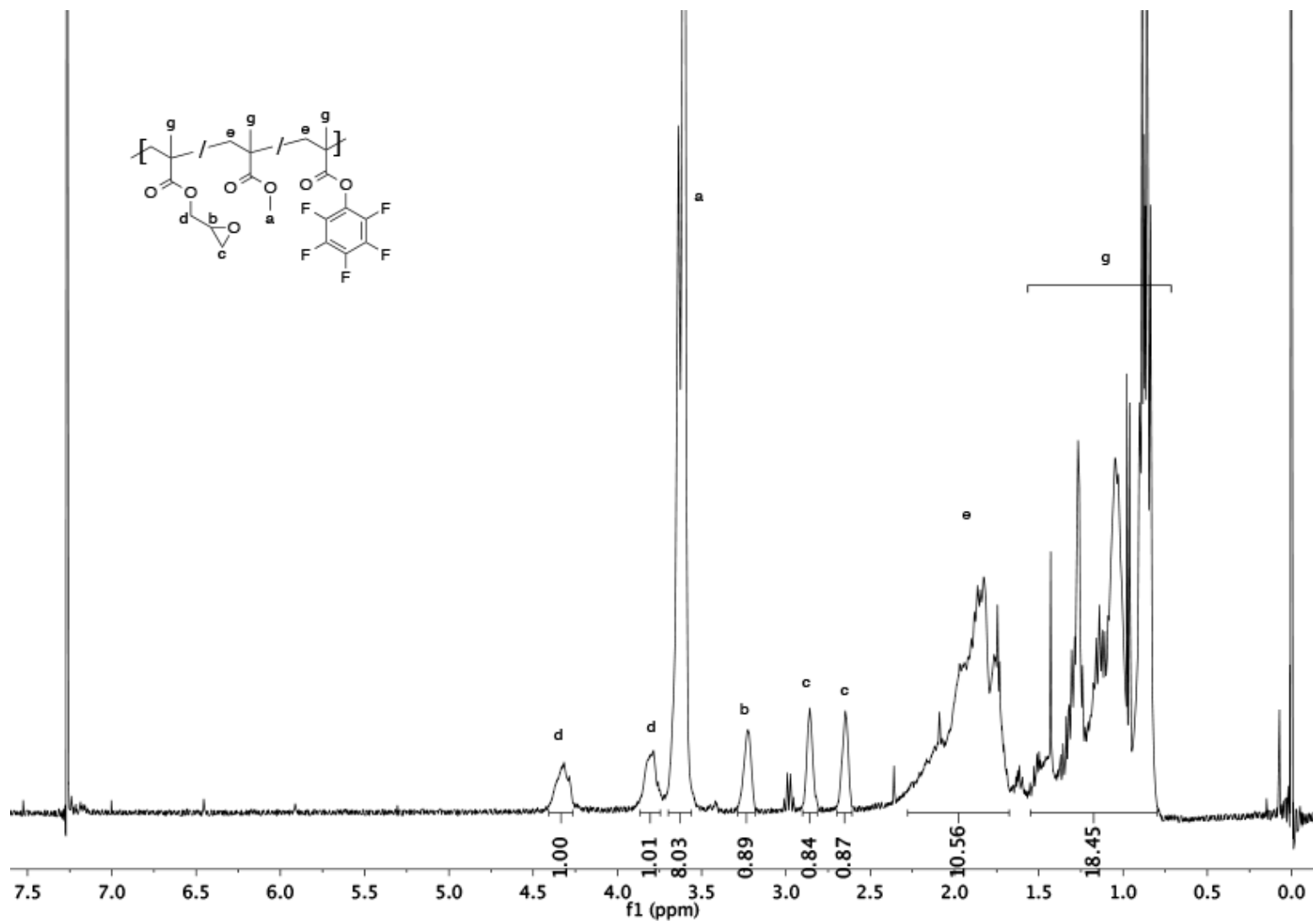


Figure A 23 Pentafluorophenyl methacrylate fluorine NMR see page 49





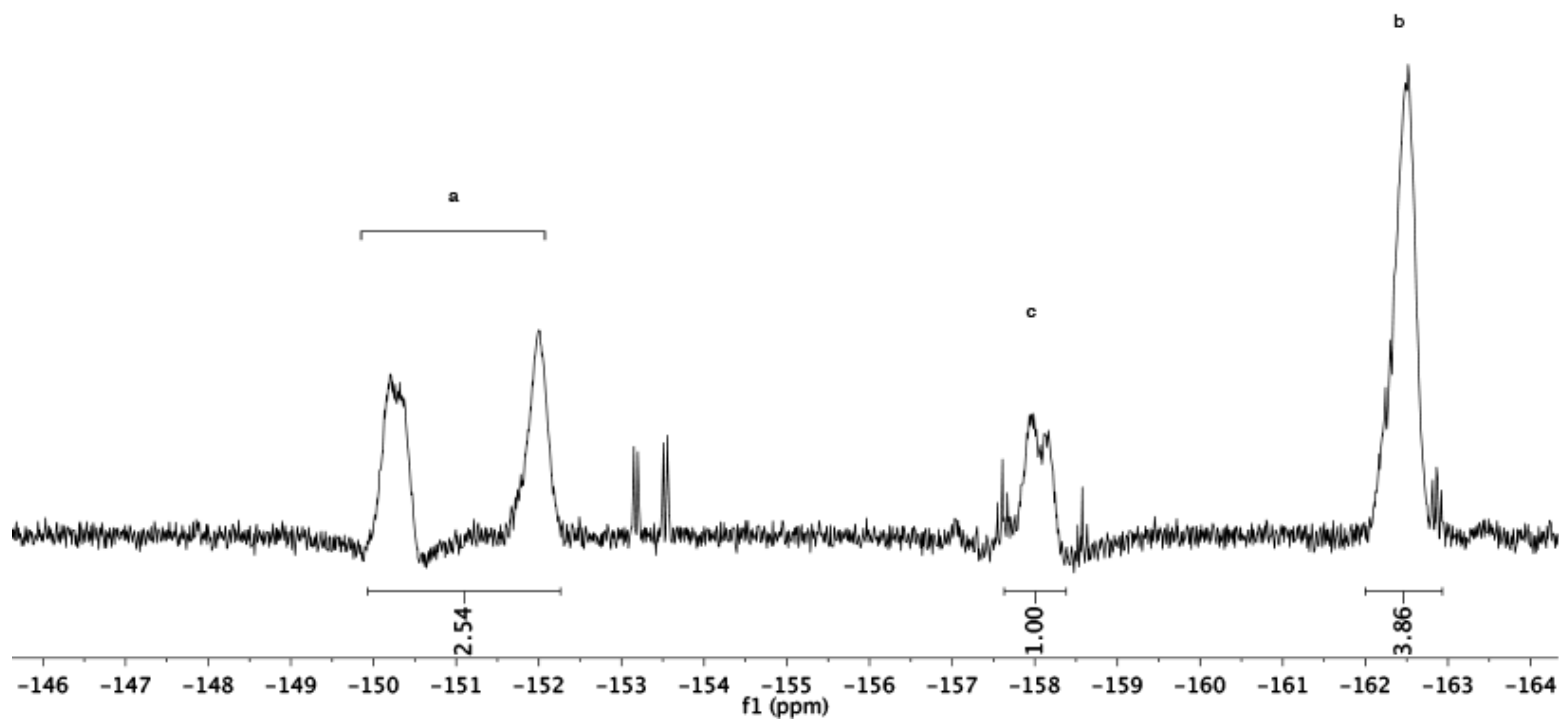
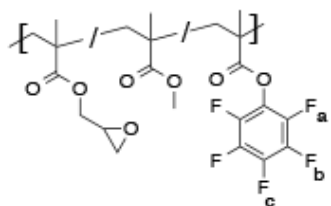


Figure A 25 P3.1 fluorine NMR see page 50

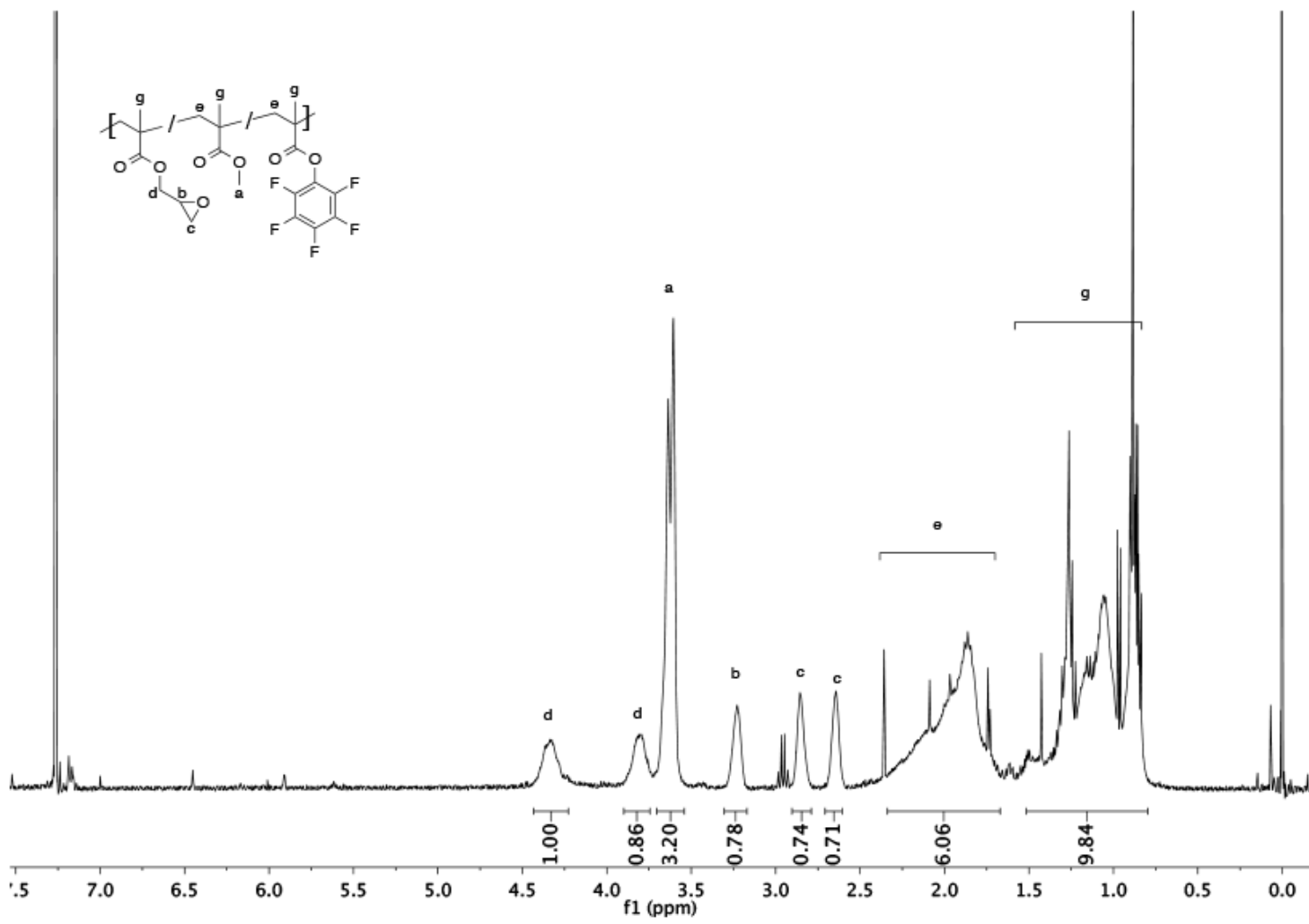


Figure A 26 P3.2 proton NMR see page 50

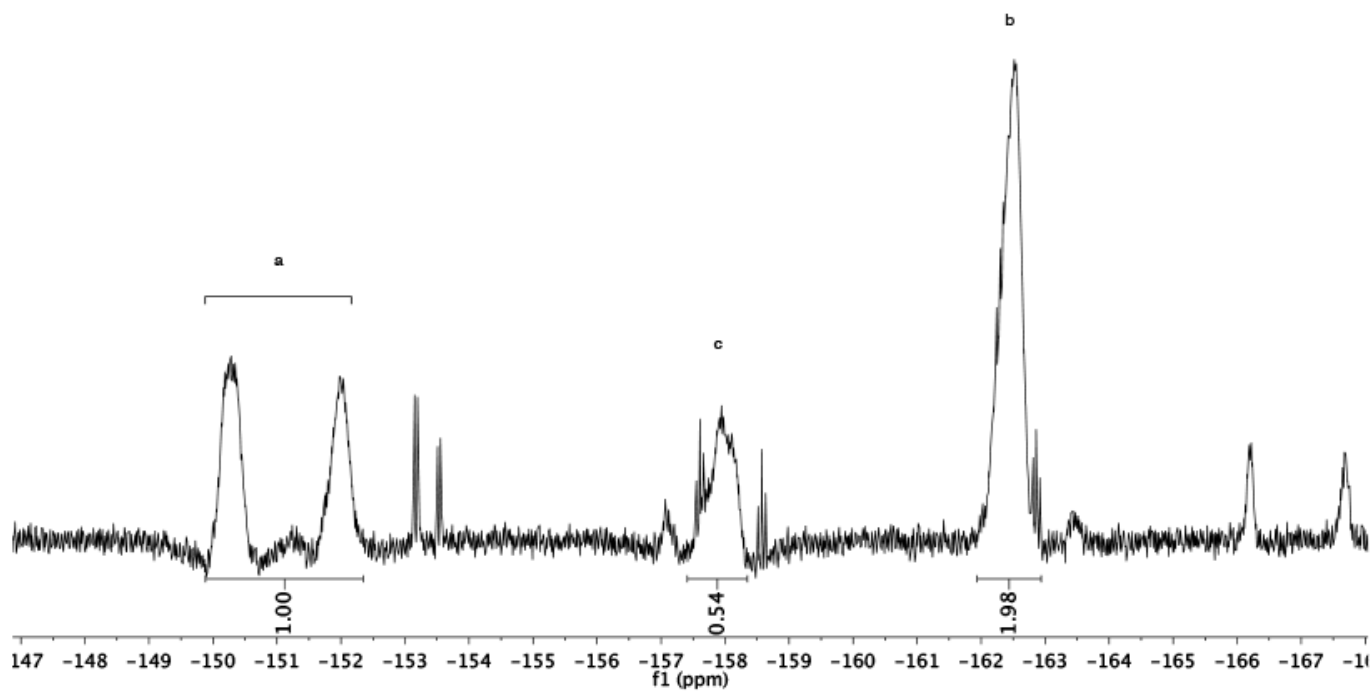
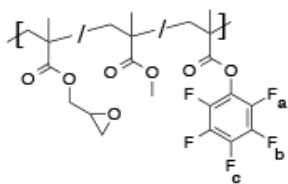


Figure A 27 P3.2 fluorine NMR see page 50

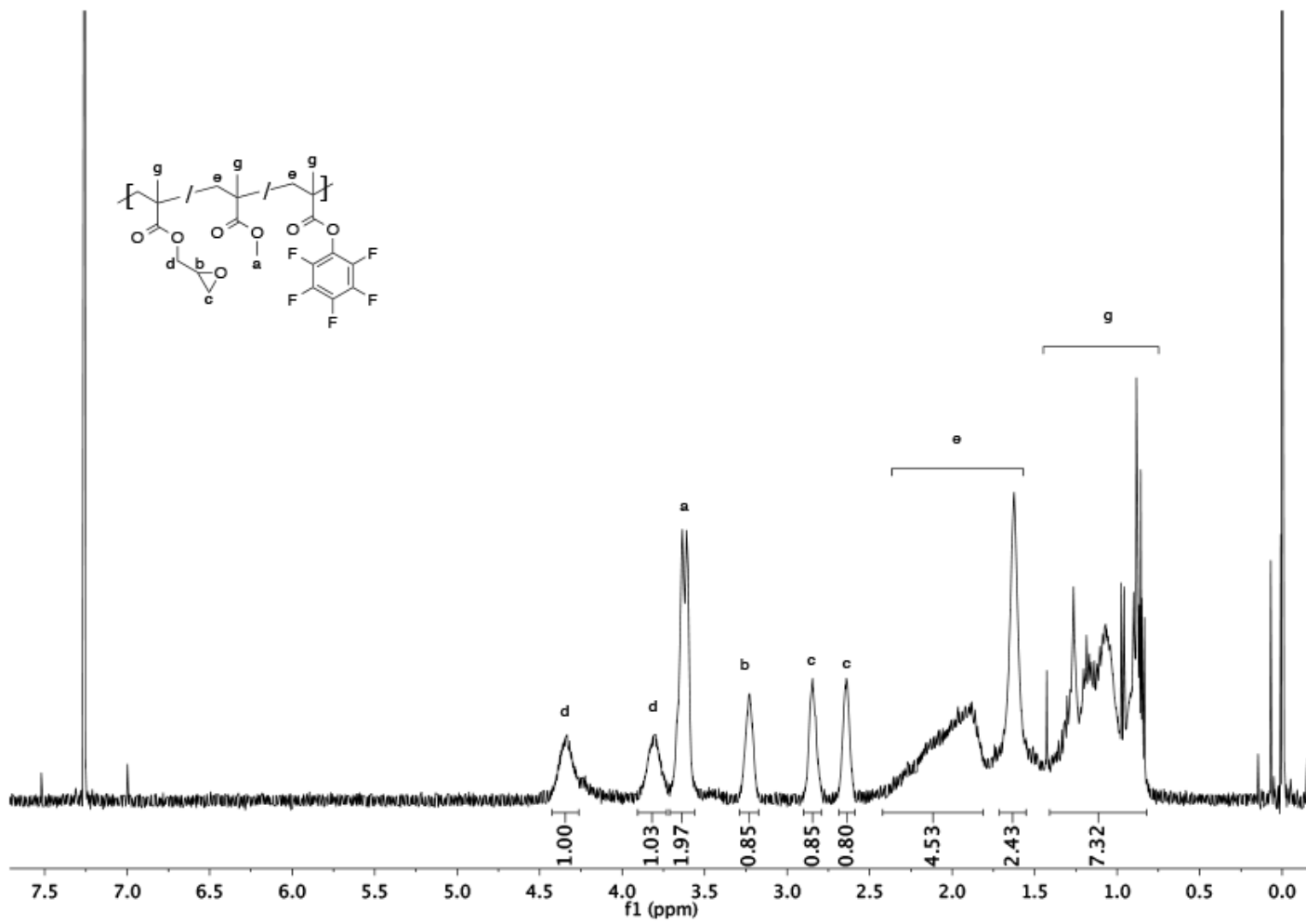


Figure A 28 P3.3 proton NMR see page 50

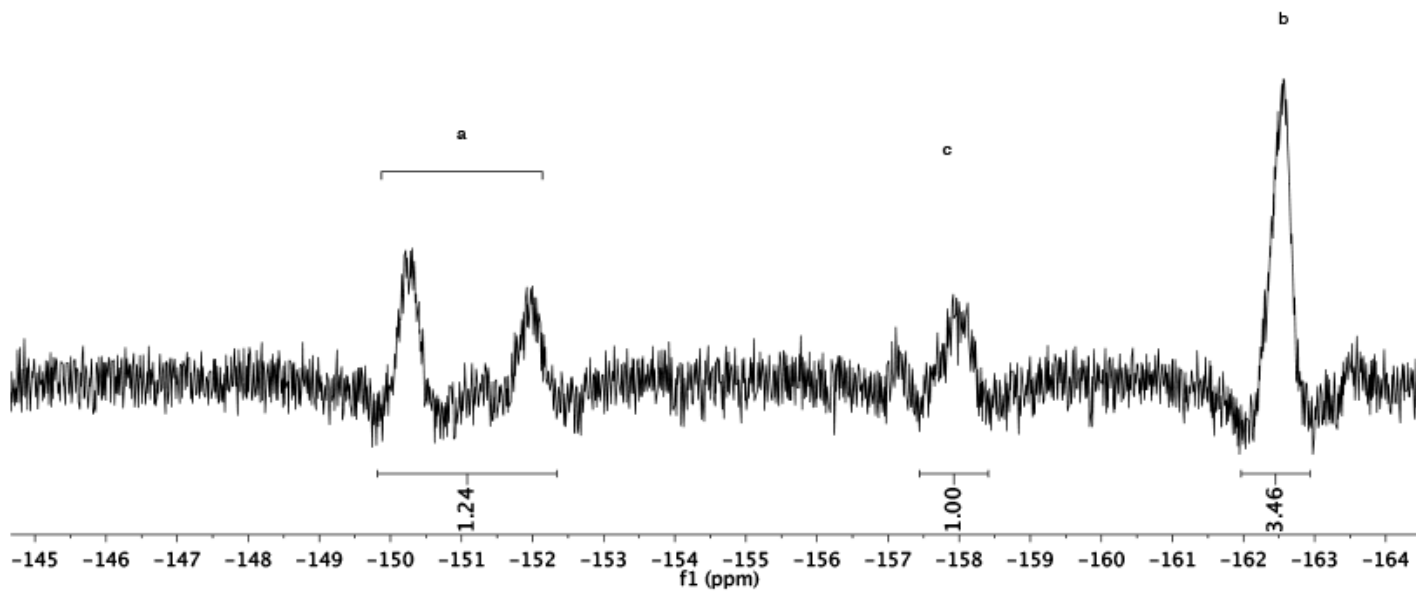
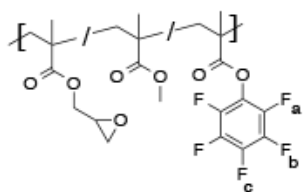


Figure A 29 P3.3 fluorine NMR see page 50

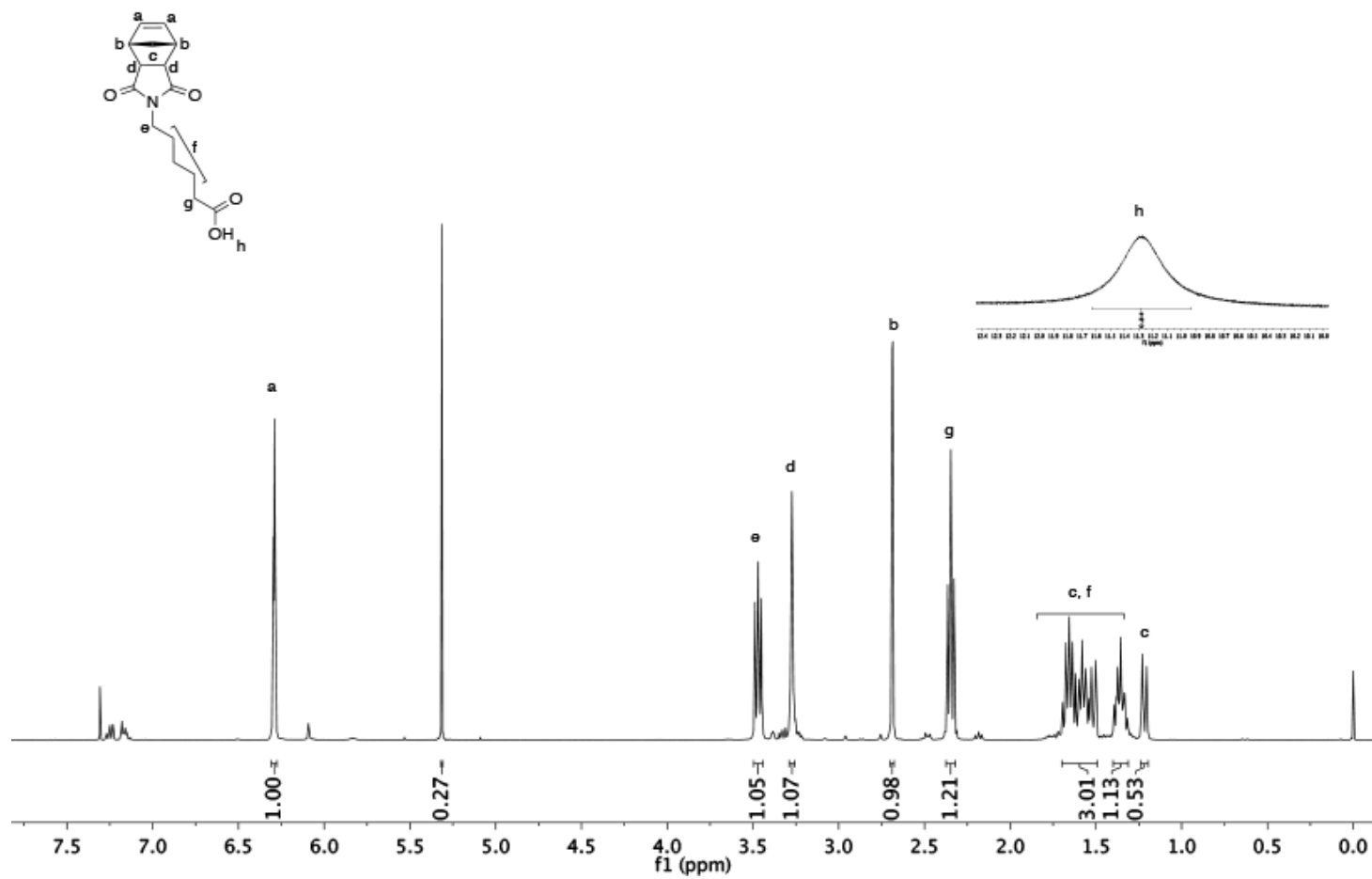


Figure A 30 hexanoic acid norbornene imide proton NMR see page 65

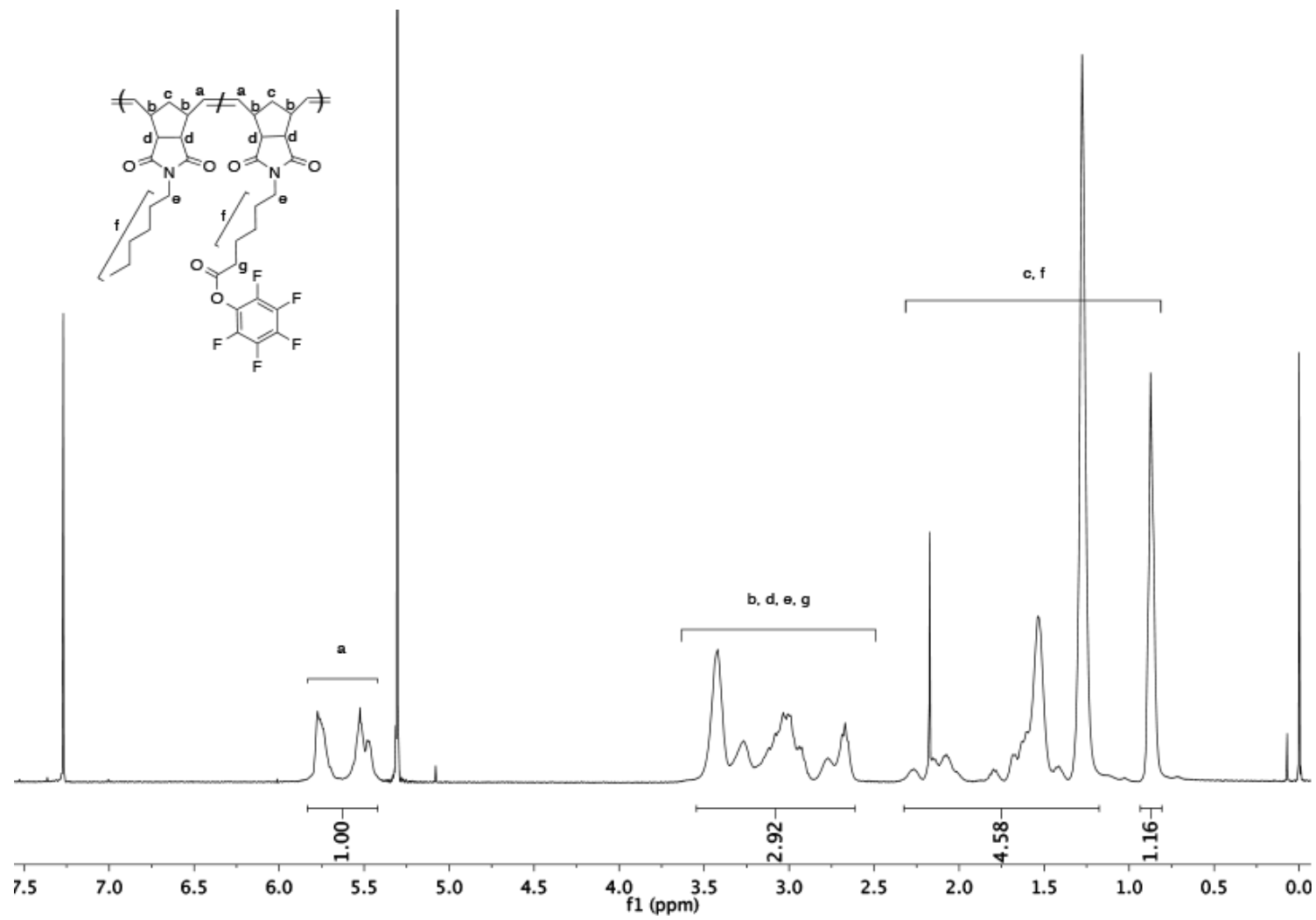


Figure A 31 P4.1 proton NMR see page 69



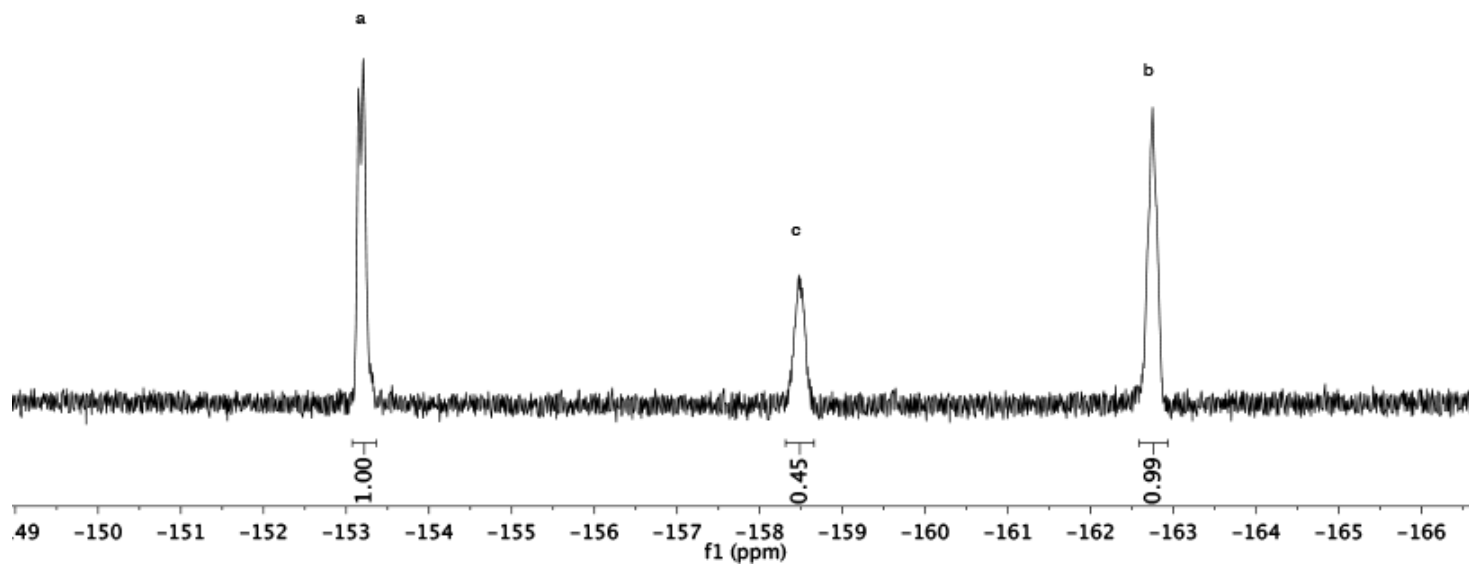
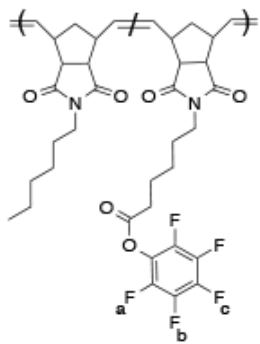


Figure A 32 P4.1 fluorine NMR see page 69

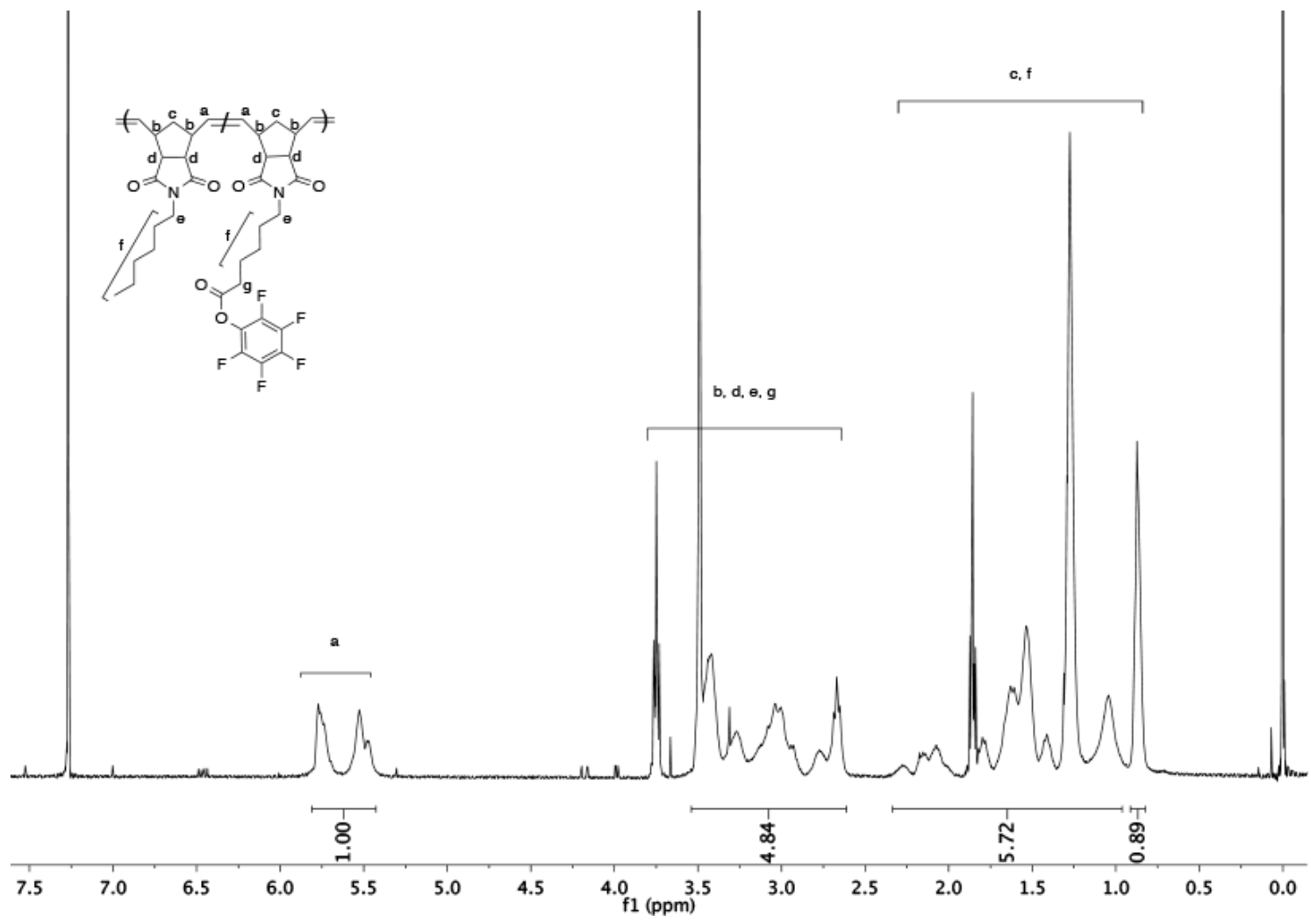


Figure A 33 P4.2 proton NMR see page

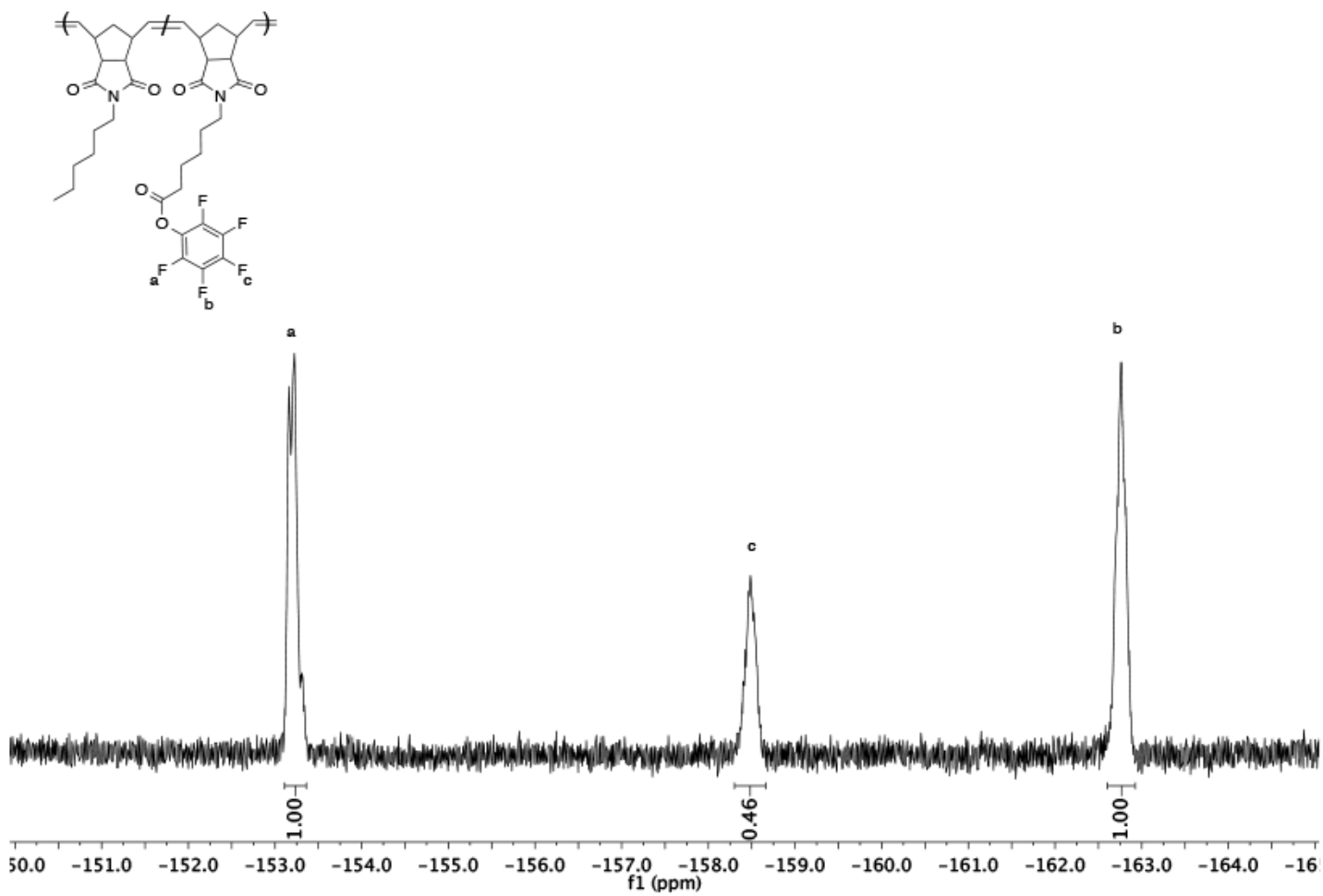


Figure A 34 P4.2 fluorine NMR see page 69

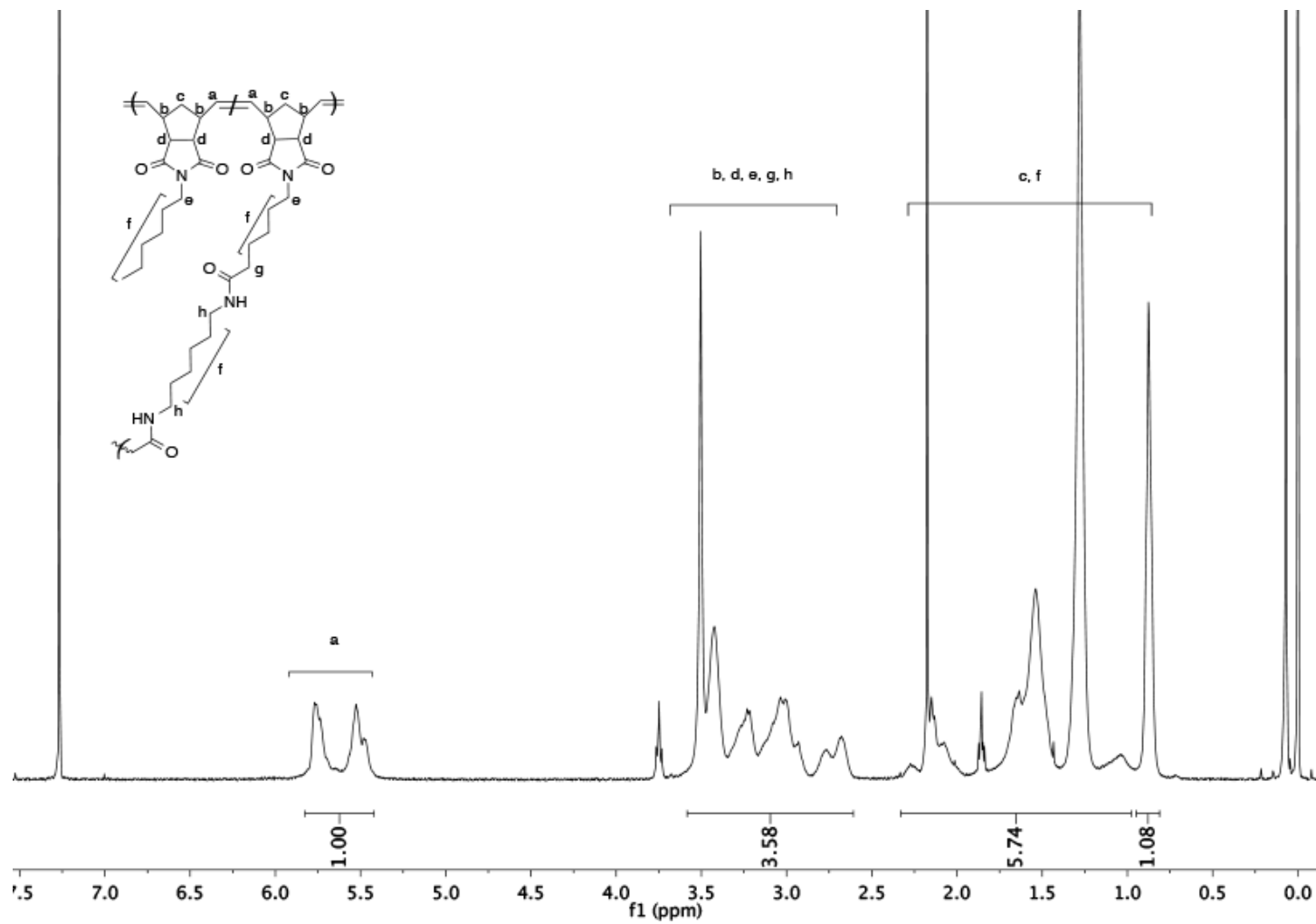


Figure A 35 Example post-polymerization modification of P4.1 proton NMR

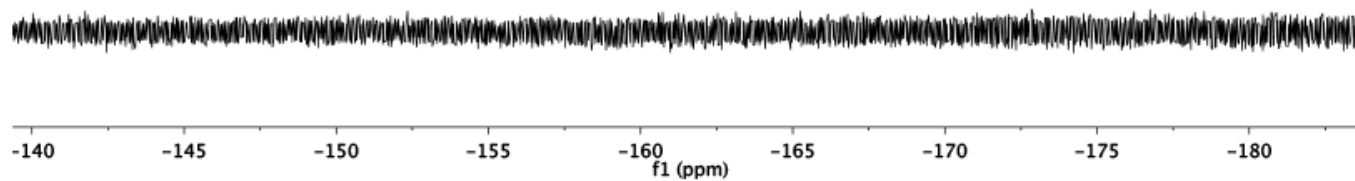
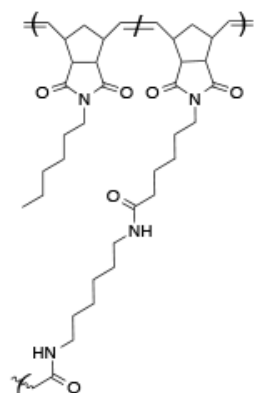


Figure A 36 Example of post-polymerization modification of P4.1 fluorine NMR

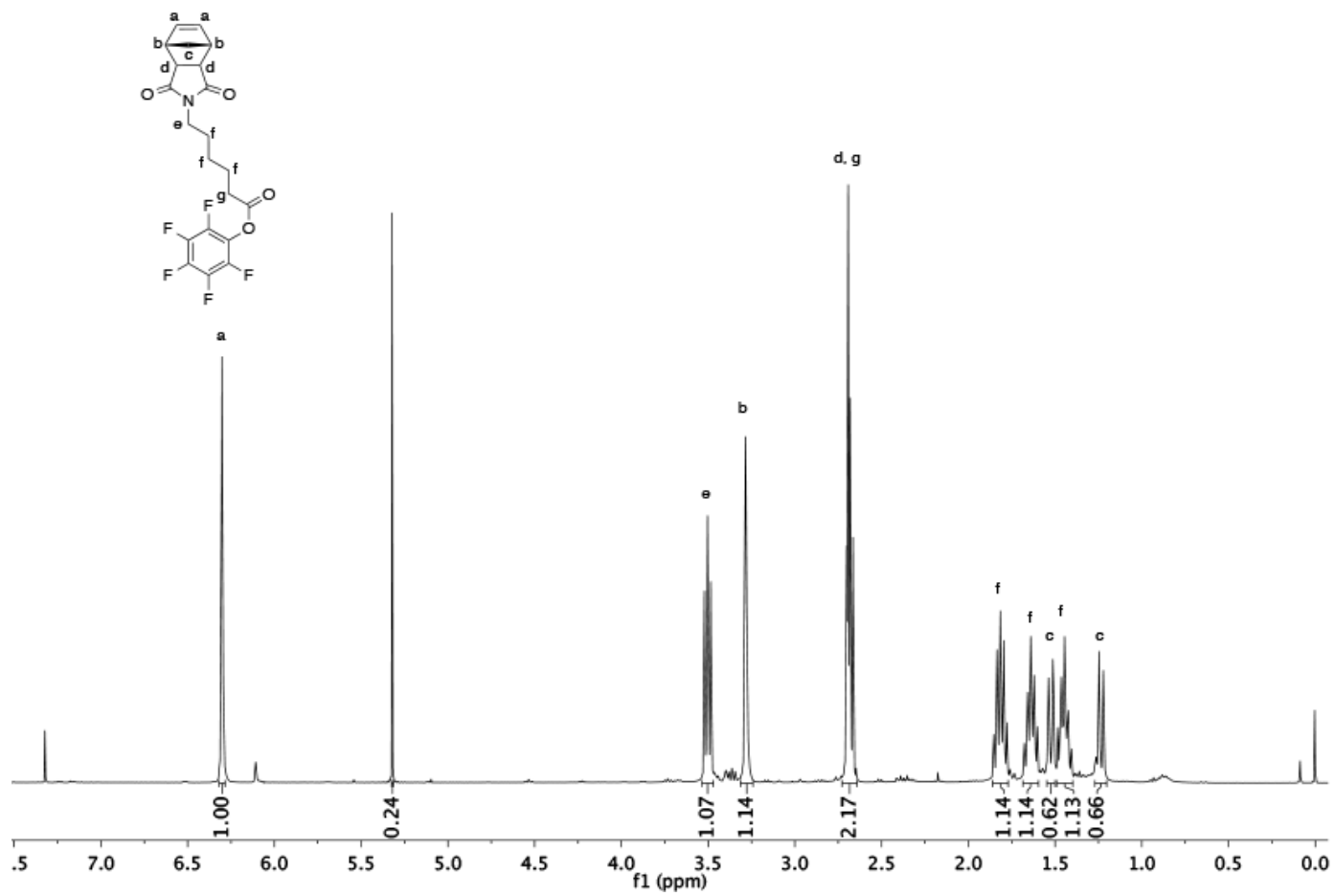


Figure A 37 Hexanoic pentafluorophenyl norbornene imide monomer proton NMR see page 66

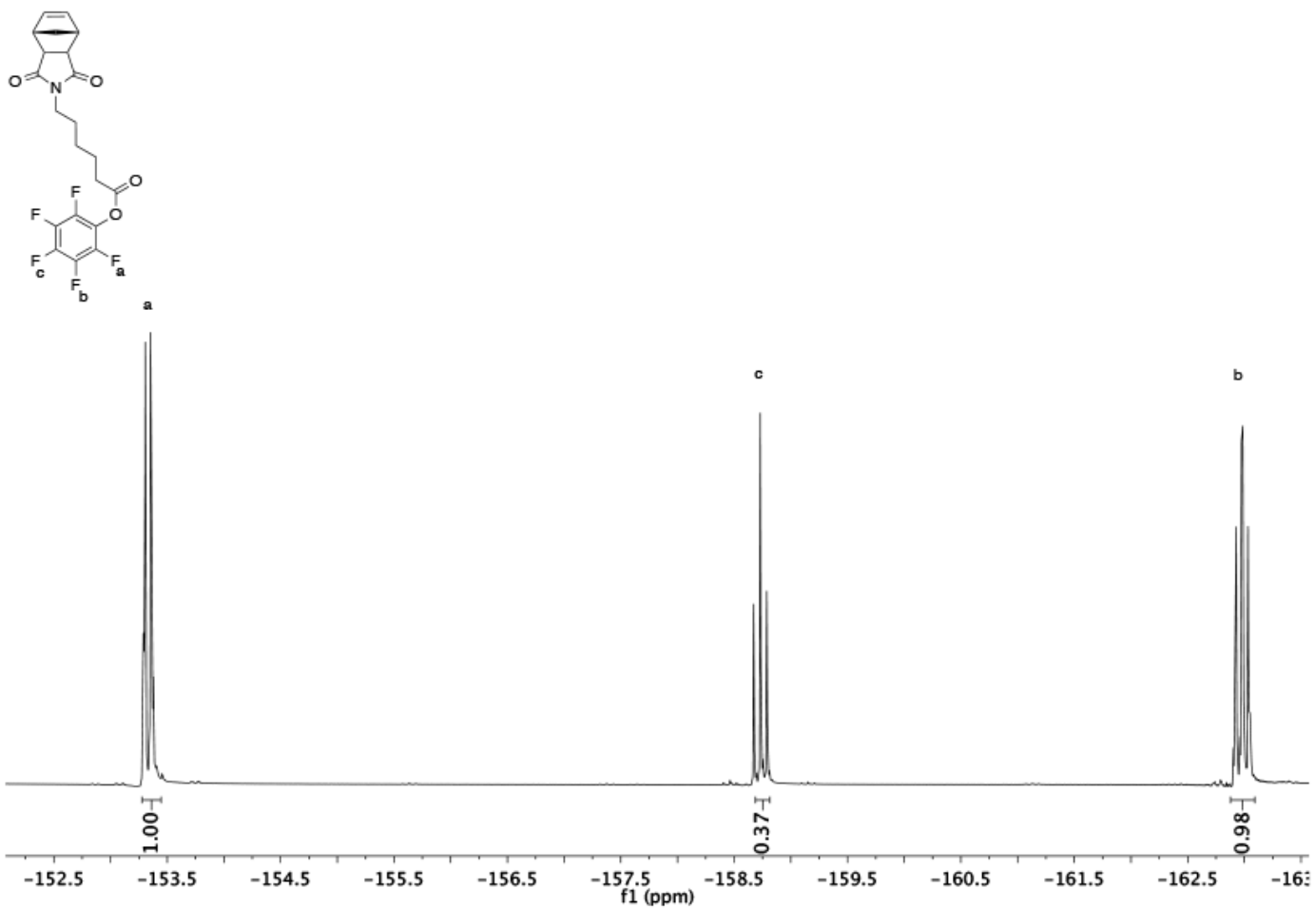


Figure A 38 Hexanoic pentafluorophenyl norbornene imide monomer fluorine NMR see page 66

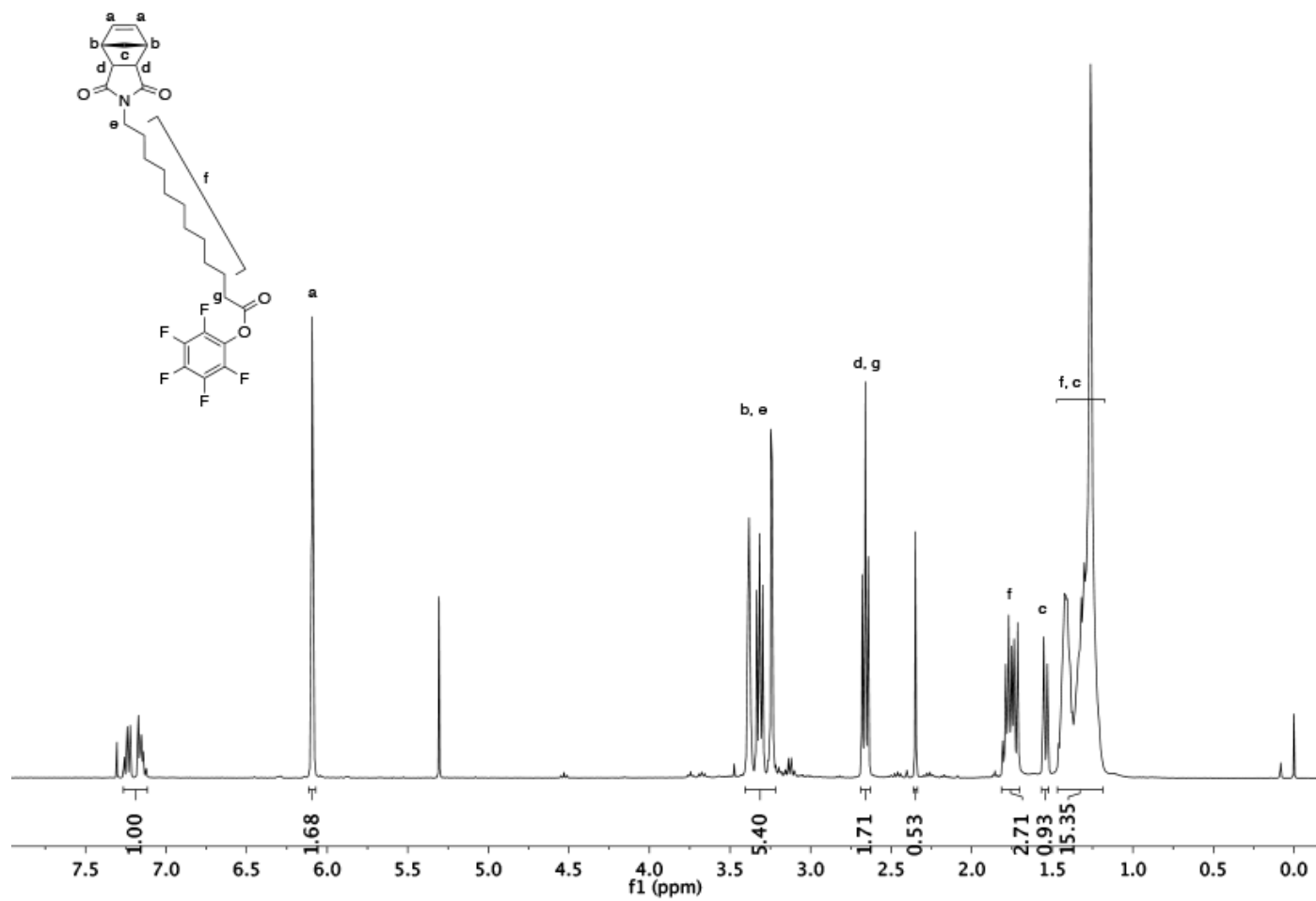


Figure A 39 Dodecanoic pentafluorophenyl esternorbornene imide monomer proton NMR see page 68



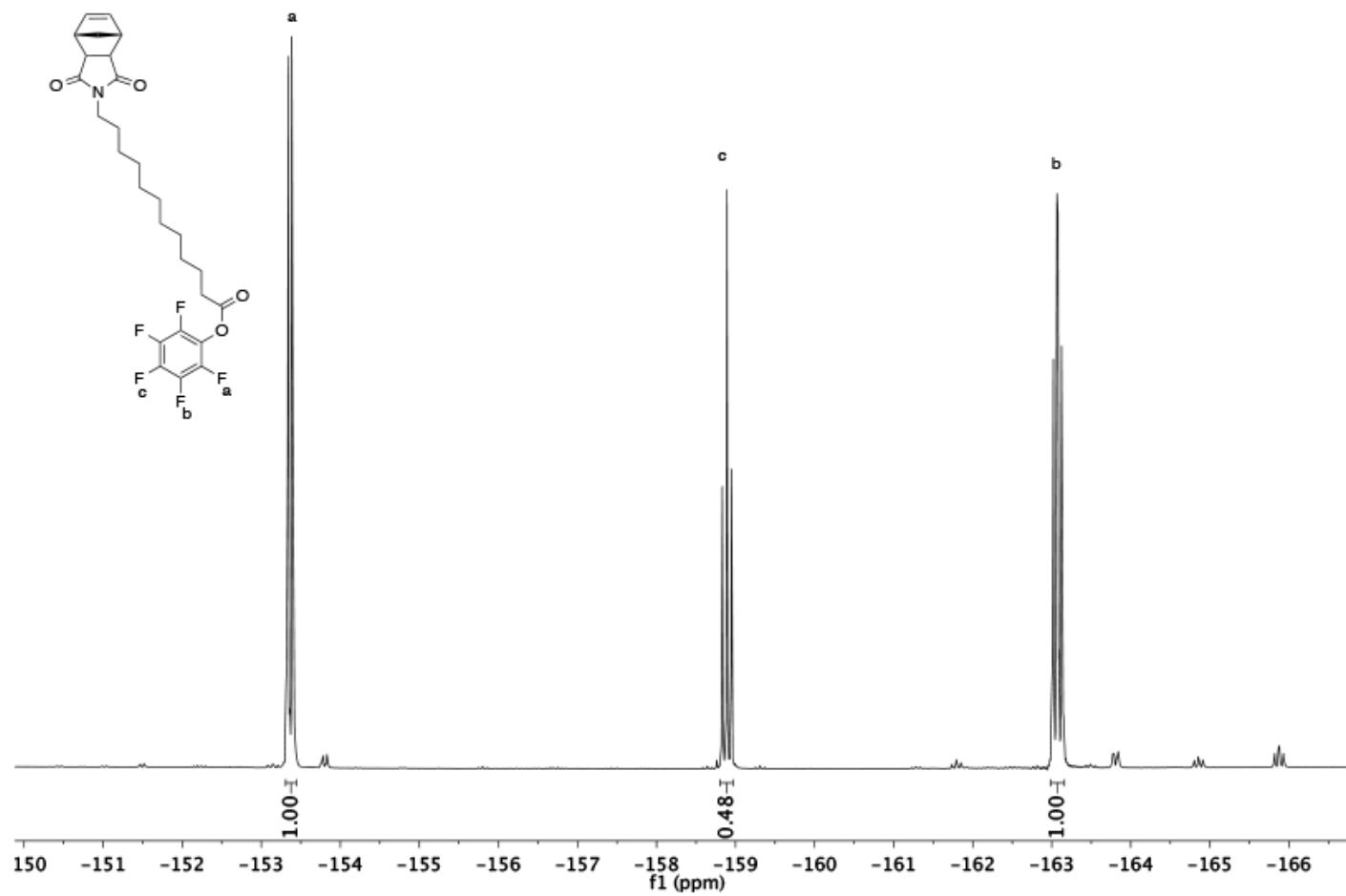


Figure A 40 Dodecanoic pentafluorophenyl esternorborene imide monomer fluorine NMR see page 68

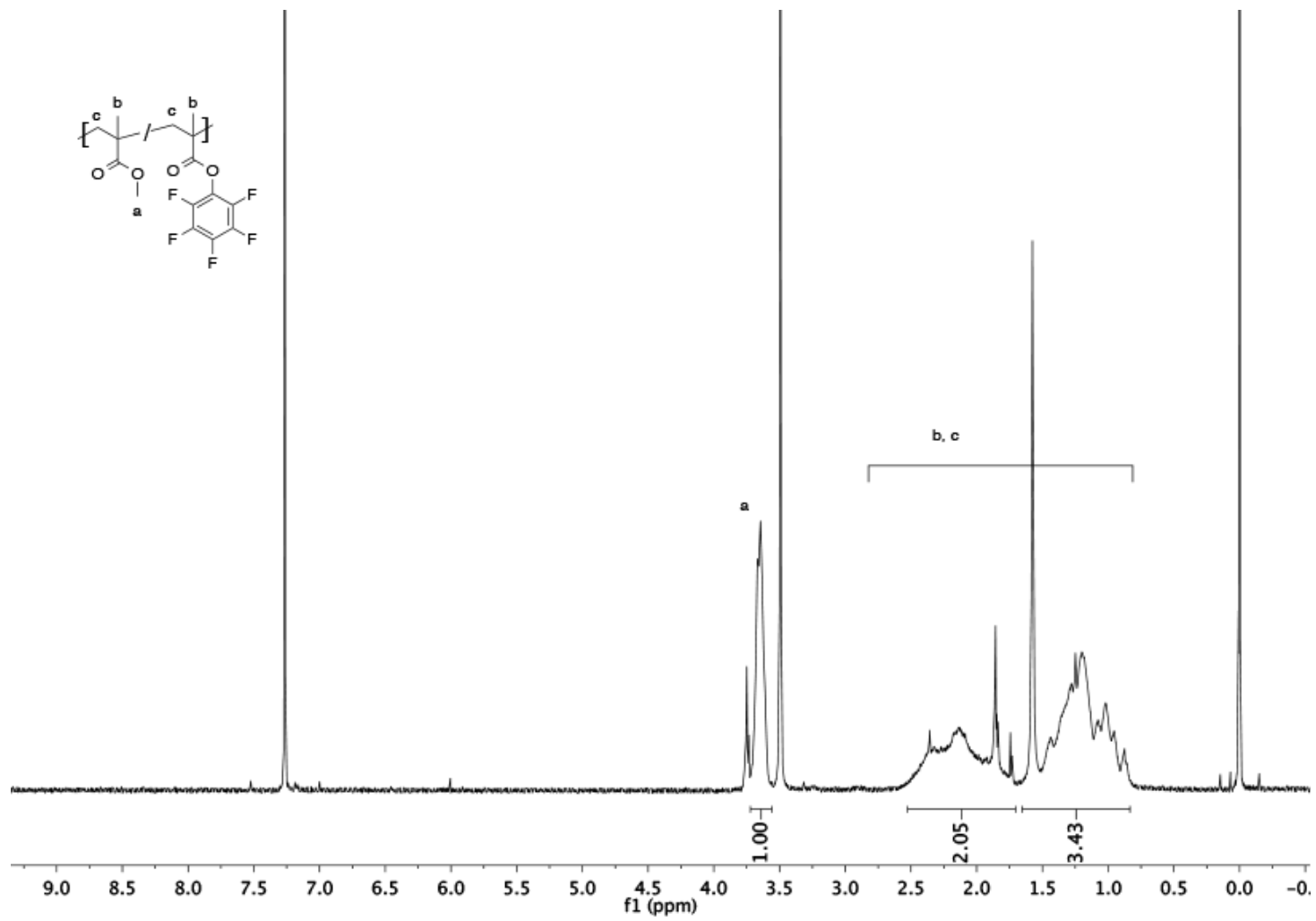


Figure A 41 P5.1 proton NMR see page 78

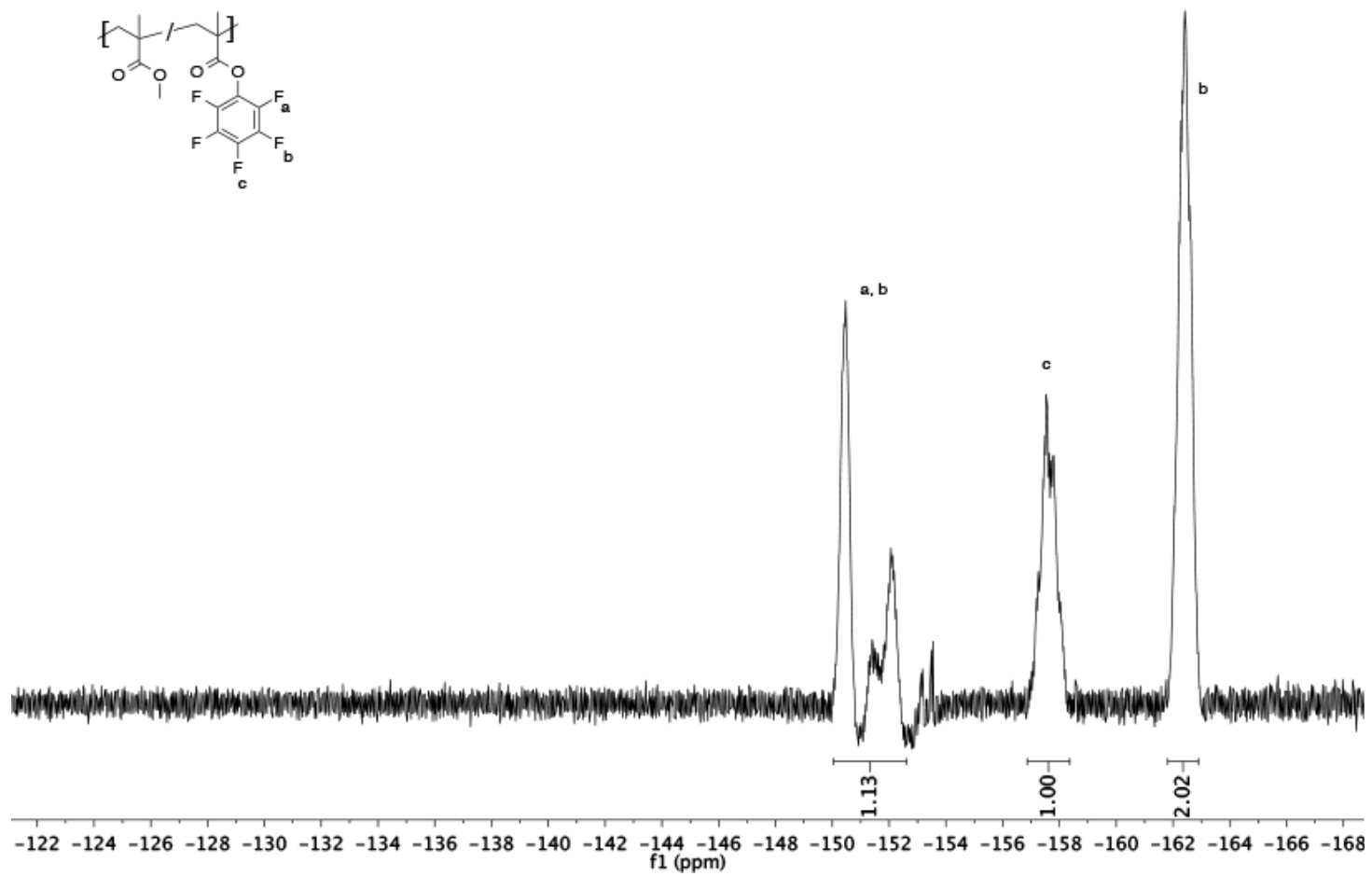


Figure A 42 P5.1 fluorine NMR see page 78

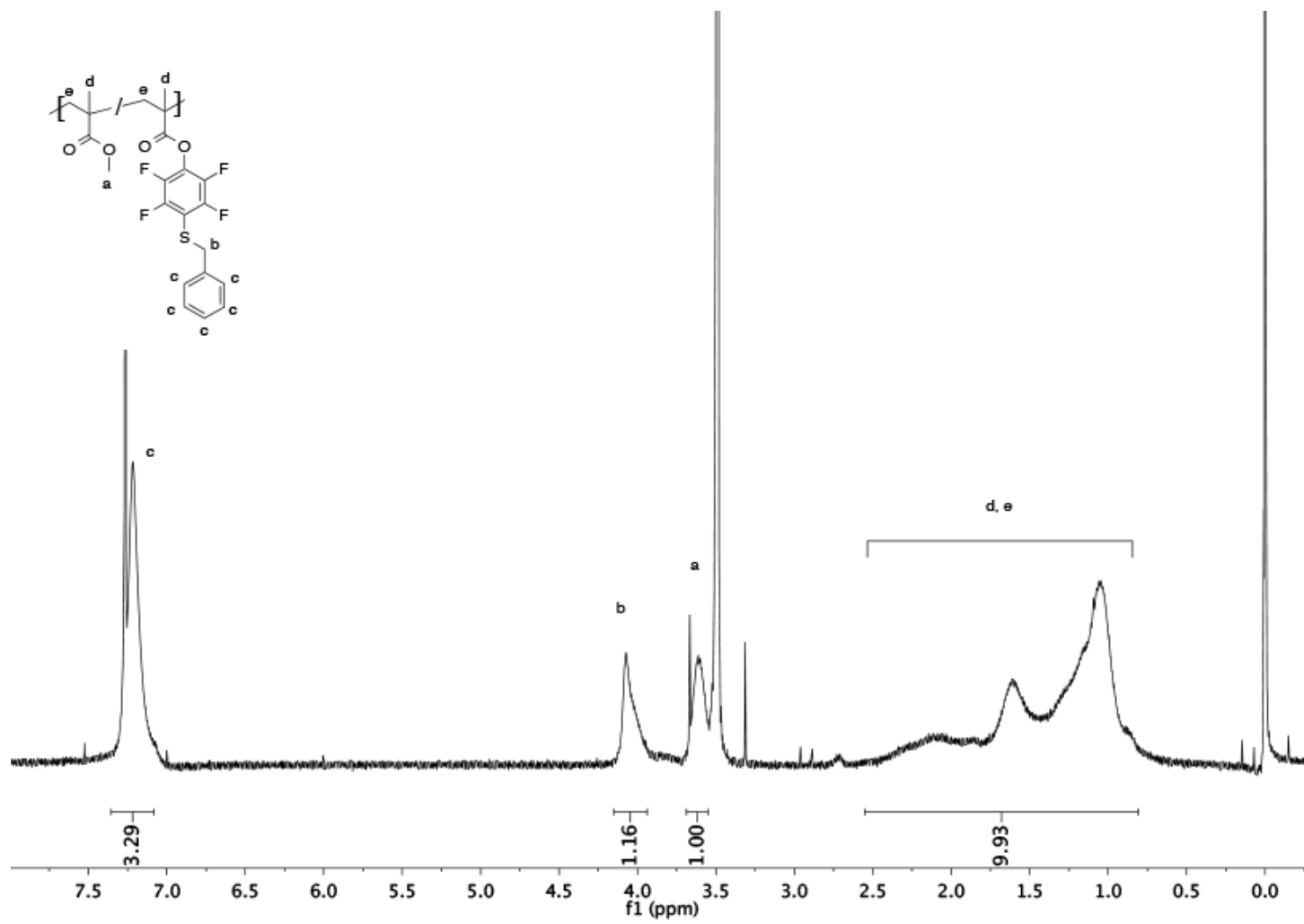


Figure A 43 P5.2 proton NMR see page 79

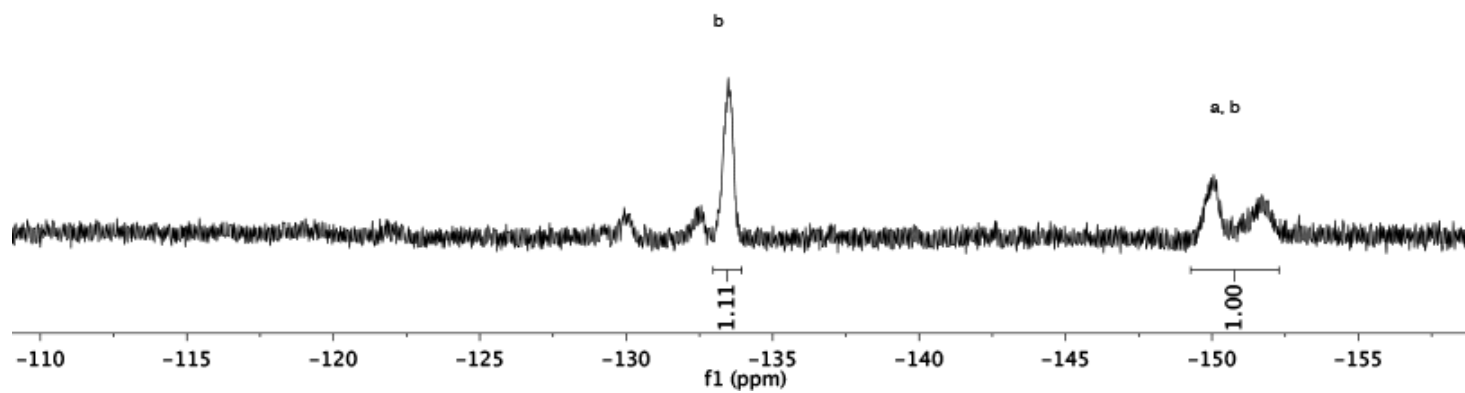
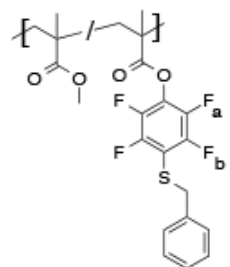


Figure A 44 P5.2 fluorine NMR see page 79

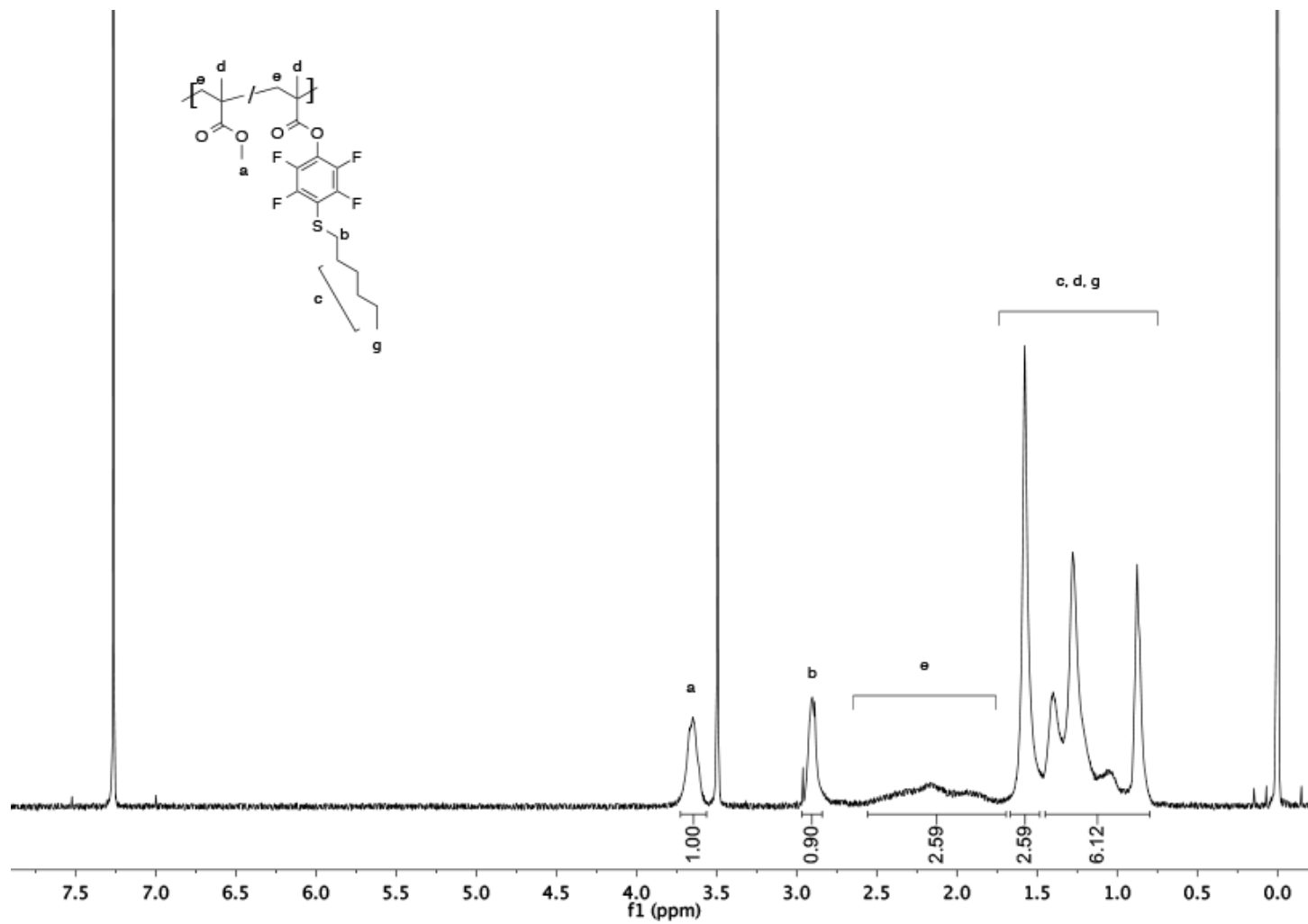


Figure A 45 P5.3 proton NMR see page 79

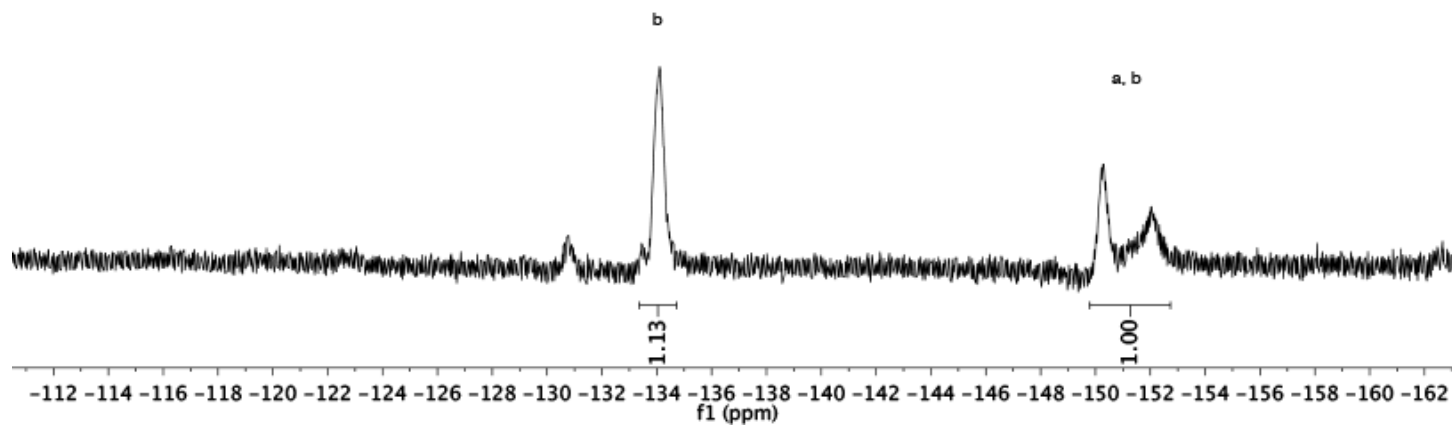
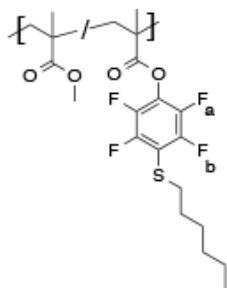


Figure A 46 P5.3 fluorine NMR see page 79

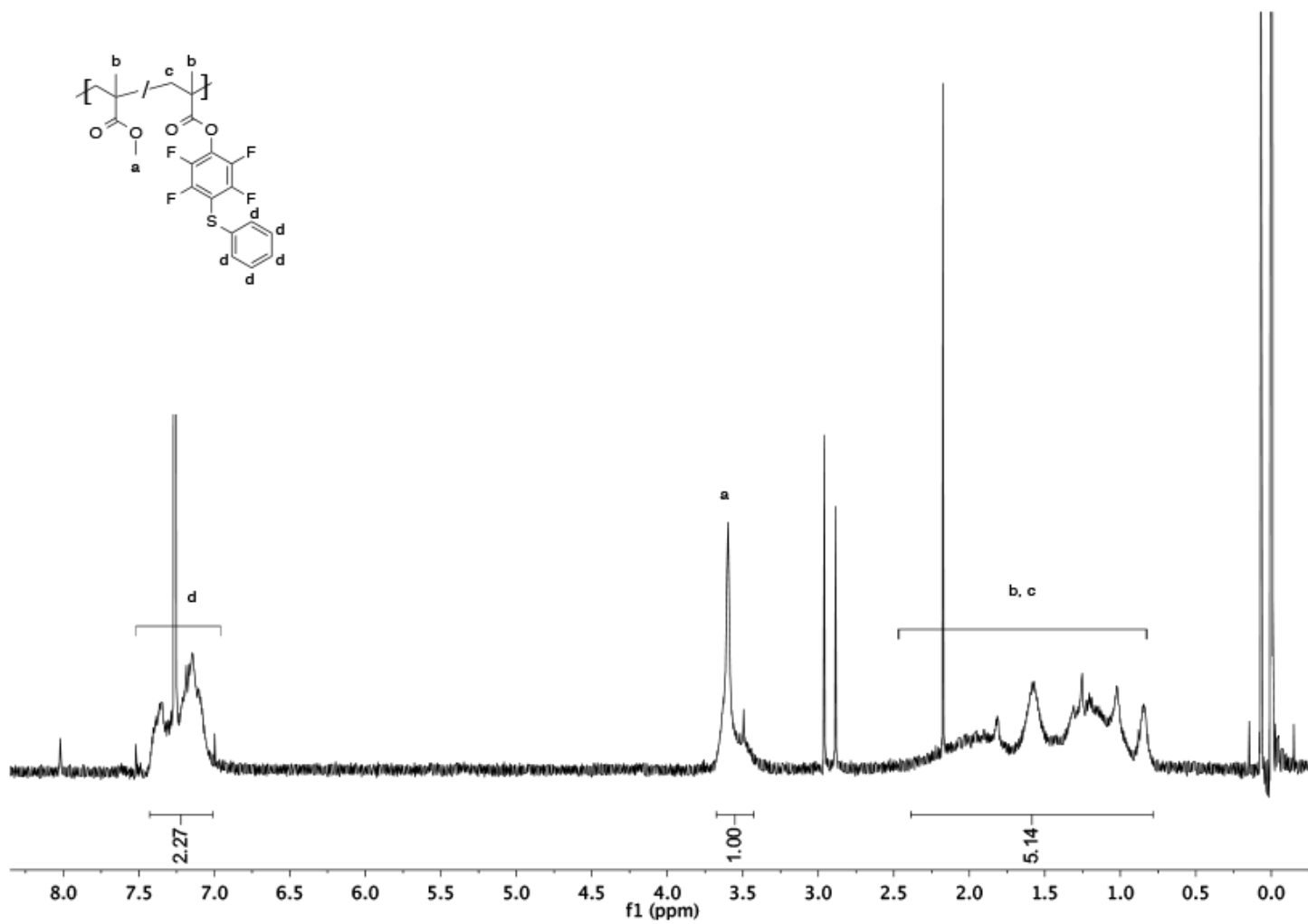


Figure A 47 P5.4 proton NMR see page 79



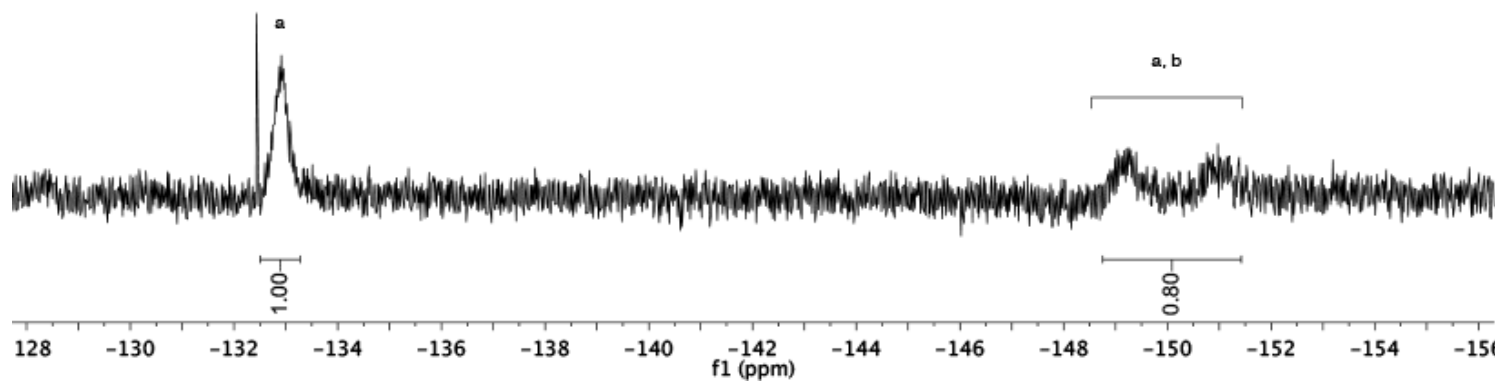
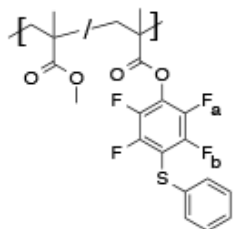


Figure A 48 P5.4 fluorine NMR see page 79

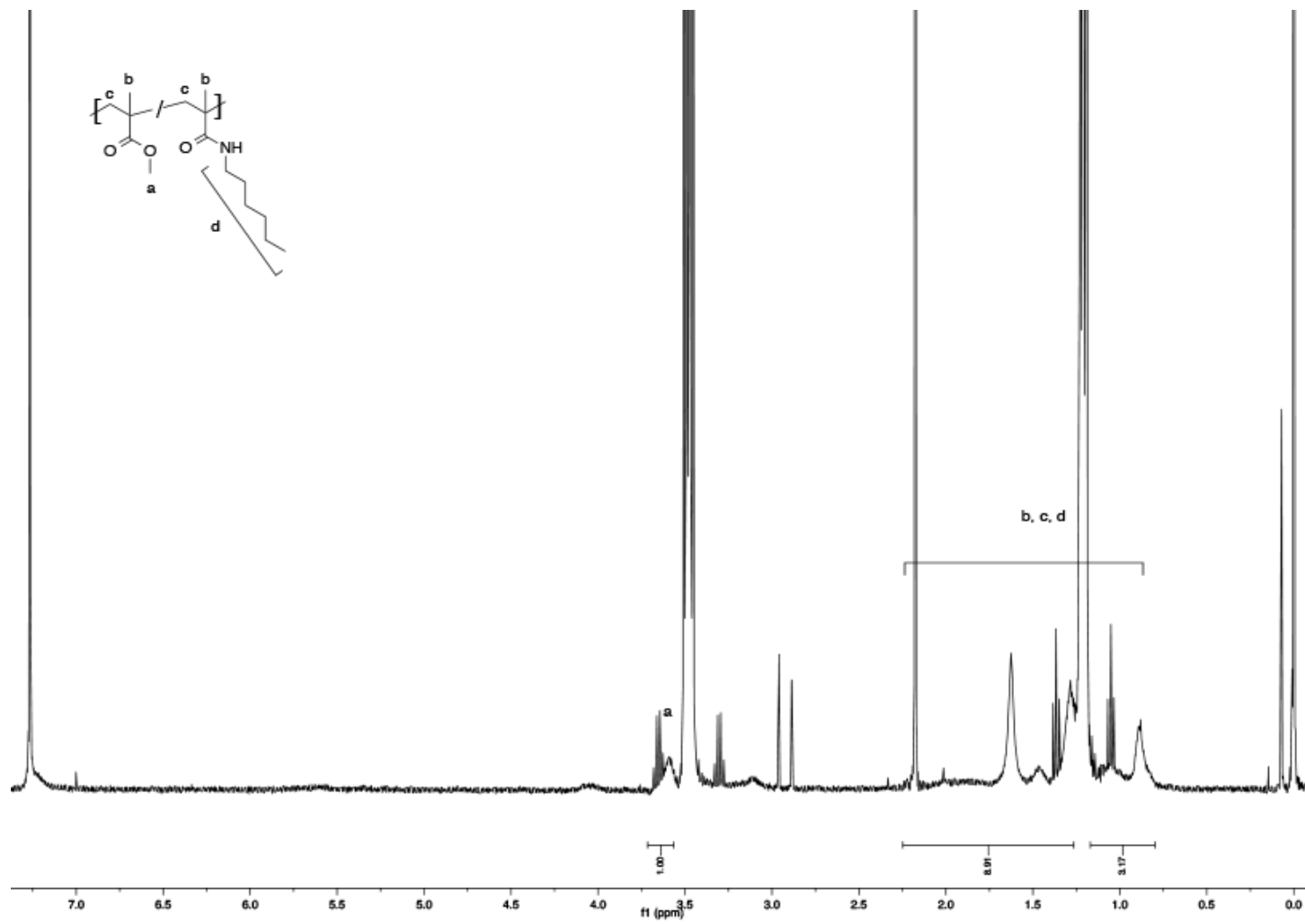


Figure A 49 P5.5 proton NMR see page 79

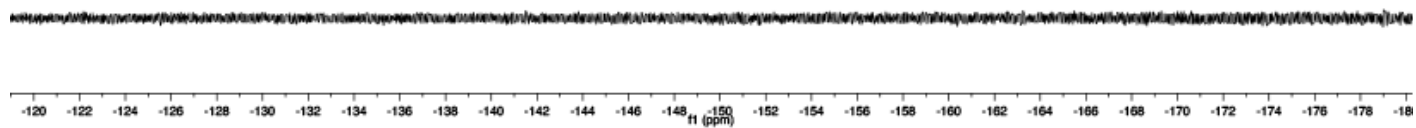
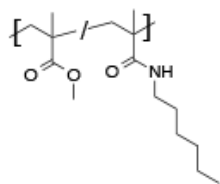


Figure A 50 P5.5 fluorine NMR see page 79

## REFERENCES

- (1) Perez-Baena, I.; Barroso-Bujans, F.; Gasser, U.; Arbe, A.; Moreno, A. J.; Colmenero, J.; Pomposo, J. A. Endowing Single-Chain Polymer Nanoparticles with Enzyme-Mimetic Activity. *ACS Macro Lett.* **2013**, *2*, 775-779.
- (2) Terashima, T.; Mes, T.; De Greef, T. F. A.; Gillissen, M. A. J.; Besenius, P.; Palmans, A. R. A.; Meijer, E. W. Single-Chain Folding of Polymers for Catalytic Systems in Water. *J. Am. Chem. Soc.* **2011**, *133*, 4742-4745.
- (3) Artar, M.; Terashima, T.; Sawamoto, M.; Meijer, E. W.; Palmans, A. R. A. Understanding the catalytic activity of single-chain polymeric nanoparticles in water. *Journal of Polymer Science Part A: Polymer Chemistry* **2014**, *52*, 12-20.
- (4) Huerta, E.; Stals, P. J. M.; Meijer, E. W.; Palmans, A. R. A. Consequences of Folding a Water-Soluble Polymer Around an Organocatalyst. *Angew. Chem., Int. Ed.* **2013**, *52*, 2906-2910.
- (5) Sanchez-Sanchez, A.; Arbe, A.; Colmenero, J.; Pomposo, J. A. Metallo-Folded Single-Chain Nanoparticles with Catalytic Selectivity. *ACS Macro Letters* **2014**, *3*, 439-443.
- (6) Gillissen, M. A. J.; Voets, I. K.; Meijer, E. W.; Palmans, A. R. A. Single chain polymeric nanoparticles as compartmentalised sensors for metal ions. *Polymer Chemistry* **2012**, *3*, 3166-3174.
- (7) He, J.; Tremblay, L.; Lacelle, S.; Zhao, Y. Preparation of polymer single chain nanoparticles using intramolecular photodimerization of coumarin. *Soft Matter* **2011**, *7*, 2380-2386.
- (8) Sanchez-Sanchez, A.; Akbari, S.; Etxeberria, A.; Arbe, A.; Gasser, U.; Moreno, A. J.; Colmenero, J.; Pomposo, J. A. "Michael" Nanocarriers Mimicking Transient-Binding Disordered Proteins. *ACS Macro Lett.* **2013**, *2*, 491-495.
- (9) Perez-Baena, I.; Loinaz, I.; Padro, D.; Garcia, I.; Grande, H. J.; Odriozola, I. Single-chain polyacrylic nanoparticles with multiple Gd(III) centers as potential MRI contrast agents. *J. Mater. Chem.* **2010**, *20*, 6916-6922.
- (10) Passarella, R. J.; Spratt, D. E.; van der Ende, A. E.; Phillips, J. G.; Wu, H.; Sathiyakumar, V.; Zhou, L.; Hallahan, D. E.; Harth, E.; Diaz, R. Targeted Nanoparticles That Deliver a Sustained, Specific Release of Paclitaxel to Irradiated Tumors. *Cancer Res.* **2010**, *70*, 4550-4559.
- (11) Hariri, G.; Edwards, A. D.; Merrill, T. B.; Greenbaum, J. M.; van der Ende, A. E.; Harth, E. Sequential Targeted Delivery of Paclitaxel and Camptothecin Using a Cross-Linked "Nanosponge" Network for Lung Cancer Chemotherapy. *Molecular Pharmaceutics* **2013**, *11*, 265-275.
- (12) Gody, G.; Maschmeyer, T.; Zetterlund, P. B.; Perrier, S. Rapid and quantitative one-pot synthesis of sequence-controlled polymers by radical polymerization. *Nat Commun* **2013**, *4*.
- (13) Berda, E. B.; Wagener, K. B.: Recent Advances in ADMET Polycondensation Chemistry. In *Materials Science and Technology*; Wiley-VCH Verlag GmbH & Co. KGaA, 2006.
- (14) Lutz, J.-F.; Ouchi, M.; Liu, D. R.; Sawamoto, M. Sequence-Controlled Polymers. *Science* **2013**, *341*.

- (15) Walter, M. V.; Malkoch, M. Simplifying the synthesis of dendrimers: accelerated approaches. *Chemical Society Reviews* **2012**, *41*, 4593-4609.
- (16) Bosman, A. W.; Janssen, H. M.; Meijer, E. W. About Dendrimers: Structure, Physical Properties, and Applications. *Chemical Reviews* **1999**, *99*, 1665-1688.
- (17) Ouchi, M.; Badi, N.; Lutz, J.-F.; Sawamoto, M. Single-chain technology using discrete synthetic macromolecules. *Nat Chem* **2011**, *3*, 917-924.
- (18) Frank, P.; Prasher, A.; Tuten, B.; Chao, D.; Berda, E. Characterization of single-chain polymer folding using size exclusion chromatography with multiple modes of detection. *Appl Petrochem Res* **2014**, 1-9.
- (19) Murray, B. S.; Fulton, D. A. Dynamic Covalent Single-Chain Polymer Nanoparticles. *Macromolecules (Washington, DC, U. S.)* **2011**, *44*, 7242-7252.
- (20) Aiertza, M. K.; Odriozola, I.; Cabanero, G.; Grande, H.-J.; Loinaz, I. Single-chain polymer nanoparticles. *Cell. Mol. Life Sci.* **2012**, *69*, 337-346.
- (21) Altintas, O.; Barner-Kowollik, C. Single Chain Folding of Synthetic Polymers by Covalent and Non-Covalent Interactions: Current Status and Future Perspectives. *Macromol. Rapid Commun.* **2012**, *33*, 958-971.
- (22) Sanchez-Sanchez, A.; Perez-Baena, I.; Pomposo, J. A. Advances in click chemistry for single-chain nanoparticle construction. *Molecules* **2013**, *18*, 3339-3355.
- (23) Gauthier, M. A.; Gibson, M. I.; Klok, H.-A. Synthesis of Functional Polymers by Post-Polymerization Modification. *Angewandte Chemie International Edition* **2009**, *48*, 48-58.
- (24) Davankov, V. A.; Ilyin, M. M.; Tsyurupa, M. P.; Timofeeva, G. I.; Dubrovina, L. V. From a Dissolved Polystyrene Coil to an Intramolecularly-Hyper-Cross-Linked "Nanosponge". *Macromolecules* **1996**, *29*, 8398-8403.
- (25) Dobish, J. N.; Hamilton, S. K.; Harth, E. Synthesis of low-temperature benzocyclobutene cross-linker and utilization. *Polymer Chemistry* **2012**, *3*, 857-860.
- (26) Duket, T. E.; Mackay, M. E.; Van Horn, B.; Wooley, K. L.; Drockenmuller, E.; Malkoch, M.; Hawker, C. J. Conformation of Intramolecularly Cross-Linked Polymer Nanoparticles on Solid Substrates. *Nano Lett.* **2005**, *5*, 1704-1709.
- (27) Harth, E.; Van Horn, B.; Lee, V. Y.; Germack, D. S.; Gonzales, C. P.; Miller, R. D.; Hawker, C. J. A Facile Approach to Architecturally Defined Nanoparticles via Intramolecular Chain Collapse. *J. Am. Chem. Soc.* **2002**, *124*, 8653-8660.
- (28) Tuteja, A.; Mackay, M. E.; Hawker, C. J.; Van Horn, B.; Ho, D. L. Molecular architecture and rheological characterization of novel intramolecularly crosslinked polystyrene nanoparticles. *J. Polym. Sci., Part B: Polym. Phys.* **2006**, *44*, 1930-1947.
- (29) Jiang, J.; Thayumanavan, S. Synthesis and Characterization of Amine-Functionalized Polystyrene Nanoparticles. *Macromolecules* **2005**, *38*, 5886-5891.
- (30) Mecerreyes, D.; Lee, V.; Hawker, C. J.; Hedrick, J. L.; Wursch, A.; Volksen, W.; Magbitang, T.; Huang, E.; Miller, R. D. A novel approach to functionalized nanoparticles: self-crosslinking of macromolecules in ultradilute solution. *Adv. Mater. (Weinheim, Ger.)* **2001**, *13*, 204-208.

- (31) Altintas, O.; Willenbacher, J.; Wuest, K. N. R.; Oehlenschlaeger, K. K.; Krolla-Sidenstein, P.; Gliemann, H.; Barner-Kowollik, C. A Mild and Efficient Approach to Functional Single-Chain Polymeric Nanoparticles via Photoinduced Diels-Alder Ligation. *Macromolecules (Washington, DC, U. S.)* **2013**, *46*, 8092-8101.
- (32) Beck, J. B.; Killops, K. L.; Kang, T.; Sivanandan, K.; Bayles, A.; Mackay, M. E.; Wooley, K. L.; Hawker, C. J. Facile Preparation of Nanoparticles by Intramolecular Cross-Linking of Isocyanate Functionalized Copolymers. *Macromolecules (Washington, DC, U. S.)* **2009**, *42*, 5629-5635.
- (33) Cherian, A. E.; Sun, F. C.; Sheiko, S. S.; Coates, G. W. Formation of Nanoparticles by Intramolecular Cross-Linking: Following the Reaction Progress of Single Polymer Chains by Atomic Force Microscopy. *J. Am. Chem. Soc.* **2007**, *129*, 11350-11351.
- (34) Ormategui, N.; Garcia, I.; Padro, D.; Cabanero, G.; Grande, H. J.; Loinaz, I. Synthesis of single chain thermoresponsive polymer nanoparticles. *Soft Matter* **2012**, *8*, 734-740.
- (35) Ruiz de Luzuriaga, A.; Ormategui, N.; Grande, H. J.; Odriozola, I.; Pomposo, J. A.; Loinaz, I. Intramolecular click cycloaddition: an efficient room-temperature route towards bioconjugable polymeric nanoparticles. *Macromol. Rapid Commun.* **2008**, *29*, 1156-1160.
- (36) Ruiz de Luzuriaga, A.; Perez-Baena, I.; Montes, S.; Loinaz, I.; Odriozola, I.; Garcia, I.; Pomposo, J. A. New Route to Polymeric Nanoparticles by Click Chemistry using Bifunctional Cross-Linkers. *Macromol. Symp.* **2010**, *296*, 303-310.
- (37) Stevens, D. M.; Tempelaar, S.; Dove, A. P.; Harth, E. Nanosponge Formation from Organocatalytically Synthesized Poly(carbonate) Copolymers. *ACS Macro Letters* **2012**, *1*, 915-918.
- (38) Dirlam, P. T.; Kim, H. J.; Arrington, K. J.; Chung, W. J.; Sahoo, R.; Hill, L. J.; Costanzo, P. J.; Theato, P.; Char, K.; Pyun, J. Single chain polymer nanoparticles via sequential ATRP and oxidative polymerization. *Polym. Chem.* **2013**, *4*, 3765-3773.
- (39) Jiang, X.; Pu, H.; Wang, P. Polymer nanoparticles via intramolecular crosslinking of sulfonyl azide functionalized polymers. *Polymer* **2011**, *52*, 3597-3602.
- (40) Sanchez-Sanchez, A.; Asenjo-Sanz, I.; Buruaga, L.; Pomposo, J. A. Naked and Self-Clickable Propargylic-Decorated Single-Chain Nanoparticle Precursors via Redox-Initiated RAFT Polymerization. *Macromol. Rapid Commun.* **2012**, *33*, 1262-1267, S1262/1261-S1262/1266.
- (41) Wen, J.; Yuan, L.; Yang, Y.; Liu, L.; Zhao, H. Self-Assembly of Monotethered Single-Chain Nanoparticle Shape Amphiphiles. *ACS Macro Lett.* **2013**, *2*, 100-106.
- (42) Zhu, B.; Ma, J.; Li, Z.; Hou, J.; Cheng, X.; Qian, G.; Liu, P.; Hu, A. Formation of polymeric nanoparticles via Bergman cyclization mediated intramolecular chain collapse. *J. Mater. Chem.* **2011**, *21*, 2679-2683.
- (43) Zhu, B.; Qian, G.; Xiao, Y.; Deng, S.; Wang, M.; Hu, A. A convergence of photo-Bergman cyclization and intramolecular chain collapse towards polymeric nanoparticles. *J. Polym. Sci., Part A: Polym. Chem.* **2011**, *49*, 5330-5338.

- (44) Whitaker, D. E.; Mahon, C. S.; Fulton, D. A. Thermoresponsive Dynamic Covalent Single-Chain Polymer Nanoparticles Reversibly Transform into a Hydrogel. *Angew. Chem., Int. Ed.* **2013**, *52*, 956-959.
- (45) Ryu, J.-H.; Chacko, R. T.; Jiwanich, S.; Bickerton, S.; Babu, R. P.; Thayumanavan, S. Self-Cross-Linked Polymer Nanogels: A Versatile Nanoscopic Drug Delivery Platform. *J. Am. Chem. Soc.* **2010**, *132*, 17227-17235.
- (46) Tuten, B. T.; Chao, D.; Lyon, C. K.; Berda, E. B. Single-chain polymer nanoparticles via reversible disulfide bridges. *Polym. Chem.* **2012**, *3*, 3068-3071.
- (47) Buruaga, L.; Pomposo, J. A. Metal-free polymethyl methacrylate (PMMA) nanoparticles by enamine "click" chemistry at room temperature. *Polymers (Basel, Switz.)* **2011**, *3*, 1673-1683.
- (48) Sanchez-Sanchez, A.; Fulton, D. A.; Pomposo, J. A. pH-responsive single-chain polymer nanoparticles utilising dynamic covalent enamine bonds. *Chem. Commun. (Cambridge, U. K.)* **2014**, *50*, 1871-1874.
- (49) Frank, P. G.; Tuten, B. T.; Prasher, A.; Chao, D.; Berda, E. B. Intra-Chain Photodimerization of Pendant Anthracene Units as an Efficient Route to Single-Chain Nanoparticle Fabrication. *Macromol. Rapid Commun.* **2014**, *35*, 249-253.
- (50) Altintas, O.; Gerstel, P.; Dingenouts, N.; Barner-Kowollik, C. Single chain self-assembly: preparation of  $\alpha,\omega$ -donor-acceptor chains via living radical polymerization and orthogonal conjugation. *Chem. Commun. (Cambridge, U. K.)* **2010**, *46*, 6291-6293.
- (51) Altintas, O.; Lejeune, E.; Gerstel, P.; Barner-Kowollik, C. Bioinspired dual self-folding of single polymer chains via reversible hydrogen bonding. *Polym. Chem.* **2012**, *3*, 640-651.
- (52) Altintas, O.; Rudolph, T.; Barner-Kowollik, C. Single chain self-assembly of well-defined heterotelechelic polymers generated by ATRP and click chemistry revisited. *J. Polym. Sci., Part A: Polym. Chem.* **2011**, *49*, 2566-2576.
- (53) Berda, E. B.; Foster, E. J.; Meijer, E. W. Toward Controlling Folding in Synthetic Polymers: Fabricating and Characterizing Supramolecular Single-Chain Nanoparticles. *Macromolecules* **2010**, *43*, 1430-1437.
- (54) Foster, E. J.; Berda, E. B.; Meijer, E. W. Metastable Supramolecular Polymer Nanoparticles via Intramolecular Collapse of Single Polymer Chains. *Journal of the American Chemical Society* **2009**, *131*, 6964-6966.
- (55) Foster, E. J.; Berda, E. B.; Meijer, E. W. Tuning the size of supramolecular single-chain polymer nanoparticles. *Journal of Polymer Science Part A: Polymer Chemistry* **2011**, *49*, 118-126.
- (56) Hosono, N.; Gillissen, M. A. J.; Li, Y.; Sheiko, S. S.; Palmans, A. R. A.; Meijer, E. W. Orthogonal Self-Assembly in Folding Block Copolymers. *J. Am. Chem. Soc.* **2013**, *135*, 501-510.
- (57) Stals, P. J. M.; Gillissen, M. A. J.; Nicolay, R.; Palmans, A. R. A.; Meijer, E. W. The balance between intramolecular hydrogen bonding, polymer solubility and rigidity in single-chain polymeric nanoparticles. *Polymer Chemistry* **2013**, *4*, 2584-2597.
- (58) Mes, T.; van der Weegen, R.; Palmans, A. R. A.; Meijer, E. W. Single-Chain Polymeric Nanoparticles by Stepwise Folding. *Angew. Chem., Int. Ed.* **2011**, *50*, 5085-5089.

- (59) Seo, M.; Beck, B. J.; Paulusse, J. M. J.; Hawker, C. J.; Kim, S. Y. Polymeric Nanoparticles via Noncovalent Cross-Linking of Linear Chains. *Macromolecules (Washington, DC, U. S.)* **2008**, *41*, 6413-6418.
- (60) Mavila, S.; Diesendruck, C. E.; Linde, S.; Amir, L.; Shikler, R.; Lemcoff, N. G. Polycyclooctadiene Complexes of Rhodium(I): Direct Access to Organometallic Nanoparticles. *Angewandte Chemie International Edition* **2013**, *52*, 5767-5770.
- (61) Croce, T. A.; Hamilton, S. K.; Chen, M. L.; Muchalski, H.; Harth, E. Alternative o-Quinodimethane Cross-Linking Precursors for Intramolecular Chain Collapse Nanoparticles. *Macromolecules* **2007**, *40*, 6028-6031.
- (62) Chao, D.; Jia, X.; Tuten, B.; Wang, C.; Berda, E. B. Controlled folding of a novel electroactive polyolefin via multiple sequential orthogonal intra-chain interactions. *Chemical Communications* **2013**, *49*, 4178-4180.
- (63) Hansell, C. F.; Lu, A.; Patterson, J. P.; O'Reilly, R. K. Exploiting the tetrazine-norbornene reaction for single polymer chain collapse. *Nanoscale* **2014**, *6*, 4102-4107.
- (64) Frank, P. G.; Tuten, B. T.; Prasher, A.; Chao, D.; Berda, E. B. Intra-Chain Photodimerization of Pendant Anthracene Units as an Efficient Route to Single-Chain Nanoparticle Fabrication. *Macromolecular Rapid Communications* **2014**, *35*, 249-253.
- (65) Willenbacher, J.; Wuest, K. N. R.; Mueller, J. O.; Kaupp, M.; Wagenknecht, H.-A.; Barner-Kowollik, C. Photochemical Design of Functional Fluorescent Single-Chain Nanoparticles. *ACS Macro Letters* **2014**, *3*, 574-579.
- (66) Altintas, O.; Willenbacher, J.; Wuest, K. N. R.; Oehlenschlaeger, K. K.; Krolla-Sidenstein, P.; Gliemann, H.; Barner-Kowollik, C. A Mild and Efficient Approach to Functional Single-Chain Polymeric Nanoparticles via Photoinduced Diels-Alder Ligation. *Macromolecules* **2013**, *46*, 8092-8101.
- (67) Li, G.; Tao, F.; Wang, L.; Li, Y.; Bai, R. A facile strategy for preparation of single-chain polymeric nanoparticles by intramolecular photo-crosslinking of azide polymers. *Polymer* **2014**, *55*, 3696-3702.
- (68) Gasparini, G.; Dal Molin, M.; Lovato, A.; Prins, L. J.: Dynamic Covalent Chemistry. In *Supramolecular Chemistry*; John Wiley & Sons, Ltd, 2012.
- (69) Pomposo, J. A.; Perez-Baena, I.; Buruaga, L.; Alegria, A.; Moreno, A. J.; Colmenero, J. On the Apparent SEC Molecular Weight and Polydispersity Reduction upon Intramolecular Collapse of Polydisperse Chains to Unimolecular Nanoparticles. *Macromolecules (Washington, DC, U. S.)* **2011**, *44*, 8644-8649.
- (70) Einstein, A. Theorie der Opaleszenz von homogenen Flüssigkeiten und Flüssigkeitsgemischen in der Nähe des kritischen Zustandes. *Annalen der Physik* **1910**, *338*, 1275-1298.
- (71) Raman, C. V. A Change of Wave-length in Light Scattering. *Nature* **1928**, *121*, 619.
- (72) Debye, P. Light Scattering in Solutions. *Journal of Applied Physics* **1944**, *15*, 338-342.
- (73) Zimm, B. H. Molecular Theory of the Scattering of Light in Fluids. *The Journal of Chemical Physics* **1945**, *13*, 141-145.
- (74) Wyatt, P. J. Light scattering and the absolute characterization of macromolecules. *Anal. Chim. Acta* **1993**, *272*, 1-40.



- (75) Tuten, B. T.; Chao, D.; Lyon, C. K.; Berda, E. B. Single-chain polymer nanoparticles via reversible disulfide bridges. *Polymer Chemistry* **2012**, *3*, 3068-3071.
- (76) Appel, E. A.; Barrio, J. d.; Dyson, J.; Isaacs, L.; Scherman, O. A. Metastable single-chain polymer nanoparticles prepared by dynamic cross-linking with nor-seco-cucurbit[10]uril. *Chem. Sci.* **2012**, *3*, 2278-2281.
- (77) Zamfir, M.; Theato, P.; Lutz, J.-F. Controlled folding of polystyrene single chains: design of asymmetric covalent bridges. *Polymer Chemistry* **2012**, *3*, 1796-1802.
- (78) Appel, E. A.; Dyson, J.; del Barrio, J.; Walsh, Z.; Scherman, O. A. Formation of Single-Chain Polymer Nanoparticles in Water through Host-Guest Interactions. *Angew. Chem., Int. Ed.* **2012**, *51*, 4185-4189, S4185/4181-S4185/4111.
- (79) Wang, P.; Pu, H.; Jin, M. Single-chain nanoparticles with well-defined structure via intramolecular crosslinking of linear polymers with pendant benzoxazine groups. *Journal of Polymer Science Part A: Polymer Chemistry* **2011**, *49*, 5133-5141.
- (80) Sugai, N.; Heguri, H.; Yamamoto, T.; Tezuka, Y. A Programmed Polymer Folding: Click and Clip Construction of Doubly Fused Tricyclic and Triply Fused Tetracyclic Polymer Topologies. *Journal of the American Chemical Society* **2011**, *133*, 19694-19697.
- (81) Schmidt, B. V. K. J.; Fechler, N.; Falkenhagen, J.; Lutz, J.-F. Controlled folding of synthetic polymer chains through the formation of positionable covalent bridges. *Nat Chem* **2011**, *3*, 234-238.
- (82) Adkins, C. T.; Muchalski, H.; Harth, E. Nanoparticles with Individual Site-Isolated Semiconducting Polymers from Intramolecular Chain Collapse Processes. *Macromolecules* **2009**, *42*, 5786-5792.
- (83) Njikang, G.; Liu, G.; Curda, S. A. Tadpoles from the Intramolecular Photo-Cross-Linking of Diblock Copolymers. *Macromolecules* **2008**, *41*, 5697-5702.
- (84) Cheng, L.; Hou, G.; Miao, J.; Chen, D.; Jiang, M.; Zhu, L. Efficient Synthesis of Unimolecular Polymeric Janus Nanoparticles and Their Unique Self-Assembly Behavior in a Common Solvent. *Macromolecules* **2008**, *41*, 8159-8166.
- (85) Li, R.; McCoy, B. J. Inter- and Intramolecular Crosslinking Kinetics: Partitioning According to Number of Crosslinks. *Macromolecular Rapid Communications* **2004**, *25*, 1059-1063.
- (86) van der Ende, A. E.; Harrell, J.; Sathiyakumar, V.; Meschievitz, M.; Katz, J.; Adcock, K.; Harth, E. "Click" Reactions: Novel Chemistries for Forming Well-defined Polyester Nanoparticles. *Macromolecules* **2010**, *43*, 5665-5671.
- (87) Corbett, P. T.; Leclaire, J.; Vial, L.; West, K. R.; Wietor, J.-L.; Sanders, J. K. M.; Otto, S. Dynamic Combinatorial Chemistry. *Chemical Reviews* **2006**, *106*, 3652-3711.
- (88) Rowan, S. J.; Cantrill, S. J.; Cousins, G. R. L.; Sanders, J. K. M.; Stoddart, J. F. Dynamic Covalent Chemistry. *Angewandte Chemie International Edition* **2002**, *41*, 898-952.
- (89) Jackson, A. W.; Fulton, D. A. Triggering Polymeric Nanoparticle Disassembly through the Simultaneous Application of Two Different Stimuli. *Macromolecules* **2012**, *45*, 2699-2708.

- (90) Nicolaÿ, R. Synthesis of Well-Defined Polythiol Copolymers by RAFT Polymerization. *Macromolecules* **2012**, *45*, 821-827.
- (91) Pauloehrl, T.; Delaittre, G.; Bastmeyer, M.; Barner-Kowollik, C. Ambient temperature polymer modification by in situ phototriggered deprotection and thiol-ene chemistry. *Polymer Chemistry* **2012**, *3*, 1740-1749.
- (92) Matson, J. B.; Grubbs, R. H. Synthesis of Fluorine-18 Functionalized Nanoparticles for use as in vivo Molecular Imaging Agents. *Journal of the American Chemical Society* **2008**, *130*, 6731-6733.
- (93) Ilker, M. F.; Coughlin, E. B. Alternating Copolymerizations of Polar and Nonpolar Cyclic Olefins by Ring-Opening Metathesis Polymerization. *Macromolecules* **2002**, *35*, 54-58.
- (94) Yan, X.; Li, S.; Pollock, J. B.; Cook, T. R.; Chen, J.; Zhang, Y.; Ji, X.; Yu, Y.; Huang, F.; Stang, P. J. Supramolecular polymers with tunable topologies via hierarchical coordination-driven self-assembly and hydrogen bonding interfaces. *Proceedings of the National Academy of Sciences* **2013**, *110*, 15585-15590.
- (95) Wang, C.; Wang, Z.; Zhang, X. Amphiphilic Building Blocks for Self-Assembly: From Amphiphiles to Supra-amphiphiles. *Accounts of Chemical Research* **2012**, *45*, 608-618.
- (96) Yebeutchou, R. M.; Tancini, F.; Demitri, N.; Geremia, S.; Mendichi, R.; Dalcanale, E. Host-Guest Driven Self-Assembly of Linear and Star Supramolecular Polymers. *Angewandte Chemie International Edition* **2008**, *47*, 4504-4508.
- (97) Zhang, B.; Yan, X.; Alcouffe, P.; Charlot, A.; Fleury, E.; Bernard, J. Aqueous RAFT Polymerization of Imidazolium-Type Ionic Liquid Monomers: En Route to Poly(ionic liquid)-Based Nanoparticles through RAFT Polymerization-Induced Self-Assembly. *ACS Macro Letters* **2015**, *4*, 1008-1011.
- (98) Lowe, A. B.; Harvison, M. A. Thiol-Based 'Click' Chemistries in Polymer Synthesis and Modification. *Australian Journal of Chemistry* **2010**, *63*, 1251-1266.
- (99) Sardon, H.; Chan, J. M. W.; Ono, R. J.; Mecerreyes, D.; Hedrick, J. L. Highly tunable polyurethanes: organocatalyzed polyaddition and subsequent post-polymerization modification of pentafluorophenyl ester sidechains. *Polymer Chemistry* **2014**, *5*, 3547-3550.
- (100) Barbey, R.; Klok, H.-A. Room Temperature, Aqueous Post-Polymerization Modification of Glycidyl Methacrylate-Containing Polymer Brushes Prepared via Surface-Initiated Atom Transfer Radical Polymerization. *Langmuir* **2010**, *26*, 18219-18230.
- (101) Kolb, H. C.; Finn, M.; Sharpless, K. B. Click chemistry: diverse chemical function from a few good reactions. *Angewandte Chemie International Edition* **2001**, *40*, 2004-2021.
- (102) Günay, K. A.; Theato, P.; Klok, H.-A. Standing on the shoulders of Hermann Staudinger: Post-polymerization modification from past to present. *Journal of Polymer Science Part A: Polymer Chemistry* **2013**, *51*, 1-28.
- (103) Singha, N. K.; Gibson, M. I.; Koiry, B. P.; Danial, M.; Klok, H.-A. Side-Chain Peptide-Synthetic Polymer Conjugates via Tandem "Ester-Amide/Thiol-Ene" Post-Polymerization Modification of Poly(pentafluorophenyl methacrylate) Obtained Using ATRP. *Biomacromolecules* **2011**, *12*, 2908-2913.

(104) Tripathi, A. K.; Tsavalas, J. G.; Sundberg, D. C. Monte Carlo Simulations of Free Radical Polymerizations with Divinyl Cross-Linker: Pre- and Postgel Simulations of Reaction Kinetics and Molecular Structure. *Macromolecules* **2015**, *48*, 184-197.

(105) Perez-Baena, I.; Asenjo-Sanz, I.; Arbe, A.; Moreno, A. J.; Lo Verso, F.; Colmenero, J.; Pomposo, J. A. Efficient Route to Compact Single-Chain Nanoparticles: Photoactivated Synthesis via Thiol-Yne Coupling Reaction. *Macromolecules* **2014**, *47*, 8270-8280.

(106) Kuhn, W.; Balmer, G. Crosslinking of single linear macromolecules. *Journal of Polymer Science* **1962**, *57*, 311-319.

(107) Gibson, M. I.; Fröhlich, E.; Klok, H.-A. Postpolymerization modification of poly(pentafluorophenyl methacrylate): Synthesis of a diverse water-soluble polymer library. *Journal of Polymer Science Part A: Polymer Chemistry* **2009**, *47*, 4332-4345.

(108) Eberhardt, M.; Mruk, R.; Zentel, R.; Théato, P. Synthesis of pentafluorophenyl(meth)acrylate polymers: New precursor polymers for the synthesis of multifunctional materials. *European Polymer Journal* **2005**, *41*, 1569-1575.

(109) Mohr, N.; Barz, M.; Forst, R.; Zentel, R. A Deeper Insight into the Postpolymerization Modification of Polypenta Fluorophenyl Methacrylates to Poly(N-(2-Hydroxypropyl) Methacrylamide). *Macromolecular Rapid Communications* **2014**, *35*, 1522-1527.

(110) Schaefer, M.; Hanik, N.; Kilbinger, A. F. M. ROMP Copolymers for Orthogonal Click Functionalizations. *Macromolecules* **2012**, *45*, 6807-6818.

(111) Gunay, K. A.; Schuwer, N.; Klok, H.-A. Synthesis and post-polymerization modification of poly(pentafluorophenyl methacrylate) brushes. *Polymer Chemistry* **2012**, *3*, 2186-2192.

(112) Schüll, C.; Nuhn, L.; Mangold, C.; Christ, E.; Zentel, R.; Frey, H. Linear-Hyperbranched Graft-Copolymers via Grafting-to Strategy Based on Hyperbranched Dendron Analogues and Reactive Ester Polymers. *Macromolecules* **2012**, *45*, 5901-5910.

(113) Eberhardt, M.; Théato, P. RAFT Polymerization of Pentafluorophenyl Methacrylate: Preparation of Reactive Linear Diblock Copolymers. *Macromolecular Rapid Communications* **2005**, *26*, 1488-1493.

(114) Wolfberger, A.; Rupp, B.; Kern, W.; Griesser, T.; Slugovc, C. Ring Opening Metathesis Polymerization Derived Polymers as Photoresists: Making Use of Thiol-ene Chemistry. *Macromolecular Rapid Communications* **2011**, *32*, 518-522.

(115) Samojłowicz, C.; Bieniek, M.; Pazio, A.; Makal, A.; Woźniak, K.; Poater, A.; Cavallo, L.; Wójcik, J.; Zdanowski, K.; Grela, K. The Doping Effect of Fluorinated Aromatic Solvents on the Rate of Ruthenium-Catalysed Olefin Metathesis. *Chemistry – A European Journal* **2011**, *17*, 12981-12993.

(116) Samojłowicz, C.; Bieniek, M.; Zarecki, A.; Kadyrov, R.; Grela, K. The doping effect of fluorinated aromatic hydrocarbon solvents on the performance of common olefin metathesis catalysts: application in the preparation of biologically active compounds. *Chemical Communications* **2008**, 6282-6284.

- (117) Ritter, T.; Day, M. W.; Grubbs, R. H. Rate Acceleration in Olefin Metathesis through a Fluorine–Ruthenium Interaction. *Journal of the American Chemical Society* **2006**, *128*, 11768-11769.
- (118) Fürstner, A.; Ackermann, L.; Gabor, B.; Goddard, R.; Lehmann, C. W.; Mynott, R.; Stelzer, F.; Thiel, O. R. Comparative Investigation of Ruthenium-Based Metathesis Catalysts Bearing N-Heterocyclic Carbene (NHC) Ligands. *Chemistry – A European Journal* **2001**, *7*, 3236-3253.
- (119) Ledoux, N.; Allaert, B.; Pattyn, S.; Mierde, H. V.; Vercaemst, C.; Verpoort, F. N,N'-Dialkyl- and N-Alkyl-N-mesityl-Substituted N-Heterocyclic Carbenes as Ligands in Grubbs Catalysts. *Chemistry – A European Journal* **2006**, *12*, 4654-4661.
- (120) Rost, D.; Porta, M.; Gessler, S.; Blechert, S. A hexafluorobenzene promoted ring-closing metathesis to form tetrasubstituted olefins. *Tetrahedron Letters* **2008**, *49*, 5968-5971.
- (121) Grandbois, A.; Collins, S. K. Enantioselective Synthesis of [7]Helicene: Dramatic Effects of Olefin Additives and Aromatic Solvents in Asymmetric Olefin Metathesis. *Chemistry – A European Journal* **2008**, *14*, 9323-9329.
- (122) Moatsou, D.; Hansell, C. F.; O'Reilly, R. K. Precision polymers: a kinetic approach for functional poly(norbornenes). *Chemical Science* **2014**, *5*, 2246-2250.
- (123) Zhang, K.; Lackey, M. A.; Wu, Y.; Tew, G. N. Universal Cyclic Polymer Templates. *Journal of the American Chemical Society* **2011**, *133*, 6906-6909.
- (124) Vogel, N.; Théato, P. Controlled Synthesis of Reactive Polymeric Architectures Using 5-Norbornene-2-carboxylic Acid Pentafluorophenyl Ester. *Macromolecular Symposia* **2007**, *249-250*, 383-391.
- (125) Santiago, A. A.; Vargas, J.; Fomine, S.; Gaviño, R.; Tlenkopatchev, M. A. Polynorbornene with pentafluorophenyl imide side chain groups: Synthesis and sulfonation. *Journal of Polymer Science Part A: Polymer Chemistry* **2010**, *48*, 2925-2933.
- (126) Zhang, K.; Tew, G. N. Cyclic polymers as a building block for cyclic brush polymers and gels. *Reactive and Functional Polymers* **2014**, *80*, 40-47.
- (127) Zhang, K.; Zha, Y.; Peng, B.; Chen, Y.; Tew, G. N. Metallo-Supramolecular Cyclic Polymers. *Journal of the American Chemical Society* **2013**, *135*, 15994-15997.
- (128) Santiago, A. A.; Vargas, J.; Gaviño, R.; Cerda, A. M.; Tlenkopatchev, M. A. Synthesis and Ring-Opening Metathesis Polymerization of New Oxanorbornene Dicarboximides with Fluorine Pendant Groups. *Macromolecular Chemistry and Physics* **2007**, *208*, 1085-1092.
- (129) Cole, J. P.; Lessard, J. J.; Lyon, C. K.; Tuten, B. T.; Berda, E. B. Intra-chain radical chemistry as a route to poly(norbornene imide) single-chain nanoparticles: structural considerations and the role of adventitious oxygen. *Polymer Chemistry* **2015**, *6*, 5555-5559.
- (130) York, A. W.; Kirkland, S. E.; McCormick, C. L. Advances in the synthesis of amphiphilic block copolymers via RAFT polymerization: Stimuli-responsive drug and gene delivery. *Advanced Drug Delivery Reviews* **2008**, *60*, 1018-1036.

(131) Watson, K. J.; Park, S.-J.; Im, J.-H.; Nguyen, S. T.; Mirkin, C. A. DNA-block copolymer conjugates. *Journal of the American Chemical Society* **2001**, *123*, 5592-5593.

(132) Baughman, T.; Wagener, K.: Recent Advances in ADMET Polymerization. In *Metathesis Polymerization*; Buchmeiser, M., Ed.; Advances in Polymer Science; Springer Berlin Heidelberg, 2005; Vol. 176; pp 1-42.

(133) Kakuchi, R.; Theato, P. Three-Component Reactions for Post-Polymerization Modifications. *ACS Macro Letters* **2013**, *2*, 419-422.

(134) Das, A.; Theato, P. Activated Ester Containing Polymers: Opportunities and Challenges for the Design of Functional Macromolecules. *Chemical Reviews* **2015**.

(135) Batz, H. G.; Franzmann, G.; Ringsdorf, H. Pharmakologisch aktive polymere, 5. Modellreaktionen zur umsetzung von pharmaka und enzymen mit monomeren und polymeren reaktiven estern. *Die Makromolekulare Chemie* **1973**, *172*, 27-47.

(136) Šubr, V.; Ulbrich, K. Synthesis and properties of new N-(2-hydroxypropyl)methacrylamide copolymers containing thiazolidine-2-thione reactive groups. *Reactive and Functional Polymers* **2006**, *66*, 1525-1538.

(137) He, L.; Szameit, K.; Zhao, H.; Hahn, U.; Theato, P. Postpolymerization Modification Using Less Cytotoxic Activated Ester Polymers for the Synthesis of Biological Active Polymers. *Biomacromolecules* **2014**, *15*, 3197-3205.

(138) Roy, D.; Nehilla, B. J.; Lai, J. J.; Stayton, P. S. Stimuli-Responsive Polymer-Antibody Conjugates via RAFT and Tetrafluorophenyl Active Ester Chemistry. *ACS Macro Letters* **2013**, *2*, 132-136.

(139) He, L.; Shang, J.; Theato, P. Preparation of dual stimuli-responsive block copolymers based on different activated esters with distinct reactivities. *European Polymer Journal* **2015**, *69*, 523-531.

(140) Slavin, S.; Burns, J.; Haddleton, D. M.; Becer, C. R. Synthesis of glycopolymers via click reactions. *European Polymer Journal* **2011**, *47*, 435-446.

(141) Becer, C. R.; Babiuch, K.; Pilz, D.; Hornig, S.; Heinze, T.; Gottschaldt, M.; Schubert, U. S. Clicking Pentafluorostyrene Copolymers: Synthesis, Nanoprecipitation, and Glycosylation. *Macromolecules* **2009**, *42*, 2387-2394.

(142) Chen, J.; Dumas, L.; Duchet-Rumeau, J.; Fleury, E.; Charlot, A.; Portinha, D. Tuning h-bond capability of hydroxylated-poly(2,3,4,5,6-pentafluorostyrene) grafted copolymers prepared by chemoselective and versatile thiol-para-fluoro "click-type" coupling with mercaptoalcohols. *Journal of Polymer Science Part A: Polymer Chemistry* **2012**, *50*, 3452-3460.

(143) Noy, J.-M.; Koldevitz, M.; Roth, P. J. Thiol-reactive functional poly(meth)acrylates: multicomponent monomer synthesis, RAFT (co)polymerization and highly efficient thiol-para-fluoro postpolymerization modification. *Polymer Chemistry* **2015**, *6*, 436-447.

(144) Cogolli, P.; Maiolo, F.; Testaferri, L.; Tingoli, M.; Tiecco, M. Nucleophilic aromatic substitution reactions of unactivated aryl halides with thiolate ions in hexamethylphosphoramide. *The Journal of Organic Chemistry* **1979**, *44*, 2642-2646.

(145) Burnett, J. F.; Zahler, R. E. Aromatic Nucleophilic Substitution Reactions. *Chemical Reviews* **1951**, *49*, 273-412.

(146) Montanari, S.; Paradisi, C.; Scorrano, G. Thiol anions in nucleophilic aromatic substitution reactions with activated aryl halides. Attack on carbon vs attack on halogen. *The Journal of Organic Chemistry* **1993**, *58*, 5628-5631.